CANADIAN THESES ON MICROFICHE

THÈSES CANADIENNES SUR MICROFICHE

National Library of Canada
Collections Development Branch

Canadian Theses on
Microfiche Service

Ottawa, Canada
K1A 0N4

Bibliothèque nationale du Canada
Direction du développement des collections

Service des thèses canadiennes
sur microfiche

NOTICE

The quality of this microfiche is heavily dependent upon the quality of the original thesis submitted for microfilming. Every effort has been made to ensure the highest quality of reproduction possible.

If pages are missing, contact the university which granted the degree.

Some pages may have indistinct print especially if the original pages were typed with a poor typewriter ribbon or if the university sent us an inferior photocopy.

Previously copyrighted materials (journal articles, published tests, etc.) are not filmed.

Reproduction in full or in part of this film is governed by the Canadian Copyright Act, R.S.C. 1970, c. C-30. Please read the authorization forms which accompany this thesis.

AVIS

La qualité de cette microfiche dépend grandement de la qualité de la thèse soumise au microfilmage. Nous avons tout fait pour assurer une qualité supérieure de reproduction.

S'il manque des pages, veuillez communiquer avec l'université qui a conféré le grade.

La qualité d'impression de certaines pages peut laisser à désirer, surtout si les pages originales ont été dactylographiées à l'aide d'un ruban usé ou si l'université nous a fait parvenir une photocopie de qualité inférieure.

Les documents qui font déjà l'objet d'un droit d'auteur (articles de revue, examens publiés, etc.) ne sont pas microfilmés.

La reproduction, même partielle, de ce microfilm est soumise à la Loi canadienne sur le droit d'auteur, SRC 1970, c. C-30. Veuillez prendre connaissance des formules d'autorisation qui accompagnent cette thèse.

THIS DISSERTATION
HAS BEEN MICROFILMED
EXACTLY AS RECEIVED

LA THÈSE A ÉTÉ
MICROFILMÉE TELLE QUE
NOUS L'AVONS REÇUE

Canada

NL 339 (r. 86/09)

EFFECTS OF DIAPHRAGMS ON WARPING AND DISTORTIONAL STRESSES IN BOX GIRDER BRIDGES

by

Ahmad Hussain Siddiqui

A thesis
presented to the University of Ottawa
in partial fulfillment of the
requirements for the degree of
Master of Applied Science
in
Civil Engineering

OTTAWA, Ontario, 1985

UNIVERSITÉ D'OTTAWA
UNIVERSITY OF OTTAWA

TABLE OF CONTENTS

ABSTRACT

The static behaviour of simply supported box girder bridges with or without intermediate diaphragms and subjected to concentrated joint loads was investigated. The purpose of this investigation was to confirm experimentally that deformation of the cross section of a box girder induces an appreciable amount of warping and distortion stresses and that these stresses can be substantially reduced by inserting rigid diaphragms at selected locations.

By starting with the governing differential equation for the Beam of Elastic Foundations and by applying the proper boundary conditions, expressions for the dimensionless moments and deflections in terms of the Beam on Elastic Foundation Analogy and support properties can be determined. These values are later used in calculating the warping and distortion stresses in the analogous box girder. In the analogy, bending stresses in the Beams on Elastic Foundation Analogy are related to the warping stresses in the box girder, and the load is related to the torsional load on the box girder. Warping stresses in the girder may be found by evaluating the moments in the Beam on Elastic Foundation Analo-

gy. Similarly, distortion stresses are obtained by finding the deflections of the corresponding Beam on Elastic Foundations.

The experimental program was limited in scope to the test of two different types of cross-sections for single cell box girders fabricated from plexiglas. The static loads, which were applied normal to the compression flange of the box girder, were kept small enough so that the strains in the plexiglas models were within the elastic range. The models were designed so that the shape of the cross section would be distorted under the test loads, thus resulting in warping and distortion stresses of easily measureable magnitudes.

The evaluation of distortion stresses was accomplished by subtracting the stresses measured by the transverse web gages due to concentric loading from those due to eccentric loading.

Similarly, the experimental warping stresses were determined by subtracting the flange stresses due to concentric loading from those obtained when the model was loaded eccentrically.

The experimental results indicate that the diaphragms are much more effective in controlling distortion stresses than warping stresses. Thus in the design process it would seem reasonable to space diaphragms to control distortion stresses, and then check the warping stresses to ensure that they are within acceptable limits.

The distortion and warping stresses determined from the B.E.F theory agree well with the experimental stresses.

ACKNOWLEDGEMENTS

The author wishes to express his sincere gratitude to Dr.S.F.Ng under whose guidance this work was carried out. His generous encouragement, helpful suggestions and valuable time spent during the course of this study are particularly appreciated. The cooperation rendered by the Civil Engineering Workshop personnel in connection with the fabrication of models for the experimental study is highly appreciated.

The author is most indebted to his wife Mrs. Rana J. Ahmad and his sons Shayaan A. Siddiqui and Shamoon A. Siddiqui for their understanding and support. The financial support offered by the National Research Council of Canada is gratefully acknowledged.

LIST OF FIGURES

NOMENCLATURE

a	top width of box girder cell
A	cross sectional area of box girder cell
A	cross sectional area of diagonal brace
A	middle surface area of diaphragm plate
b	bottom width of box girder cell
BEF	beam on elastic foundation
c	slant width of box girder web plate
d	stiffness spacing
d	effective width of plate acting with a stiffener
D	flexural rigidity of a plate
E	modulus of elasticity
E	modulus of elasticity for a brace
F	parameter related to distortion stress
G	shear modulus of reference material
G	shear modulus of plate element
h	depth of box girder cell
I	moment of inertia of plate per unit width
I	moment of inertia of equivalent beam on elastic foundation
I	moment of inertia of box girder cell
k	foundation modulus for BEF
l	panel length of box girder between diaphragms
L	span of box girder
L	length of a cross brace

m	diamensionless moment
M	moment
p	distributed vertical, distributed torsional load
P	concentrated vertical load, concentrated torsional load
P_1	concentric load
P_2	medium eccentric load
P_3	maximum eccentric load
q	dimensionless brace stiffness
Q	brace stiffness
r	dimensionless reaction of BEF
R	reaction of BEF
S	section modulus of plate element per unit length
t	thickness of plate element
t_p	thickness of diaphragm plate
v	y-direction (transverse displacement, Eq.3.3.8)
V	shear in BEF
w	dimensionless deflection of BEF
Y	N.A.of box girder cell below middle surface of deck plat
β	beam on elastic foundation parameter
δ_1	unit vertical deflection due to torsional load
δ_b	brace distortion box girder cell
ν	poisson's ratio
σ_b	bending stress
σ_t	distortion stress at extreme fibers
σ_w	warping axial stress
τ	shear stress in plane of plate element
θ	slope in BEF

$\phi(\beta x)$ function for BEF

Chapter I

INTRODUCTION

1.I GENERAL

Closed-section girder type bridges have become increasingly popular as a major component in highway bridge systems. The interest in box girder bridges is due to the advantages that they have over other types of bridges. Due to the boxes, the bridges have a high torsional stiffness and consequently, a better transverse distribution of loads, with fevourable effects on the load carrying capacity and, therefore, on economy. The maintenance cost is reduced in these bridges because a smaller percentage of the total section is exposed. Utilities and services can be contained within the boxes. The clean and simple lines of the boxes make them aesthetically pleasing.

The cross section of box girder bridges may be either i) steel box- steel plates to be cut into desired shapes and the resultant pieces to be joined by welding ii) concrete box- the entire section made by concrete and iii) composite construction- a concrete deck acting with the steel box in a composite fashion. The primary appeal of com-

posite construction is economy, since loads may be carried with less weight of material when the concrete and steel are acting compositely.

It is a well known fact that the cross sections of box girder bridges do not always retain their original shapes under eccentrical loading. In this case, the deformation of the cross-section is accompanied by additional stresses, such as the distortion and warping stresses in thin-plate members. Hence diaphragms or cross bracings are usually installed in the box girders to prevent such unfavourable distortion and its harmful effect.

The beam on elastic foundation analogy (25) is used to obtain distortion and warping stresses in the box girder cell caused by the deformation of the cross section. The beam on elastic foundation analogy finds its widest applicability in steel and composite box girders.

1.2 OBJECTIVE

The objective of this thesis is to examine the effect of diaphragms in reducing warping and distortion stresses that are caused by the deformation of the box girder cross section. Model tests were conducted on plexiglas models for two different types of box girder sections. Re-

sults were compared with values obtained from the so called"B.E.F analogy" modified to fit the model sections under investigation.

1.3 OUTLINE OF THESIS

Since the problems studied in this thesis are related to the effects of interior diaphragms in box girder bridge sections, existing literature relating to the topics are briefly reviewed in chapter 2. In chapter 3, theoretical formulation of the Beam on Elastic Foundations Analogy is presented. Chapter 4 presents the experimental set-up and subsequent testing details. Analysis and discussion of the tests can be found in chapter 5.

In the final chapter, chapter 6, conclusions based on the theory and experimental results are summarized. Whenever possible,such results are compared with solutions obtained by other investigators.

Chapter II

REVIEW OF LITERATURE

The increasing use of box girder bridges in the last few years is due to the fact that box sections often lead to economical and aesthetical designs. For bridge of longer spans,transverse stiffeners or intermediate diaphragms are used to prevent excessive distortion of the cross section of the box elements.

Several analytical methods have been developed in recent years for the elastic analysis of box girder bridges. A comprehensive revew of current methods can be found in references (1,2).

The greatest degree of generality is achieved by the finte element methods but, due to the associated high computing costs, the method is used only for very complicated geometries. The accuracy of the results depends mainly on the assumptions used in the formulation of the element stiffness matrix and on the fineness of the mesh. More detailed descriptions of this method can be found in several references (3,4,5 and 6).

For box girder analysis, a three dimensional assemblage of elements may be necessary. Sisodiya, Ghali and Cheung (7) used the finite element method of analysis to investigate the effect of transverse stiffeners in single cell and double cell box girder bridges with various angles of skew. Scordelis (8) applied rectangular finite elements in the analysis of continuous concrete box girders with rigid interior diaphragms and obtained results which are in good agreement with those given by the folded plate theory.

There is no logical limit to structural complexity. However, even for simple bridges, a large number of elements is necessary to obtain desirable accuracy. The resulting computational cost is high, also the amount of input preparation and output data reduction for clear interpretation of the results can be excessive.

Cheung,Y.K (9,10,11) developed a shell strip for the analysis of prismatic folded plate structures and box girders. The assumed deflexion function consists of a one-way slab function (a third order polynomial) across the width of the strip and a characteristic function in the longitudinal direction. Cheung gave several examples to demonstrate the power of the method when dealing with rectangular plates with various combinations of boundary conditions. Loo and Cusens (12) developed the finite strip method for

orthotropic plates by assuming a fifth order polynomial as the transverse displacement function and obtained satisfactory results with a small number of strips. Branco,F.A (13) used the finite strip method to study the influence of the bracing system on the open box girders.

Scordelis (14) applied the folded plate method to box girders considering the bending of each plate out of its plane according to the plate flexural theory and the bending in the plane according to plane stress theory. The external loads were represented by a Fourier series. This analysis can only be applied to constant cross section box girders.

The application of grillage analysis for box girder bridges was first proposed by Sawko (15). The application to box girders (16,17), while not being the most rigorous, has the benifit that computing costs are low and output is simple to understand.

There are several methods developed to study the effect of the cross section deformation. Knittle's method (18) analyses the transverse bending stresses and the transverse normal stresses due to torsional distortion of the section. The loads are assumed to act at the webs. The distortion of the flanges due to concentric loading out of the webs is not considered. Richmond (19) developed the equiva-

lent beam method, and considered only the antisymmetric load case. The transverse bending stresses, transverse normal stresses and distortional warping stresses are obtained. The loads are considered as acting on the webs. It is assumed that there are rigid diaphragms at the supports but these do not restrain warping. The analysis is simplified by considering the flanges of the box girder replaced by equivalent flanges of two beams, lattiçed together in the planes of the flanges. A similar method proposed by Kupfer's (20), considers two independent structural systems which are deformationally compatible. In the first, the box girder is treated as a hinged folded plate structure considering only the longitudinal behaviour of the walls. Secondly, the box is considered as a rigid joint close-frame and only transverse structural action is obtained.

P.Nimityongskul,R.P.Pama and Seng-Lip Lee (21) presented an accurate and efficient method of analysis for box girder bridges and takes into account the influence of intermediate diaphragms. The elements in the box section are treated as rectangular plates subjected to lateral and in-plane boundary forces. The solutions due to unit vertical and horizontal loads applied at the joints for the case without intermediate diaphragms are obtained and used as influence coefficients to derive the solutions for any combination of concentrated live loads applied at the joints as well as the effect of intermediate diaphragms.

Abdul-Samad,Wright and Robinson (22) applied thin walled beam theory (23) to box girder of deformable cross section. Thin-walled beam theory is extended to cover stiffened plate elements and of deformable interior diaphragms. A simplified formulation was studied by Dalton and Richmond (24) to obtain the solution for girders of trapezoidal cross section by assuming that only the diaphragms or cross frames resists the cross section distortion.

Wright, Abdel Samad and Robinson (25) have developed an analogy to the well known "theory of beam on elastic foundation" (B.E.F) to obtain an approximate analysis procedure which accounts for the effects of diaphragms or cross braces on the warping and distortion stresses of box girders. Comparison with more refined analysis show that the B.E.F analogy is an adequate substitute for these much more refined procedures. Rajagopalan,N, Rajagoplan,B.K (26) extended this B.E.F analogy for support diaphragms.

Even though there were many paper published referring to the distortional behaviour of the girder itself, only/a few proposal have been given with respect to design criteria for intermediate diaphragms so far. These are Merrison's rule (27),proposal by Sakai and Nagai (28,29). Merrison's rule adopted the results obtained by Wright, Abdel-Samad and Robinson (25), who applied B.E.F (beam on elastic

foundation) analogy. In that rule, the approximate formulae for the additional stresses induced in box girders and those for the required minimum rigidity and stresses of diaphragms are listed. Sakai and Nagai (28,29) have presented at first beam analogy to formulate the distortional behaviour of box girders. The theory is based on the assumption that the influence of elastic foundation uniformly distributed spanwise on the distortional behaviour may be neglected under the sufficiently rigid condition of diaphragms. Then they derived the compratively simple formulae as proposed by Merrison's rule. Further more , they proposed for the first time the critical space of diaphragms being such that the additional warping stress becomes negligible in comparison with the primary bending stress. Sadao Komatsu and Masatsugu Nagai (30) have presented a recomendation for design of intermediate diaphragms in the box girders on the basis of B.E.F analogy.

Myers and Cooper (31) reported stress distribution in a plexiglas model of a one cell box girder with various diaphragm arrangements for loading. The results are in general in agreement with those predicted by thin walled beam theory using the beam on elastic foundation analogy. Variation between experiment and theory can be attributed to difficulties in achieving rigid joints, stress relaxation in the plexiglas, and two way plate action in the short panel

lengths between diaphragms. Godden and Aslam (32) presented the results of an experimental study on the static response of skew box girder bridges and theoretical results based on a finite element analysis was used for comparison. An experimental investigation to study the behaviour of composite simply supported box girder bridge with end diaphragms was carried out by Mattock and Johnstone (33) and the result agreed well with those obtained by the folded plate theory (34). Maggard and Parr (35) have reported a series of static tests on steel box girder models in which the loads were applied at the diaphragms. The experimental results were compared with stresses obtained from a simple flexural analysis superimposed with the St.Venant torsional stresses. This work is being extended to give further data with respect to the stresses in the immediate vicinity of normally spaced diaphragms. Vlasov (23) reported test results on a box girder model for confirmation of the thin walled beam theory. These tests considered an applied warping load. While agreement between theory and experiment is good, the loading is not representative of a box girder bridge. Pama R.P (36) experimentally studied the influence of intermediate diaphragms on the behaviour of a simply supported straight double-cell box girder bridge. The experimental results are compared with theoretical values suggested by Nimityongskul, Pama and Lee (21).

Recently, experimental research was developed and several tests were conducted using 1/4 scale model of an open box girder (13,37). These test results were used to check the results of an analytical study.

Chapter III

INTRODUCTION TO BEAM ON ELASTIC FOUNDATION ANALOGY

The beam on elastic foundation analogy (B.E.F) was developed by Wright, R.,N., Abdel-Samad, S.,R. and Robinson,A.,R. (25) to obtain an approximate analysis procedure which accounts for the effects of diaphragms or cross braces on the warping and distortion stresses of box girders. This chapter summarizes the salient features of the beam on elastic foundation analogy (B.E.F).

3.1 OUTLINE OF THE B.E.F. ANALOGY

The response of a box cell to loading that causes deformation of the cross section can be represented by a differential equation identical in form to that of a beam on elastic foundations. A direct analogy exists between the physical properties of the box cell and the beam on elastic foundation. A similar analogy has proved useful for evaluation of bending stresses in cylindrical shells.

Deformation of the cross-section produces distortion in the plane of the cross section. One basic assumption

regarding this in-plane motion is borrowed from the theory of torsion of thin-walled beams of open sections. It is assumed that the distortions are accompanied by sufficient warping to annul the average shear strain in the plates which form the cross section. It can be seen that if the deformation is not constant along the beam, some warping displacement must then be present. It is emphasized that for the box cell this warping displacement arises from the deformation of the cross section, and is not the warping associated with St.Venant torsion. Just as in thin walled beam theory for open sections, warping can be regarded as in-plane bending of the plates forming the cross section.

The warping displacements are not in general constant along the axis of the box cell. Longitudinal stresses arise from constraint. If, in turn, these warping stresses vary along the girder, shearing forces are required by considerations of longitudinal equilibrium. These shear force in the plane of the plates also change from section to section, resulting in a net resistance to deformation of the cross section which adds to the resistance caused by the flexural stiffness of the cross section in its own plane.

3.2 BASIC RELATIONS OF B.E.F

An element of B.E.F is shown in figure 3.1 with the positive quantities indicated: deflection,W; concentrated load,P; distributed load, p; shear, V; and moment,M. The governing differential equation is

$$EId^4W/dx^4+kW= p \qquad (3.2.1)$$

Here k is the foundation modulus and I is the moment of inertia of the beam cross section. The solution is written in terms of the B.E.F. parameter β , which includes the flexural rigidity of the beam as well as the elasticity of the supporting medium, and is an important factor influencing the shape of the elastic line. For this reason the factor β is called the characteristic of the system, and since its dimension is inverse length, the term $1/\beta$ is frequently referred to as the characteristic length. Consequently , βx will be an absolute number.

$$\beta = \sqrt[4]{K/4EI} \qquad (3.2.2)$$

The general solution in terms of the end conditions , w_o , θ_o , v_o , and M_o , is given by

$$W = W_o\phi_1(\beta x)+\theta_o\phi_2(\beta x)/2\beta -M_o\phi_3(\beta x)/2EI\beta^2$$
$$-V_o\phi_4(\beta x)/4EI\beta^3+p(1-\phi_1(\beta x))/4EI\beta^4 \qquad (3.2.3)$$

$$\Theta = -W_o\beta\Phi_4(\beta x)+\theta_o\Phi_1(\beta x)-M_o\Phi_2(\beta x)/2EI\beta$$
$$-V_o\Phi_3(\beta x)/2EI\beta^2+p\Phi_4(\beta x)/4EI\beta^3 \qquad (3.2.4)$$

$$W^{ii} = -W_o 2\beta^2\Phi_3(\beta x)-\theta_o\beta\Phi_4(\beta x)-M_o\Phi_1(\beta x)/EI$$
$$-V_o\Phi_2(\beta x)/2EI\beta+p\Phi_3(\beta x)/2EI\beta^2 \qquad (3.2.5)$$

$$W^{iii} = -W_o 2\beta^3\Phi_2(\beta x)-\theta_o 2\beta^2\Phi_3(\beta x)+M_o\beta\Phi_4(\beta x)/EI$$
$$-V_o\Phi_1(\beta x)/EI+p\Phi_2(\beta x)/2EI\beta \qquad (3.2.6)$$

$$W^{iv} = -W_o 4\beta^4\Phi_1(\beta x)-\theta_o 2\beta^3\Phi_2(\beta x)+M_o 2\beta^2\Phi_3(\beta x)/EI$$
$$+V_o\beta\Phi_4(\beta x)/EI+p\Phi_1(\beta x)/EI \qquad (3.2\ 7)$$

Where,

$$\Phi_1(\beta x)=\cosh(\beta x)\cos(\beta x)$$
$$\Phi_2(\beta x)=\cosh(\beta x)\sin(\beta x)+\sinh(\beta x)\cos(\beta x)$$
$$\Phi_3(\beta x)=\sinh(\beta x)\sin(\beta x)$$
$$\Phi_4(\beta x)=\cosh(\beta x)\sin(\beta x)-\sinh(\beta x)\cos(\beta x)$$

The four function Φ_1 , Φ_2 , Φ_3 and Φ_4 are the special functions associated with deflection, slope , moment, and shear respectively.

3.3 ELEMENTARY SOLUTIONS

Solutions are presented for B.E.F with simple, undeflecting support at each end and loads either uniformly distributed or concentrated at midspan. These show how the response quantities of interest are non-dimensionalized for

plotting in a generally useful form.The same dimensionless parameters and response quantities are later used for more complex boundary conditions.

For simple span B.E.F under uniformly distributed load p, the origin x=0 is taken at midspan where $\theta_o = 0$ and V =0.Boundary conditions at the support are $W(\ell/2)=M(\ell/2)=0$. Using equation (3.2.3-3.2.7), the solutions for dimensionless deflection at midspan, w_o, moment at midspan, m_o and reaction at the support, r, are

$$w_o = 4EI\,\beta^4 W_o/p = 1 - \rho_1/\rho_1^2+\rho_3^2 \qquad (3.2.8)$$

$$m_o = 2\beta^2 M_o/p \quad = \rho_3/\rho_1^2+\rho_3^2 \qquad (3.2.9)$$

$$r = R/p\ell \quad = 1/2\beta\ell\,(-\rho_3 w_o + \rho_4 m_o + \rho_2) \qquad (3.2.10)$$

Here the term $\rho_i = \Phi_i(\beta\ell/2)$. The quantity $\beta\ell$ may be considered the dimensionless span.

For a simple span B.E.F with concentrated load P at midspan the origin x=0 is taken at midspan where $\Theta = 0$ and V =-P/2. Boundary conditions at the support are $W(\ell/2)=M(\ell/2)=0$. Using equation (3.2.3-3.2.7) the solutions for dimensionless midspan deflection, w_o, midspan moment m_o, and reaction, r, are

$$w_o = 8EI\,\beta^3 W_o/P = \frac{-\rho_1\rho_4+\rho_3\rho_2}{\rho_1^2+\rho_3^2} \qquad (3.2.11)$$

$$m_o = 4\beta M_o/P = \frac{\rho_1\rho_2 + \rho_3\rho_4}{\rho_1^2 + \rho_3^2} \qquad (3.2.12)$$

$$r = R/P = 1/2 - 1/4(w_o\rho_2) + 1/4(m_o\rho_4) \qquad (3.2.13)$$

Here the ρ terms are as defined above.

3.4 DEVELOPMENT OF CROSS SECTION PARAMETERS

A symmetrical single cell girder of the type shown in Figure 3.2 is considered to be loaded by a uniformly distributed unit line torsional load . The longitudinal flexural properties of the cross section are computed assuming the web and bottom flanges to be made of material of Young's modulus E. The deck may have a different modulus E_a.The thickness t_a , t_b ,and t_c of the deck ,flanges,and web respectively (Fig.3.3), are effective values including longitudinal stiffeners. The transformed area is given by

$$A = at_a E_a/E + 2ct_c + bt_b \qquad (3.3.1)$$

The centroid is located at distance $\bar{Y}$ below the top flange middle surface ,where

$$\bar{Y} = (h/A)(bt_b + ct_c) \qquad (3.3.2)$$

The moment of inertia of the cell, neglecting thickness squared terms, is

$$I_c = at_a E_a \bar{Y}^2/E + 2ct_c(h^2/12 + (h/2-\bar{Y})^2) + bt_b(h-\bar{Y})^2 \quad (3.3.3)$$

Figs. 3.4-3.8 show the forces acting on an element of the girder of unit length in the span direction. The twisting moment of the torsional loading is balanced by the gradient of the St.Venant torsion in the cell walls. Consider now an element of unit length cut along the span of the structure and assume that a twisting moment $M_T = pa$ is applied as shown in Figure 3.4. This twisting moment will transfer a shear equivalent to $pa/(a+e)$ at the inflection points as shown in Figure 3.4c. This also causes a unit shearing forces τ_s given by the expression

$$\tau_s = M_T/2A = Pa/h(a+b) \quad (3.3.4)$$

Where A is the area enclosed by the median line of the box section.

The statical problem of evaluating the bending moments acting in the walls of the box section has one redundancy. If the box section is cut at its axis of symmetry, the forces acting will be as shown in Figure 3.5 .

Equilibrium of forces in the vertical direction yields,

$$q_o + pa/a+e = q_o + \tau_s h \quad (3.3.5)$$

Substituting for γ_s from equation (3.3.4) and solving for q_o,

$$q_o = q_u + pa(e-b)/(a+b)(a+e) \qquad (3.3.6)$$

With q_o expressed in terms of the unknown shear force q_u, the strain energy in bending may be evaluated with out any difficulty. Assuming that the deflection of point A is zero so that $(\partial u/\partial q_u)=0$, after some transformation, the unknown shear force q_u may be determined, thus;

$$q_u = Pa/(a+b)(a+e) \cdot (2a+b)(a+e)bc - a^3P(e-b) / 2c(a^2+ab+b^2) + b^3 + a^3P \qquad (3.3.7)$$

Where, $P = EI_r/EI_p = (t_r/t_p)^3$

t_r = thickness of web plate

t_p = thickness of top plate

setting $q_u = v$

$$v = (1/D_c)(2a+b)abc + (1/D_a)ba^3 / (a+b)((a^3D_a + (2c(a^2+ab+b^2)/D_c + b^3/D_b) \qquad (3.3.8)$$

In equation (3.3.8) D_a, D_b, and D_c denotes the transverse flexural rigidity per unit length of the deck, web and flange plates, respectively. For an unstiffened plate.

$$D = Et^3/12(1-\nu^2) \qquad (3.3.9)$$

For a transversely stiffened plate the effective width of plate acting with a stiffener is computed by

$$d_o = d \tanh(5.6d/b)/(5.6/b)(1-\nu^2) \qquad (3.3.10)$$

Where d is the spacing of the transverse stiffeners. Then D= EI where I is the moment of inertia of combined section of transverse stiffener and effective width of plate, divided by the stiffener spacing.

The deflection δ_1 of the loaded node, Figure 3.9, resulting from transverse flexural deformation is obtained using the principle of virtual displacements, noting that if no work from the shear flow gradient is considered no torsional deflection is included.

$$\delta_1 = ab/24(a+b).(c/D_c(2ab/a+b - v(2a+b) + a^2/D_a(b/a+b - v)) \qquad (3.3.11)$$

Where, v is given by eq (3.3.8)

Observe that δ_1 is constant along the length of the box if the torsional load and cross section remain constant and no diaphragms are present. The distortion stress at the bottom of the web is given by (Figs.3.7 & 3.8)

$$\sigma_d = F_d = bv/2S \qquad (3.3.12)$$

At the top of the web the distortion stress is given by (Figs. 3.7 & 3.8)

$$\sigma_t = F_d = (a/2S)(b/a+b-v) \qquad (3.3.13)$$

In Equation (3.3.12) and (3.3.13), S is the section modulus of the web per unit length in the box span direction.

The change in distance between opposite corners of the cell caused by the deformation of the cross section is given by

$$\delta_b = 1/\sqrt{1+(a+b/2h)^2}\,.\,((a^3/12D_a)(b/(a+b)-v) + (abc/12D_c)(2a/a+b-v(1+2a/b)) \qquad (3.3.14)$$

or simply

$$\delta_b = 2(1+a/b)\,\delta_t/\sqrt{1+(a+b/2h)^2} \qquad (3.3.15)$$

This deformation quantity is used in the relation of bracing stiffness to cell stiffness.

3.5 ANALOGY TO BEAM ON ELASTIC FOUNDATION

As noted by Vlasov (23), the stiffness $\frac{1}{\delta_1}$ with which a box cell responds to a unit uniform deformation of the cross section may be linked to the stiffness k of an elastic foundation supporting an elastic beam . A long uniformly

loaded beam on elastic foundation ,Figures 3.10 & 3.11, has no axial stresses. In the analogy between the beam on elastic foundation and the deformable section box girder, the bending stresses in the beam are related to the warping stresses in the box girder,and the load on the B.E.F is related to the torsional load on the box girder.

The properties of the analogous B.E.F are defined from the box girder properties,E is the reference Young's modulus of Equation 3.3.1, I_b is approximated by one fourth of the transformed section moment of inertia of the box cell(25),I_c of equation (3.3.3),and $k= 1/\delta_1$,where δ_1 is given by equation (3.3.11). The beam foundation parameter β becomes,

$$\beta = \sqrt[4]{K/4EI_b} = \sqrt[4]{1/EI_c\delta_1} \qquad (3.4.1)$$

Using one fourth the moment of inertia of the box girder cell as I_b, the moment of inertia of the analogous B.E.F, give good results for normal bridge cell proportions(25).

The dimensionless stiffness of a flexible support of the B.E.F, q, is expressed by relating the support stiffness, Q k/in , to the stiffness k, k/in ,of the elastic foundation summed over support spacing ℓ

$$Q = qk\ell = 4q\beta\ell EI_b\beta^3 = q\beta\ell EI_c\beta^3 \qquad (3.4.2)$$

The B.E.F support stiffness analogous to the stiffness of a box girder diaphragm or cross bracing is obtained using the brace area A_b corresponding to one of a pair of actual braces, or to a plate diaphragm as given by Equation below (3.4.4), and the brace elongation δ_b of Equation (3.3.15). The brace stiffness is defined as the magnitude of concentrated torsional load which must act through the displacement δ_1 of Figure 3.9 to produce unit δ_1 when the cross section itself acts as a linkage.

$$Q = E_b A_b / L_b \, (\delta_b / \delta_1) \qquad (3.4.3)$$

where,

$$A_b = G_p t_p h^2 \; / \; E_b (a+b).(1+(a+b/2h)^2)^{3/2} \qquad (3.4.4)$$

or,

$A_b = G_p t_p L_b^2 / 2E_b A_p$

A_b = Cross sectional area of plate diaphragm

L_b = brace length

E_b = Young's modulus of brace

t_p = thickness of plate diaphragms

A_p = middle suraface area of a plate diaphragm

G_p = shear modulus of plate diaphragms

$$q = Q\delta_1/\ell = (E_b A_b / L_b)(\delta_b / \ell \delta_1) \qquad (3.4.5)$$

B.E.F solution for various loading and boundary conditions are plotted in Figure 3.12 - 3.14 (25).

For concentrated torsional loads the analogy is directly extended.The loading on the box girder is a force P acting up at one top node and an equal force P acting down at the adjacent top node. The analogous B.E.F is loaded by a single load P as shown in Figure 3.11. Figure 3.12 to 3.14 give dimensionless deflection w and dimensionless moment m for the B.E.F subjected to concentrated load.

$$w = 8EI_b\beta^3W/P = 2EI_c\beta^3W/P = 2W/P\beta\delta_1 \qquad (3.4.6)$$

$$m = 4\beta M/P \qquad (3.4.7)$$

Distortion stresses in the box girder subjected to concentrated torsional load are obtained by considering the deformed shape of the box girder to be the same for the same node deflection for uniform or concentrated torsional load. Distortion stress is given by the factor F_d of Equation (3.3.12) or (3.3.13) multiplied by W/δ_1 .

$$\sigma_t = F_d \cdot Pw/2EI_c\beta^3\delta_1 = 1/2\ F_d\beta Pw \qquad (3.4.8)$$

Warping stress in the box girder is computed from the moment in the analogous B.E.F

$$\sigma_\omega = My/I_b = Pym/I_c\beta \qquad (3.4.9)$$

Theoretical values of bending and shear stresses were computed for concentric and eccentric loading using the fundamental flexural formula and shear formula. The deflec-

tion is computed as the sum of bending and shear deflections as computed from elastic theory for concentric loading.

3.6 SAMPLE CALCULATION

In this sample calculation, the distortion and warping stresses were computed by inserting diaphragms at selected locations in the box girder. Since the testing program was divided into three major parts (illustrated in detail in section 4.7 and Table-1) the corresponding theoretical values are calculated for the above three cases (case-I, case-II and case-III).

The cross section for a trapezoidal box girder having a span length of 46 inches (1168mm) is shown in the following figure. The actual dimensions of the model are used for this calculation.

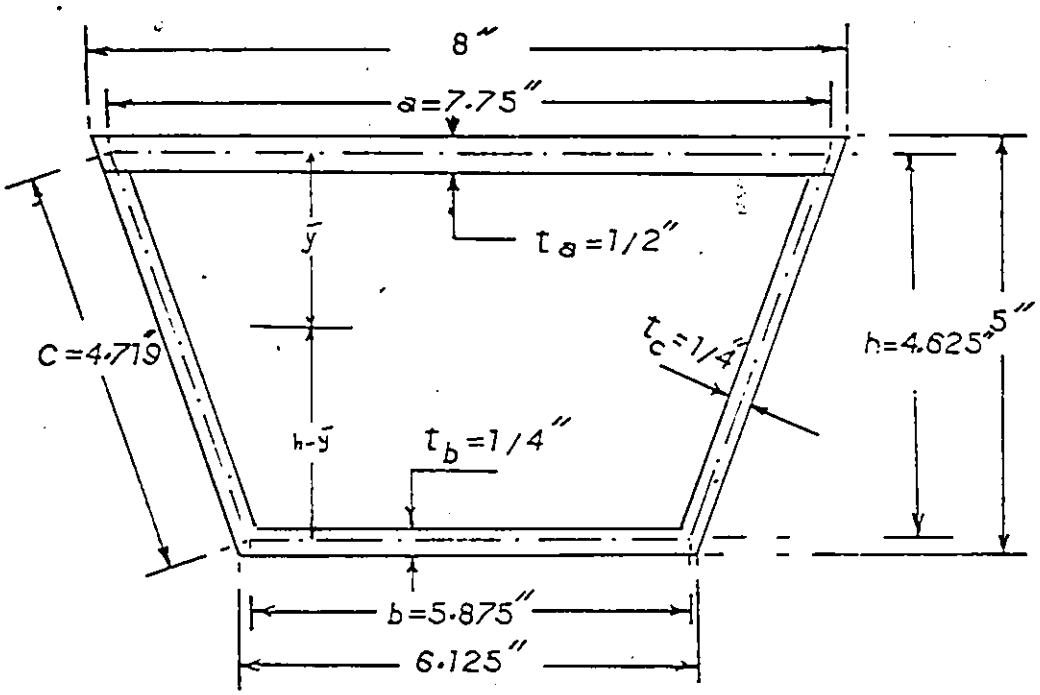

The cell dimension in the above figure are

a = 7.75 in.(197mm)

b = 5.875 in.(149mm)

c = 4.719 in.(120mm)

h = 4.625 in.(118mm)

t_a = 1/2 in.(12.7mm)

$t_b = t_c$ = 1/4 in.(6.4mm)

E = 0.440×10^6 psi(3.03×10^9 N/m²)

ν = 0.37

The various B.E.F analogy parameters have been calculated as follows.

Using the B.E.F Equation 3.3.1, the cross sectional area of box girder cell is

$$A = at_a + 2ct_c + bt_b$$

$$= 7.75 \times 0.5 + 2 \times 4.719 \times 0.25 + 5.875 \times 0.25$$

$$= 7.70 \text{ in.}^2 \ (4.97 \times 10 \text{ mm}^2)$$

The centroid is located at a distance $\bar{Y}$ below the top flange middle surface (Eq. 3.3.2) as shown in the previous figure

$$\bar{Y} = (h/A)(bt_b + ct_c)$$

$=(4.625/7.703)(5.875x0.25+4.719x0.25)$

$=1.59$ in.$(40.4mm)$

Moment of inertia of the cell, neglecting terms involving squared is (using Eq.3.3.3)

$$I_c = at_a\bar{Y}^2+2ct_c(h^2/12+(h/2-\bar{Y})^2+bt_b(h-\bar{Y})^2$$

$$=7.75x0.5x(1.59)^2+2x4.719x0.25((4.625)^2/12$$
$$+(4.625/2-1.590)^2)+ 5.875x0.25(4.625-1.590)^2$$
$$= 28.76 \text{ in.}^4 \ (1.20x10^7 \text{ mm}^4)$$

The transverse flexural rigidity is (Eq.3.3.9).

$$D= Et^3/12(1-\nu^2)$$

$$D_a/D_c = t_a^3/t_c^3 = (0.50)^3/(0.25)^3$$
$$=8.000$$

$$D_c/D_a = (0.25)^3/(0.50)^3 = 0.125$$

The redundant shear normal to the middle surface of the bottom flange is (using Eq. 3.3.8)

$$v =(1/D_c)((2a+b)abc)+(1/D_a)(ba^3)/(a+b)((a^3/D_a$$
$$+(2c(a^2+ab+b^2)/D_c+b^3/D_b)$$
$$=((2a+b)abc)+(D_c/D_a)(ba^3)/(a+b)((D_c/D_a)a^3$$
$$+(c(a^2+ab+b^2))+(D_c/D_b)b^3)$$
$$=((2x7.75+5.875)7.75x5.875x4.719)$$

$+0.125(5.875x(7.75)^3)/$

$(7.75+5.875)(0.125(7.75)^3+(2x4.719((7.75)^2$

$+7.75x5.875+(5.875)^2)+(5.875)^3)$

$= 0.23$

The vertical deflection for unit torsional load is (Eq.3.3.11)

$$\delta_1=ab/24(a+b)\ x(c/D_c)((2ab/a+b-v(2a+b))$$
$$+(a^2/D_a)(b/a+b-v))$$

where,

$D_c=440x(0.25)^3/12(1-0.37^2)$

$=0.664$ k-in.(72.75 N-m)

$D_a=440x(0.50)^3/12(1-0.37^2)$

$=5.310$ k-in. (599.85 N-m)

$\therefore \delta_1=7.75x5.875/24(7.75+5.875)$

$x\ (4.719/0.664)(2x7.75x5.875/$

$7.75+5.875\ -0.2287(2x7.75+5.875)+((7.75)^2/5.310)$

$(5.875/7.75+5.875\ -0.2287))$

$=2.10\ in^2/k$ (304.6mm^2/KN)

The brace elongation for unit torsional load is (Eq. 3.3.15)

$\delta_b = 2(1+a/b) \times \delta_1 / \sqrt{1+(a+b/2h)^2}$

$= 2(1+7.75/5.875) \times 2.0957$

$/ \sqrt{1+(7.75+5.875/2\times 4.625)^2}$

$= 5.46$ in.^{2}/k (791.95 mm^2/KN)

Area of brace(Equation 3.4.4)

$A_b = G_p t_p (L_b)^3 / 2E_b A_p$ $\quad G/E = 1/2(1+v) = 0.364$

where,

t_p =thickness of plate diaphragm =0.25 in.

$L_b = \sqrt{(4.625)^2+(6.8125)^2}$

=8.24 in.(209.3mm)

$A_b = 0.364 \times 0.25 \times (8.234)^3 / 2 \times (7.75+5.875/2) \times 4.25$

=.88 in.^{2}(567.74mm^2)

By using Equation 3.4.5

$q\ell/A_b = E\delta_b / L_b \delta_1 = 0.440 \times 10^3 \times (5.46)^2 / 8.234 1 \times 2.0957$

$= 760.10$ in^{-1}.(29.9mm^{-1})

The B.E.F parameter β may be calculated by using Equation 3.4.1

$\beta = \sqrt{1/EL\delta_1} = \sqrt{1/0.440 \times 10^3 \times 28.763 \times 2.0957}$

=0.078 in^{-1}.(0.003 mm^{-1})

Using Equation 3.4.9

$\sigma_\omega/Pm = Y/I_c\beta$,where Y is the distance from the bottom flange to the neutra axis.

$\sigma_\omega/Pm = Y/I_c\beta = 3.035/28.763x0.0784$

$= 1.35\ in^{-2}\ (0.002mm^{-2})$

$S = t^3/6 = (0.25)^3/6$

$= 1.042x10\ in^3/in.$

The factor F_d for distortion stress at bottom of web is (Eq. 3.3.12)

$F_d = bv/2S$

$= 5.875x0.2287/2x1.042x10$

$= 64.49\ in^{-1}\ (2.54mm^{-1})$

Equation 3.4.8

$\sigma_t = 1/2\ F_d\beta\ P\ w$

or, $\sigma_t/P_\omega = 1/2\ F$

$= 1/2x64.4934x0.0784$

$= 2.53\ in^{-2}(0.004mm^{-2})$

The factor F_d for distortion stress at top of web is (Eq. 3.3.13)

$F_d = a/2S(b/a+b-v)$

$= 7.75/2x1.042x10(5.875/7.75+5.875 -0.2287)$

$= 75.30\ in^{-1}\ (2.96mm^{-1})$

Using Equation 3.4.8

$\sigma_t/Pw = 1/2\ F_d\beta$

$=1/2x75.3032x0.0784$

$=2.95\ in.^{-2}\ (0.005mm^{-2})$

SUMMARY OF B.E.F PARAMETERS

Parameters	Equation	Results
A, in in^2 (mm^2)	3.3.1	7.70 ($4.97x10^3$)
I_c, in in^4 (mm^4)	3.3.3	28.76 ($1.20x10^7$)
$h-\bar{Y}$, in in (mm)	3.3.2	3.04 (77)
v	3.3.8	0.23
δ_t, in in^2/K (mm^2/KN)	3.3.11	2.10 (304.61)
δ_b, in in^2/K (mm^2/KN)	3.3.15	5.46 (791.95)
α, in in^{-1} (mm^{-1})	3.4.1	0.078 (0.003)
ql/A_b, in in^{-1} (mm^{-1})	3.4.5	760.10 (29.9)
S, in in^3/ in (mm^3/mm)		1.04x10 (170.42)
σ_c/Pw, in in^{-2} (mm^{-2}) bottom	3.4.8	2.53 (0.004)
σ_t/Pw, in in^{-2} (mm^{-2}) top	3.4.8	2.95 (0.005)
σ_ω/Pm, in in^{-2} (mm^{-2})	3.4.9	1.35 (0.002)
A_b, in in^2 (mm^2)	3.4.4	0.88 (567.74)

The bending stresses at the bottom flange were computed for loading 123.8 pounds (550.66 N) using the fundamental flexural formula and given in the following table.

Location	Calculation	Results in psi (N/m)
Load at A measure at A 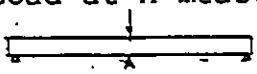	123.8x46x3.04/4x28.76	350.22 (1.04×10^6)
Load at B measure at B 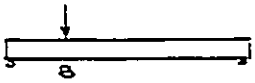	123.8x37.5x8.5x3.04/46x28.76	90.52 (6.24×10^5)
Load at A measure at B 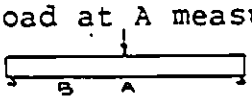	123.8x8.5x3.04/2x28.76	55.52 (3.83×10^5)
Load at B measure at A 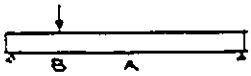	123.8x8.5x23x3.04/46x28.76	55.52 (3.83×10^5)

CALCULATION OF DISTORTION & WARPING STRESSES -

	ℓ in (mm)	$\beta\ell$	A_b in in (mm)	q	Stresses for concentratd torsional load				
					Distortion			Warping	
					Location	w Fig. 3.13	σ_E psi (N/m²)	m Fig. 3.14	σ_w psi (N/m²)
CASE-I	46 (1168)	3.6	.88 (567.7)		B.of Web	1.16[a]	181.53 (125×10^6)	1.06	88.30 (6.09×10
					T.of Web		211.96 (1.46×10^6)		
					B.of Web		83.62 (5.77×10^5)		75.11 (5.18×10
					T.of Web		97.64 (6.73×10^5)		
CASE-II	12 (305)	.94	.88	55.32	B.of Web	0.15	23.47 (1.62×10^5)	0.68	56.65 (3.91×10^5)
					T.of Web		27.41 (1.89×10^5)		
	17 (432)	1.33	.88	39.05	B.of Web	0.26	40.69 (2.81×10^5)	0.80	66.65 (4.6×10^5)

continued

				T.of Web		47.51 (3.28x10)			
CASE-III									
5 (127)	0.39	.88	132.76	B. of Web	0.035	5.48 (3.78x10^4)		0.36	29.99 (2.07x10^5)
				T.of Web		6.4 (4.41x10^4)			
8 (203)	0.63	.88	82.97	B.of Web	0.07	11.03 (7.6x10^4)		0.49	4.82 (3.32x10^4)
				T.of Web		12.88 (8.88x10^4)			

a Fig. 3.12

DETERMINATION OF STRESSES AT GAGE LOCATION

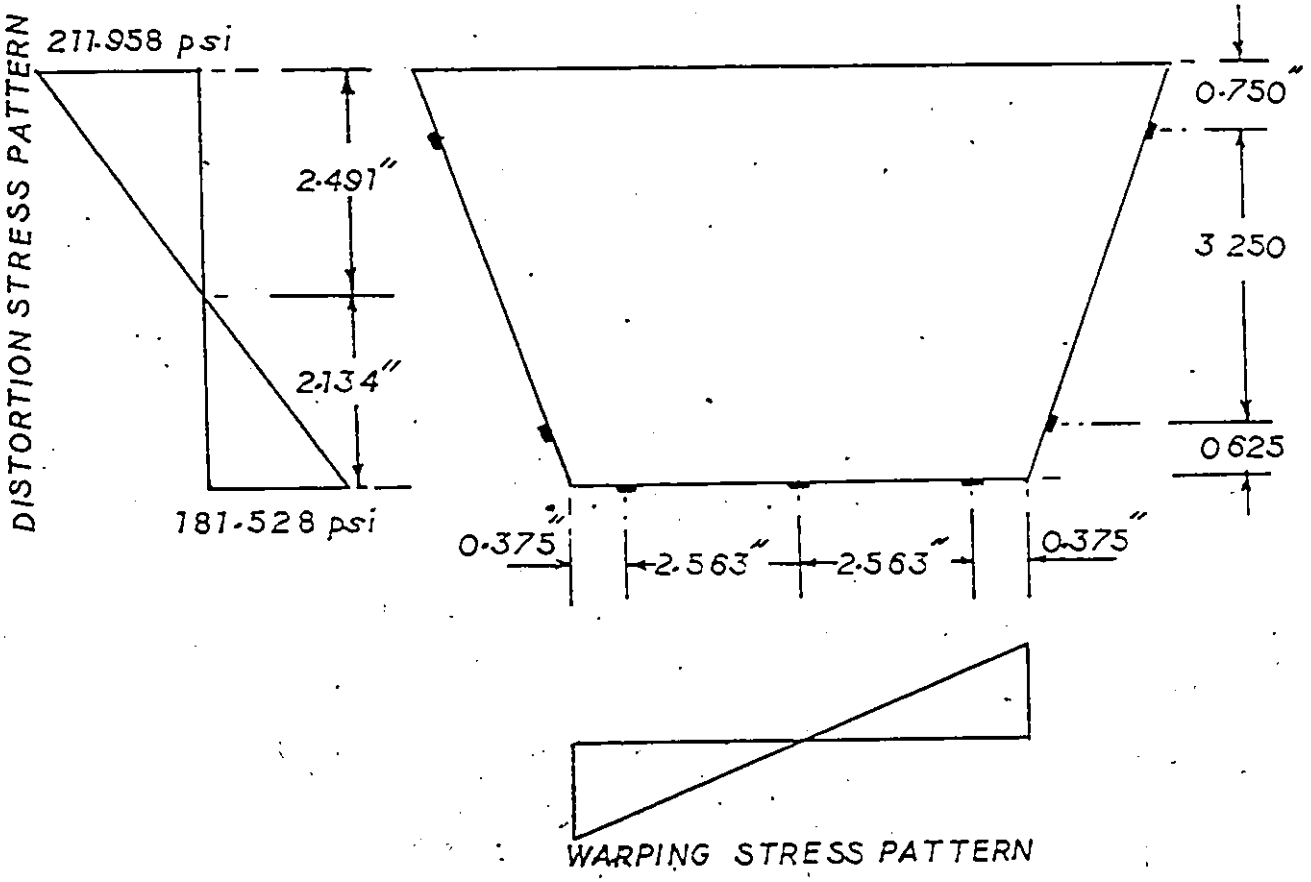

Distortion stress at lower gage location

= 1.5087xExtreme fiber stress/2.1337

= 0.707x EFS

Distortion stress at upper gage location

= 1.7413x Extreme fiber stress/2.4913

= 0.699x EFS

Warping stress at outside gage location

= 2.5625x Extreme fiber stress/2.9375

= 0.872x EFS

Summary of Theoretical stresses at gage location

(P=123.8 #(550.66N), Maximum Eccentricity)

Values in brackets are in N/m

CASE I	LOAD AT A	LOAD AT B
1)Distortion stress at lower gage location	128.34 psi (8.85×10^5)	59.12 psi (4.08×10^5)
2)Distortion stress at upper gage location	148.16 psi (1.02×10^5)	68.25 psi (4.71×10^5)

continued

3)Warping stresses	77.00 psi (5.31×10)	65.49 psi (4.52×10)
CASE II		
1)distortion stress at lower gage location	15.93 psi (1.10×10^{5})	28.76 psi (1.98×10^{5})
2)Distortion stress at upper gage location	18.392 psi (1.27×10^{6})	33.21 psi (2.29×10^{5})
3)Warping stresses	49.396 psi (3.41×10^{5})	58.64 psi (4.04×10^{5})
CASE III		
1)Distortion stress at lower gage location	3.87 psi (2.67×10^{4})	7.80 psi (5.38×10^{4})
2)Distortion stress at upper gage location	4.52 psi (3.12×10^{4})	9.04 psi (6.21×10^{4})
3)Warping stresses	26.15 psi (1.80×10^{5})	35.59 psi (2.45×10^{5})

Computation of Deflection by elastic theory ,for concentric loading.

$$\Delta = PL^3/48EI(1+12\alpha_s EI/GAL^2)$$

Where,

$E = 0.440 \times 10^6$ psi

$I = 28.763$ in.^{4}

$A = 7.7033$ in.^{2}

$G = E/2(1+\nu) = 0.161 \times 10^6$ psi

$\alpha_s = A/A_w = 7.7033/2.36 = 3.265$

$L = 46$ in.

$\Delta = (P \times (46)^3/48 \times 0.440 \times 10^6 \times 28.763)(1+12 \times 3.265 \times 0.440 \times 10^6 \times 28.763 / 0.161 \times 10^6 \times 7.7033 \times (46)^2)$

$= 1.905 \times 10^{-4} \times P$ in.

For loading 120# $= 0.0229$ in.

Chapter IV

EXPERIMENTAL PROGRAM

4.1 INTRODUCTION

The experimental program was limited in scope to tests on two different types of cross sections single cell box girder fabricated from plexiglas. The static loads, which were applied normal to the compression flange of the box girder, were kept small so that the strains in the plexiglas models were within the elastic range.The models were designed so that the shape of the cross section would be distorted under the test loads, thus resulting in warping and distortion stresses of easily measurable magnitudes.

The purpose of this investigation was to confirm experimentally that deformation of the cross section of a box girder induces an appreciable amount of warping and distortion stresses and that these stresses can be substantially reduced by inserting rigid diaphragms at selected location. The entire experimental program,including the determination of material properties,establishment of experimental technique for plexiglas,design and fabrication of model,test set-up,test measurements and the test program,was

designed with this goal in mind. The experiment was conducted on two different types of cross section as shown in Figures 4.1 and 4.2. Later the results were compared with values obtained from the so called " B.E.F analogy",an approximate analytical method of box girder analysis which considers the stresses caused by warping and distortion.

4.2 DETERMINATION OF MATERIAL PROPERTIES

Before any meaningful model tests could be conducted, certain physical properties had to be determined for the model material. The literature indicates that more accurate results may be obtained if the modulus of elasticity of each model component is determined rather than relying on the results of tests on an isolated coupon. Therefore two tensile coupons from the model shown in Fig.4.1 and Fig 4.2 corresponding to the top flange and web/bottom flange , was fabricated and tested. In all cases the coupons were cut from a piece of plexiglas adjacent to the component they represented, Fig.4.3. It was found that the modulus of elasticity for all model component differ by approximately 10 percent.

The dimensions of a typical coupon is shown in Fig.4.3. Two holes of 1/4 in.(6.4mm) were made at the ends of the coupon. One end was hung by means of a 3/8 in.

(9.5mm) diameter bar and at the other end static loads were applied at increments of 20 pounds (88.96N) and 10 pounds (44.48N) for 1/2 in. (12.7mm) and 1/4 in.(6.4mm) thick coupons respectively. The coupon test set-up are shown in Fig.4.4. A typical stress-strain curve is shown in Fig.4.5 and Fig.4.6 for model one and model two respectively. The tests were repeated with nearly identical results. The value of $E=0.440\times10^{6}$ psi (3.03×10^{9} N/m^2) and $E=0.485\times10^{6}$ psi (3.34×10^{9} N/m^2) were found for models one and two respectively.

4.3 EXPERIMENTAL TECHNIQUES

It is known that plexiglas is a poor heat conductor. The heat input during the warming up of a strain gage is not immediately dissipated as in the case of metals, but contributes to an added local deformation. To overcome this problem, a procedure was developed in which each gage was alloted the same amount of time to warm up. In all cases the current was applied to each gage for exactly five minutes before reading the gage. Readings were taken at 20 pound (88.96N) load increments.

4.4 MODEL DESIGN

The experiments were conducted on two box girder models having a length of 48 in. (1219mm) and cross sections shown in Figure 4.1 and Figure 4.2 As stated in preceding sections, the models were designed so that there would be substantial deformation of the cross section when no interior diaphragms were used. Since the calculated distortion stresses were much larger than the corresponding warping stresses for a given torsional loading, the models were designed so that the smaller warping stresses would be sufficiently large to be measured at anticipated load levels. A peak ratio of warping to bending stresses of one-half was used as design criteria for model one and 0.43 for model two.

A maximum load of 120 pounds (533.76N) was chosen so that the peak bending plus warping stress would not exceed the elastic range of the plexiglas. The material properties test had indicated that plexiglas behaves elastically up to 400 psi (2.76×10^6 N/m^2); which is compatible with previous experiments (38). Actually some extreme fibers may have been subjected to stresses slightly above the yield point due to the unequal distribution of the warping stress across the bottom flange (Fig.5.27).

A detachable top flange (Fig4.7) was used to permit the installation of interior diaphragms for the later tests. The top flanges were fastened to the webs with NO.4 screws at 2 in.(50.8mm) center to center for model no.1 and NO.6 screws at 1 in.(25.4mm) center to center for model no.2. This fastening method has been shown to result in adequate shear transfer to develop full composite action . After fastening the top flange to the webs, the bottom flange and end diaphragms were cemented into place with Ethylene Dichloride, a plexiglas solvent cement that is easy to use and produces medium strength joints. After the application of ethylene dichloride,Tensol No.6 was used to produce stronger joints. When interior diaphragms were needed for later tests, the top flange was removed to permit cementing/screwing them into position. In model no.1 the interior diaphragms were cemented into position with ethyline dichloride and Tensol No.6 while in model no.2 the interior diaphragms were screwed in position.

4.5 TEST SETUP

For all of the tests the box girder models were supported on the rounded surfaces of steel bearing blocks spaced 46 in.(1168.4mm) center to center (Fig.4.7 and Fig.4.8). These blocks were bolted to two 7 in.(177.8mm) diameter and 30 in. (762mm) height concrete base. The load

was transmitted by means of special hanger as shown in Figure 4.7 to the model by a 1 in. x 1/2 in. (25.4x12.7mm) steel bearing block.

4.6 TEST MEASUREMENTS

Static loads were applied manually to the box girder models by means of a specially designed hanger. Loads were applied to the model with an increment of 20 pounds (88.96N) from 0-120 pounds (0-533.76N) plus the weight of hanger which was 3.8 pounds (16.9N). All load readings were taken when the strain indicator readings were steady. The model was located in a temperature controlled room.

Since the warping stresses are maximum under the load point, strain were measured at the loaded sections with KFC-5-C1-11 and KFC-10-C1-11 gages. These gages were mounted at the locations indicated in Figure 4.9 to Figure 4.12 using Bean CA-200SL adhesive. The gages on the webs were used to measure the transverse strains (corresponding to the distortion stresses) while the gages on the flanges were used to measure longitudinal strains. The measured longitudinal strains include both bending and warping strains . For concentric loading the longitudinal strains were due to bending only, and thus the experimental flexural strains could be determined. With eccentric loading the difference

between the flexural strains and the measured strain in the flanges could be directly attributed to warping. Hook's law was used to convert the strains to stresses. The value of Young's modulus of elasticity were taken to be 0.440×10^6 psi and 0.485×10^6 psi for (3.03×10^9 N/m^2 and 3.34×10^9 N/m^2) for models no.1 and 2 respectively as determined from material properties tests.

A BLH Electronic,Inc. ,model 1200B, digital strain indicator in conjunction with a BLH Electronic,Inc., model 1225 switching and balancing unit was used to measure the strains.

Throughout the model testing all load cycles were repeated so that the strain gages and instruments could be checked. The maximum deviation between the strains of two test cycles was 20×10^{-6} in./in., while in most cases the strain were reproduced exactly. Considering the problems inherent with plexiglas, this small discrepancy is considered to be within the accuracy of the strain measuring equipment and the procedures used.

Dial gages, located at midspan and shown in Figures 4.9 and 4.11, were used to measure vertical deflections of the models due to both concentric and eccentric loadings. This data proved valuable in establishing the distortion patterns of the cross section (Fig.4.13c). Such patterns

were used to verify the signs of the distortion stresses at various points on the cross section.

4.7 TEST PROGRAM

The testing program was divided into three major parts. Initially for case I, the model contained only the end diaphragms. The load ranging in 20 pounds (88.96N) increments from 0-120 pounds (0-533.76N), was applied at two cross sections (one at midspan and the other at 8.5 in.(216mm) from support) as shown in Figure 4.14 and separately at three points across each cross section (Fig.4.15). Strains were measured at various points on cross sections A and B (Fig.4.9,4.10,4.11 and 4.12)for all of the loads on each of the six load locations.

For case II,two interior diaphragms were inserted (Fig.4.14,4.16) and for case III four more interior diaphragms were placed in the models (Figs.4.14,4.17 and 4.18). The same loading and measuring procedures were employed as in case I. Table-I summarizes the load and diaphragm locations which were used in the program.

Chapter V

TEST RESULTS

The graphical presentation of the data from the test program is given on Figures 5.1 to 5.33.These results can be divided conveniently into four sections:

1) Deflections
2) Bending stresses
3) Distortion stresses
and 4) Warping stresses.

A general discussion of the results, including qualitative and quantitative comparisons with theory and explanations of any discrepancies is presented in this chapter.

5.1 DEFLECTIONS

Deflections at midspan due to loadings at midspan were recorded by two dial gages as shown in Figures 4.9 and 4.11. The average value of the dial gage reading was compared to the sum of the bending and shear deflections as computed from elastic theory, for concentric loading. The

experimentally determined deflections are somewhat higher than those predicted from theory for both models (Fig.5.1-5.9). This discrepancy can be attributed to the stress relaxation that occurred before the dial readings were recorded. The two dial readings were almost identical for concentric loading because there was no deformation or twisting of the cross section (Fig.4.13c)

When eccentric loads are applied to a model, two types of cross section deformation were possible in addition to that observed for concentric loading. The first is the rigid body rotation where the cross section is not deformed (Fig.4.13b). The second type of motion is the deformation of the cross section as shown in Figure 4.13c.

With eccentric loads the deflection of one edge of the cross section increases approximately as much as the other side decreases relative to that for concentric loadings as shown in Fig.5.4 for model no.1 and Fig.5.7 for model no.2. In case II and case III (Figs.5.5,5.6 for model no.1 and 5.8,5.9 for model no.2) there is not as much difference between deflection caused by concentric and eccentric loadings as there is in case I. This is an indication that additional diaphragms tend to decrease the deformation of the cross section.

5.2 BENDING STRESSES

The bending stresses in the bottom flange due to concentric loading were checked with theoretical values to give an indication of the effectiveness of the strain gages and the experimental techniques. The average of the gage readings was used to represent the strain in the extreme surface of the bottom flange plate.

There appreared to be a shear lag (39) on the bottom flange at the loaded cross section. The longitudinal stresses across the bottom flange for concentric loading were not linear as conventional beam theory predicts (Fig.5.10). It may be hypothesized that a short distance away from the load the stress distribution would approch linearity. The average of the flexural stresses for all of the gage locations on the bottom flange was compared with simple beam theory. In general the results were reasonably close regardless of the diaphragm locations. Therefore the comparison for case I only is shown in Figures 5.11-5.14.

From these results it was concluded that the gages were working properly and the girder was acting as a composite section.

5.3 DISTORTION STRESSES

The evaluation of distortion stresses was accomplished by subtracting the stresses measured by the transverse web gages due to concentric loading from those due to eccentric loading.

Distortion stresses measured in sections A and B for both the models were compared with theoretical values obtained from the B.E.F analogy. Only distortion stresses at the loaded cross section are plotted because the stresses were negligible at the other section that was gaged. The signs of these stresses were consistent with the deformation pattern (Fig.4.13c). It is also readily seen from a comparison of Figures 5.15-5.26 that diaphragms are quite effective in reducing distortion stresses.

As can be observed, the distortion stresses at the bottom and top of the webs are generally in good agreement with the B.E.F theory for both the models.

The ratio of the distortion stress caused by medium eccentric loading to that due to maximum eccentric loading varied from 20-70 percent for model no.1. This ratio should always be half according to theory. The largest variation occurred in the gage near the top of the web which

could be explained by the fact that the stresses were so small at these positions that a minor difference could be easily magnified out of proportion. In model no.2, the ratio between medium eccentric loading to maximum eccentric loading varied from 45 - 60 percent, this model shows good agreement with theory.

5.4 WARPING STRESSES

The experimental warping stresses were determined by subtracting the flange stresses due to concentric loading from those obtained when the model was loaded eccentrically. However the warping stresses at the loaded cross section are not exactly linear across the bottom flange as B.E.F theory predicted (Fig.5.27). A possible explanation of this observation can be that there is a shear lag caused by shear deformation at the point of loading, and that a short distance away the warping stress pattern becomes linear. In an effort to verify this interpretation, the warping stresses were measured at cross section B when load was applied at cross section A. These values appeared to be linear, but they were too small in magnitude to formulate a firm conclusion. In the comparison with the B.E.F. analogy, the average of the stresses was used.

The warping stresses at A due to load at A (Fig.5.28-5.30) are somewhat higher than predicted by the B.E.F. theory. However,the panel under consideration is assumed to be restrained by adjacent panels at each end when in reality it is not.

When the models were loaded and stresses were measured at B (Fig.5.31-5.33) the experimental and theoretical stresses are generally in good agreement with the B.E.F theory for both the models.

The ratio of the experimental warping stresses caused by medium eccentric loading to that due to maximum eccentric loading were quite close to half, which agreed well with the theory.

Experimental results for the reduction of distortion and warping stresses have been summarized in Table-2 and Table-3 for model no.1 and 2 respectively. From these tables it is evident that the interior diaphragms are more effective in reducing the distortion stress than the warping stress. The maximum warping stresses at A for load at A for model no.1 was approximately 60 percent of the maximum flexural stress at this point, and the maximum warping stress at B for load at B was nearly equal to the flexural stress. For model no.2 the maximum warping stress at A for load at A

was approximately 41 percent of the maximum flexural stress at this point, and the maximum warping stress at B for load at B was also nearly equal to the maximum flexural stress at this point. Thus it would appear to be inadvisable to ignore completely the stresses induced by deformation of the cross section for a prototype having the same general dimensions as the models under consideration.

Chapter VI

CONCLUSIONS

The following conclusions were substantiated in this experimental investigation. All of the conclusions apply only to conditions as specified in the scope of the study.

1) The effect of deformation of the cross section induced substantial warping and distortion stresses in model box girders. Thus for model dimensions and test conditions under consideration, it would seem to be inadvisable to employ design procedures that do not account for deformation of the cross section.

2) Diaphragms are much more effective in controlling distortion stress than in controlling warping stress. The distortion of the cross section of a box girder without intermediate diaphragms is more prominient when loaded along the side joints. When the diaphragms are sufficiently far from the applied loads, the distortion stress remain practically the same, but is considerably reduced when the diaphragms is near the loads. The use of intermediate diaphragms decreases effectively cross section distortion

throughout the span. Thus in design process it would seem reasonable to space diaphragms to control distortion stresses and then check warping stresses.

3) The distortion and warping stresses determined from the B.E.F theory agreed well with the experimental stresses although the magnitude varied somewhat.

4) The tension flange stresses and midspan deflections of a concentrically loaded box girder model can be predicted fairly accurately using simple beam theory including the shear deflections.

5) Plexiglas can be a very effective model material if the proper experimental techniques are employed.

6) It is observed from table 2 and 3 that the maximum decrease in magnitude of distortion and warping stresses occurs when diaphragms are introduced at a spacing of L/4. Any further decrease in spacing does not appreciably reduce the stresses any further. Hence a spacing of L/4 is recommanded for the purpose of design.

FIGURES

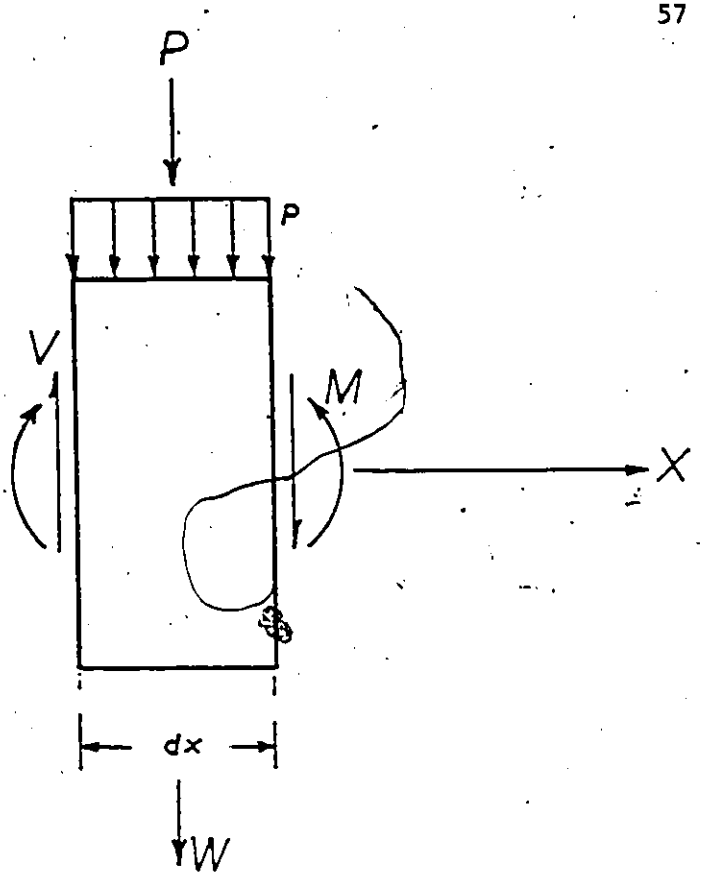

FIG.3.1 SIGN CONVENTION FOR BEAM ON ELASTIC FOUNDATION

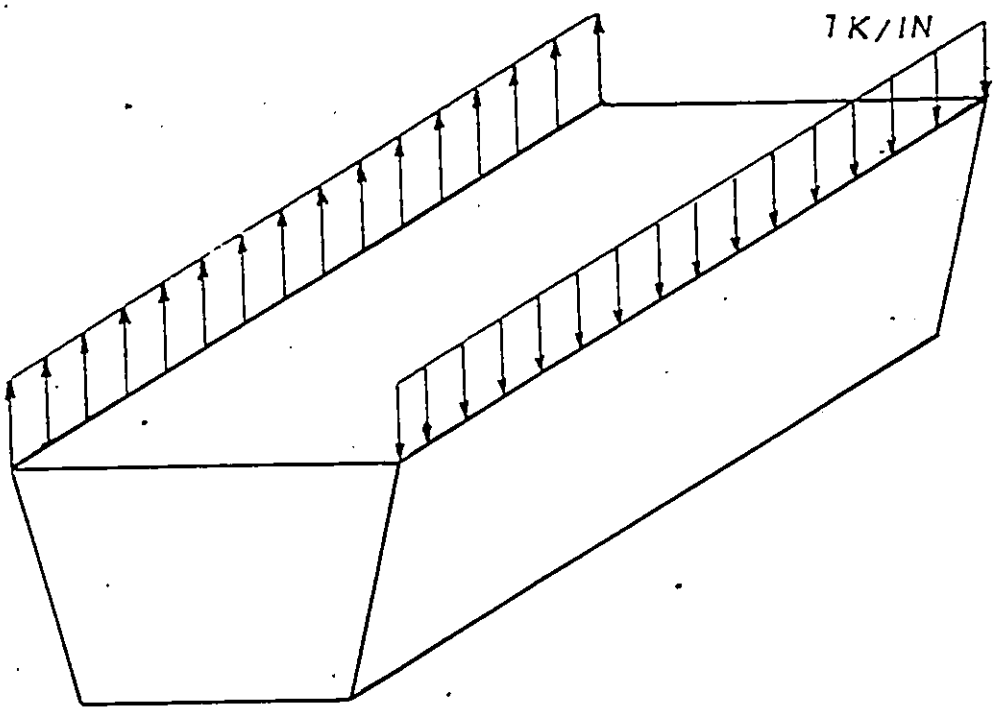

FIG.3.2 SEGMENT OF BOX LOADING

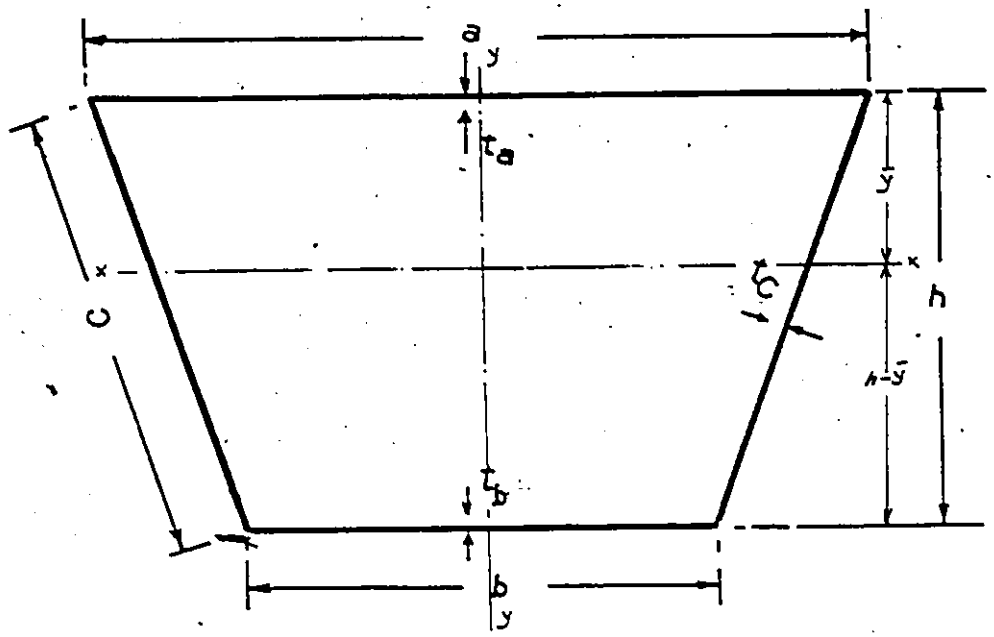

FIG.3.3 NOTATION FOR DIMENSION

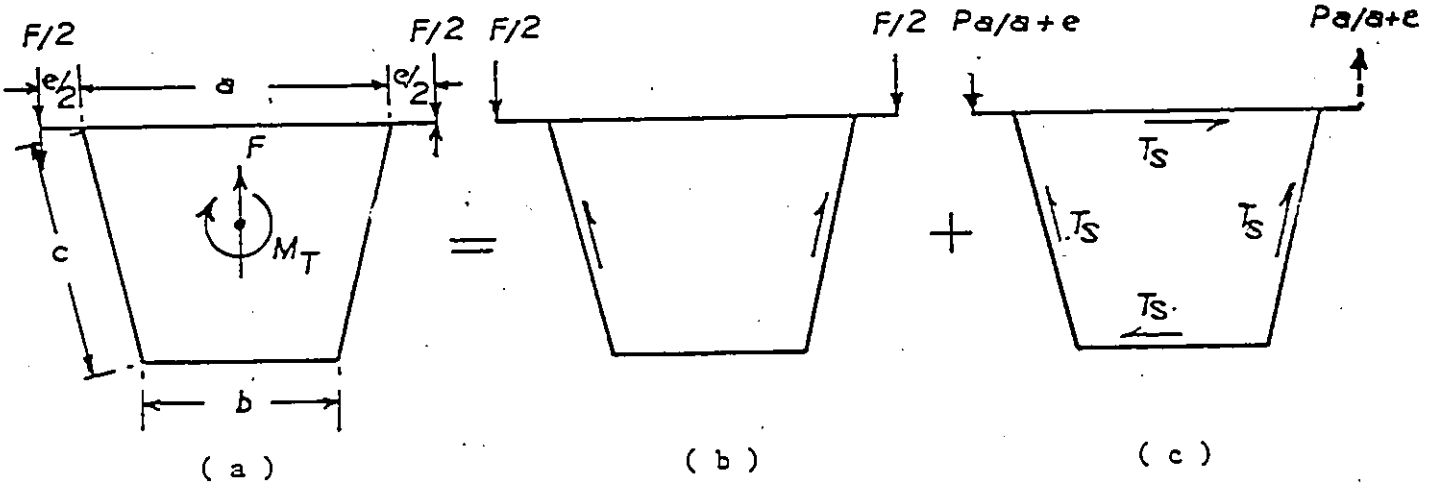

FIG.3.4 FORCES ACTING ON DECK WITH CLOSED RIB

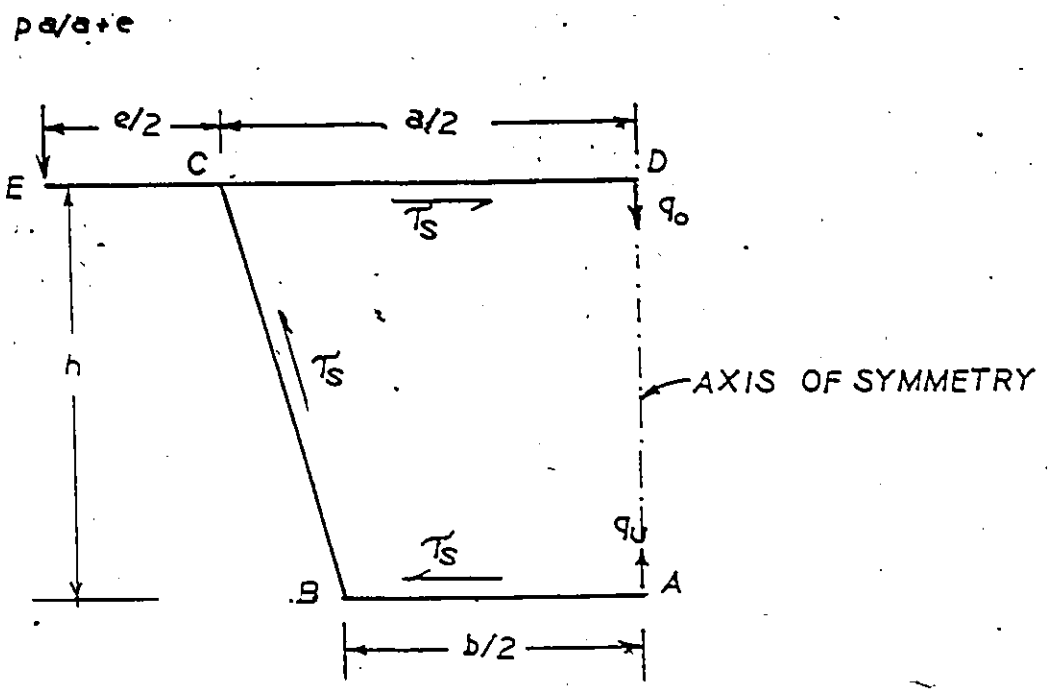

FIG.3.5 SHEAR FLOW IN DECK WITH TRAPEZOIDAL RIBS

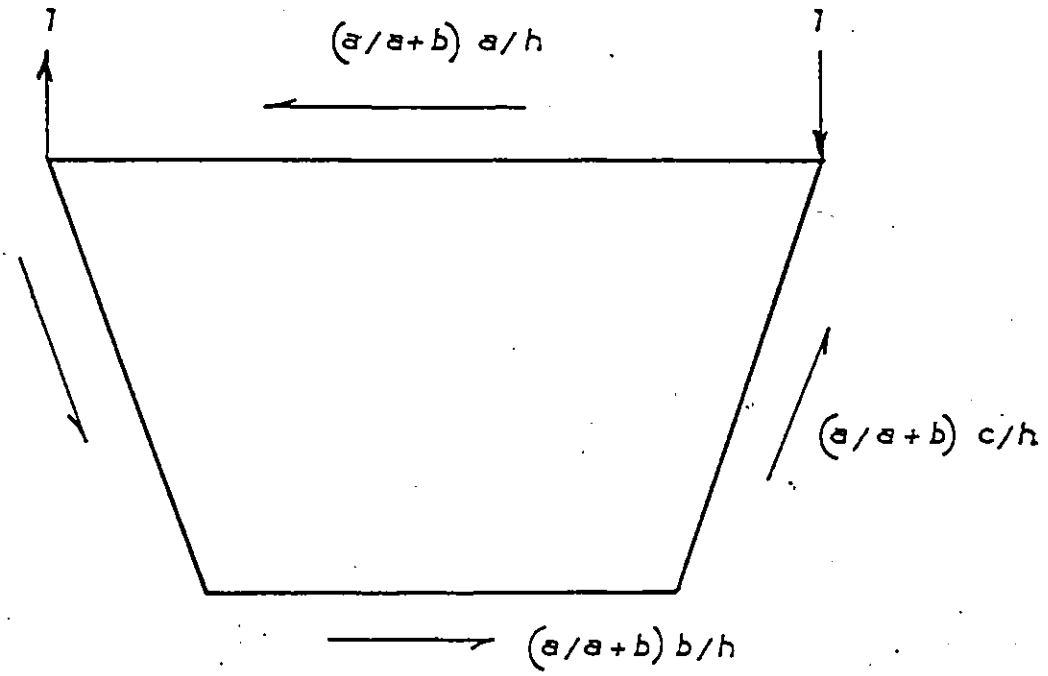

FIG.3.6 SHEAR FLOW GRADIENT

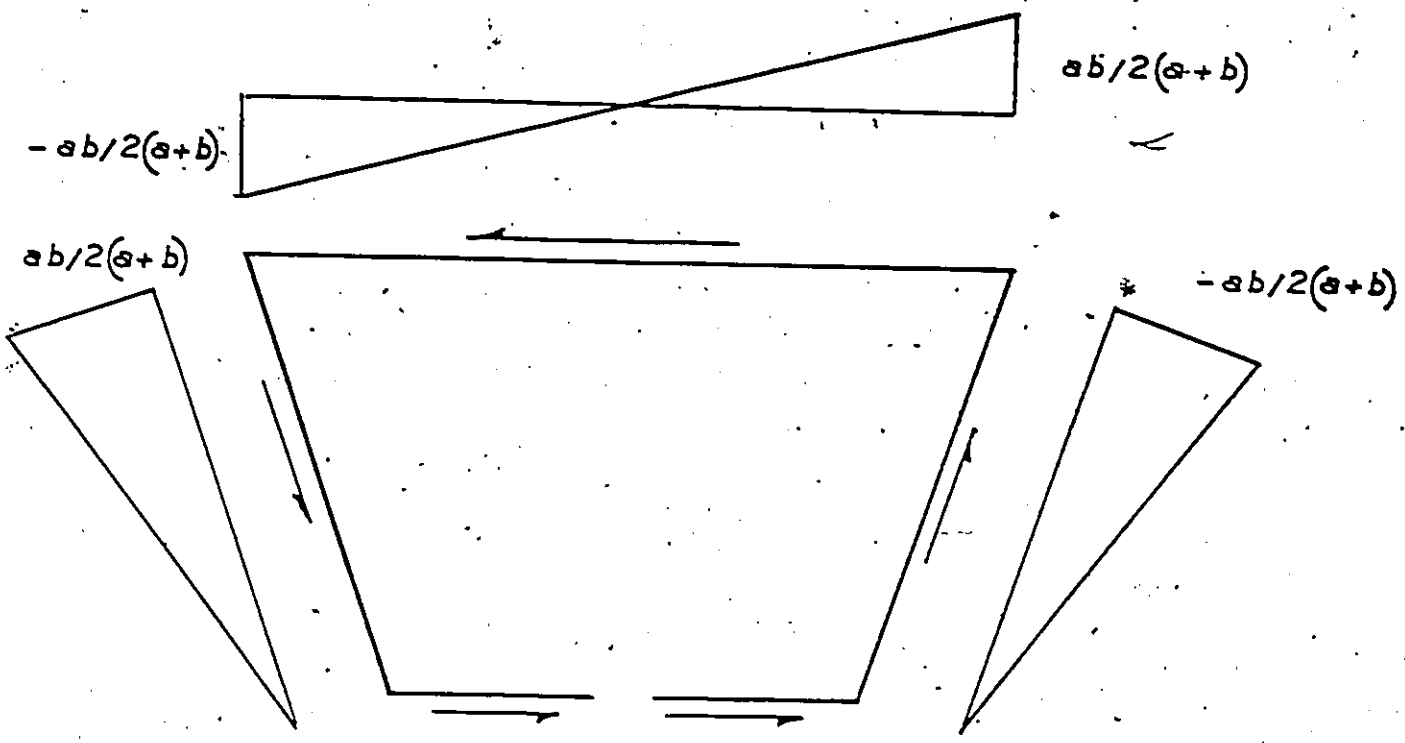

FIG.3.7 MOMENTS IN PRIMARY STRUCTURE INDUCED BY SHEAR FLOW GRADIENT

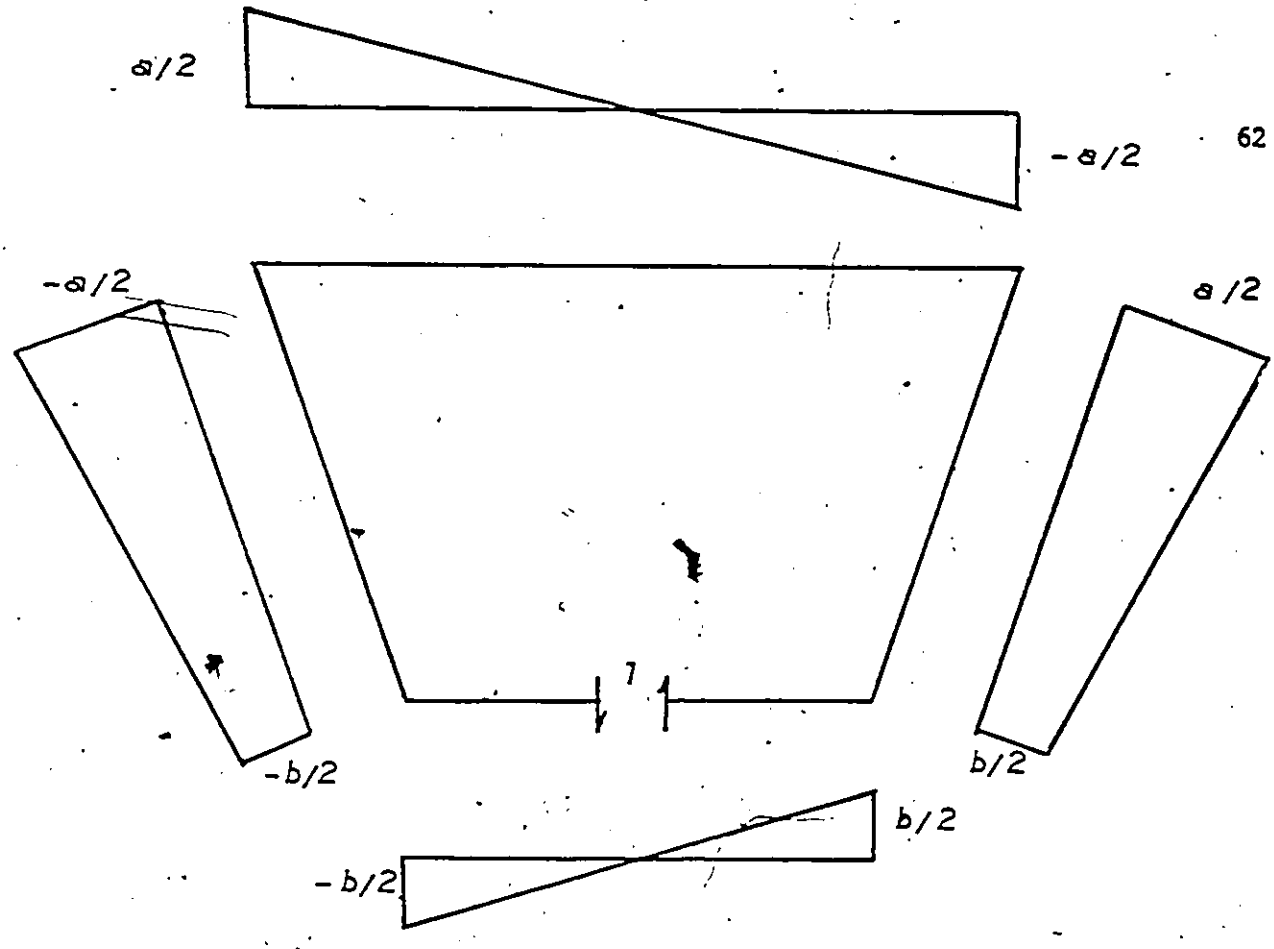

FIG.3.8 MOMENTS FOR UNIT REDUNDANT SHEAR

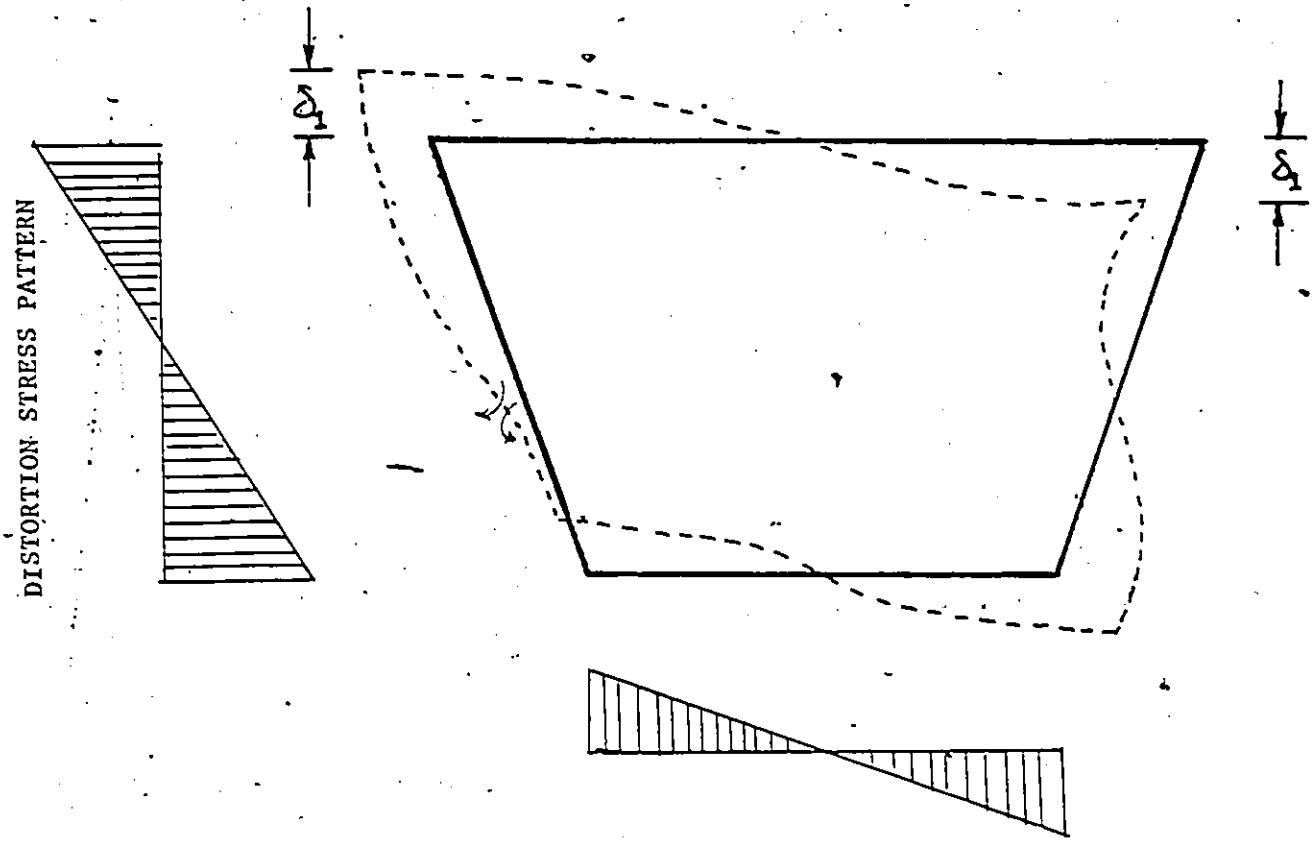

FIG.3.9 DEFORMATION OF THE CROSS SECTION

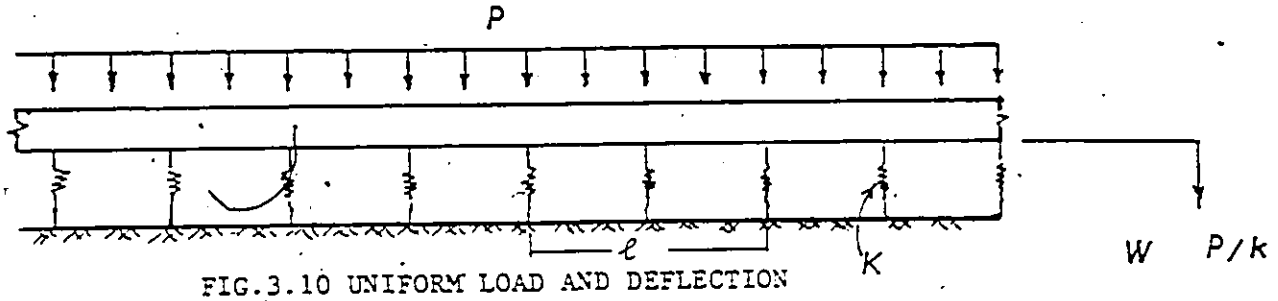

FIG.3.10 UNIFORM LOAD AND DEFLECTION

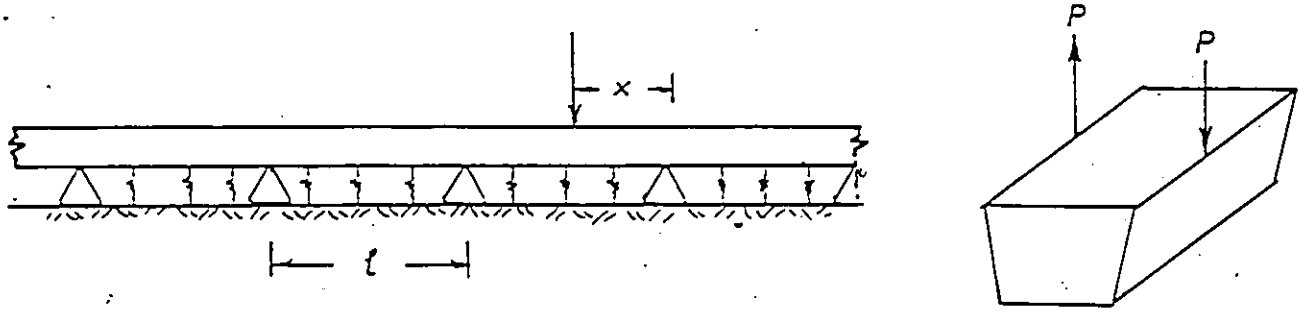

FIG.3.11 CONCENTRATED LOAD AND RIGID SUPPORTS

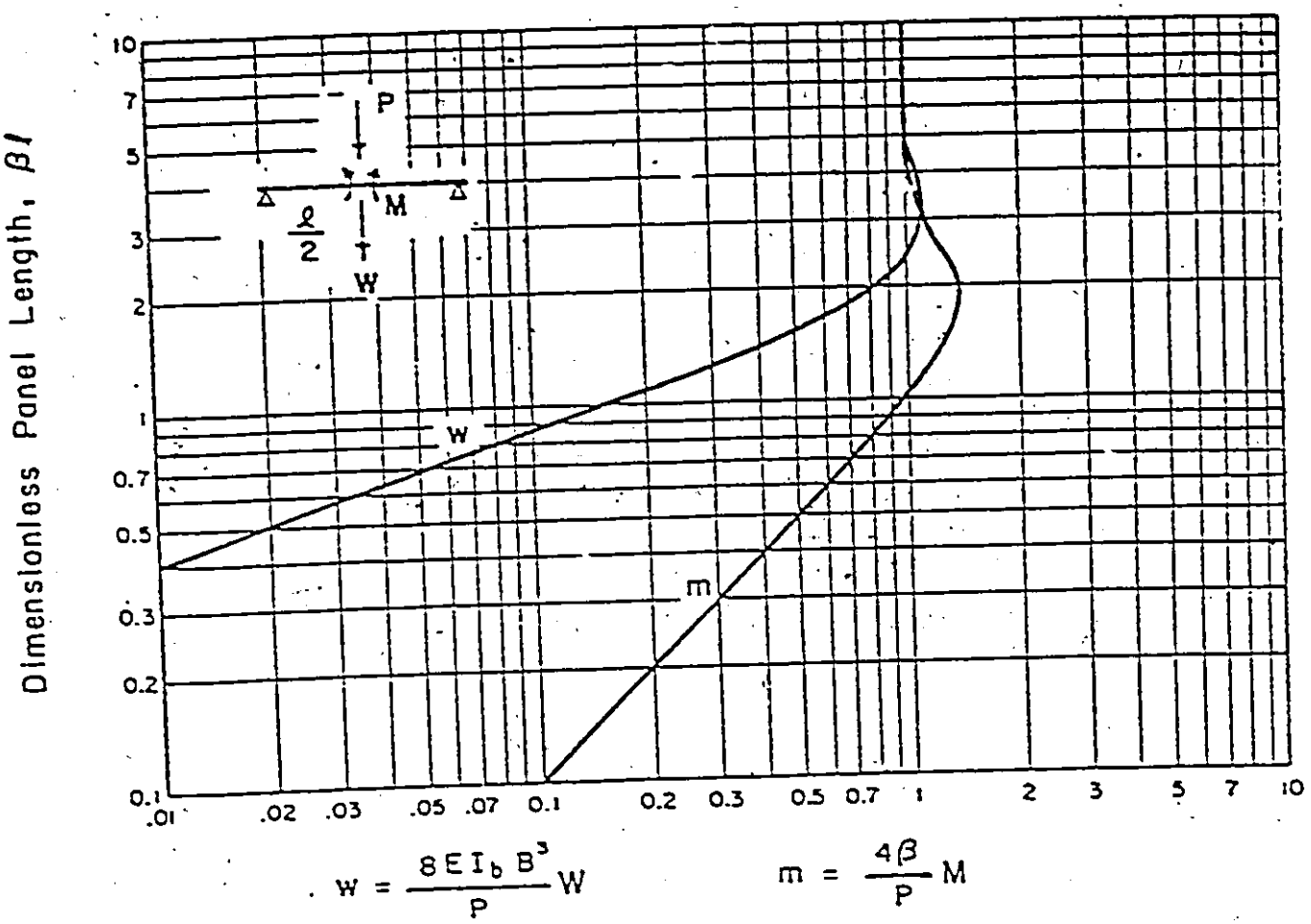

Figure 3.12* Concentrated Load, Simply Supported BEF, Analogy for Warping and Distortion Stresses

* (REF. 25)

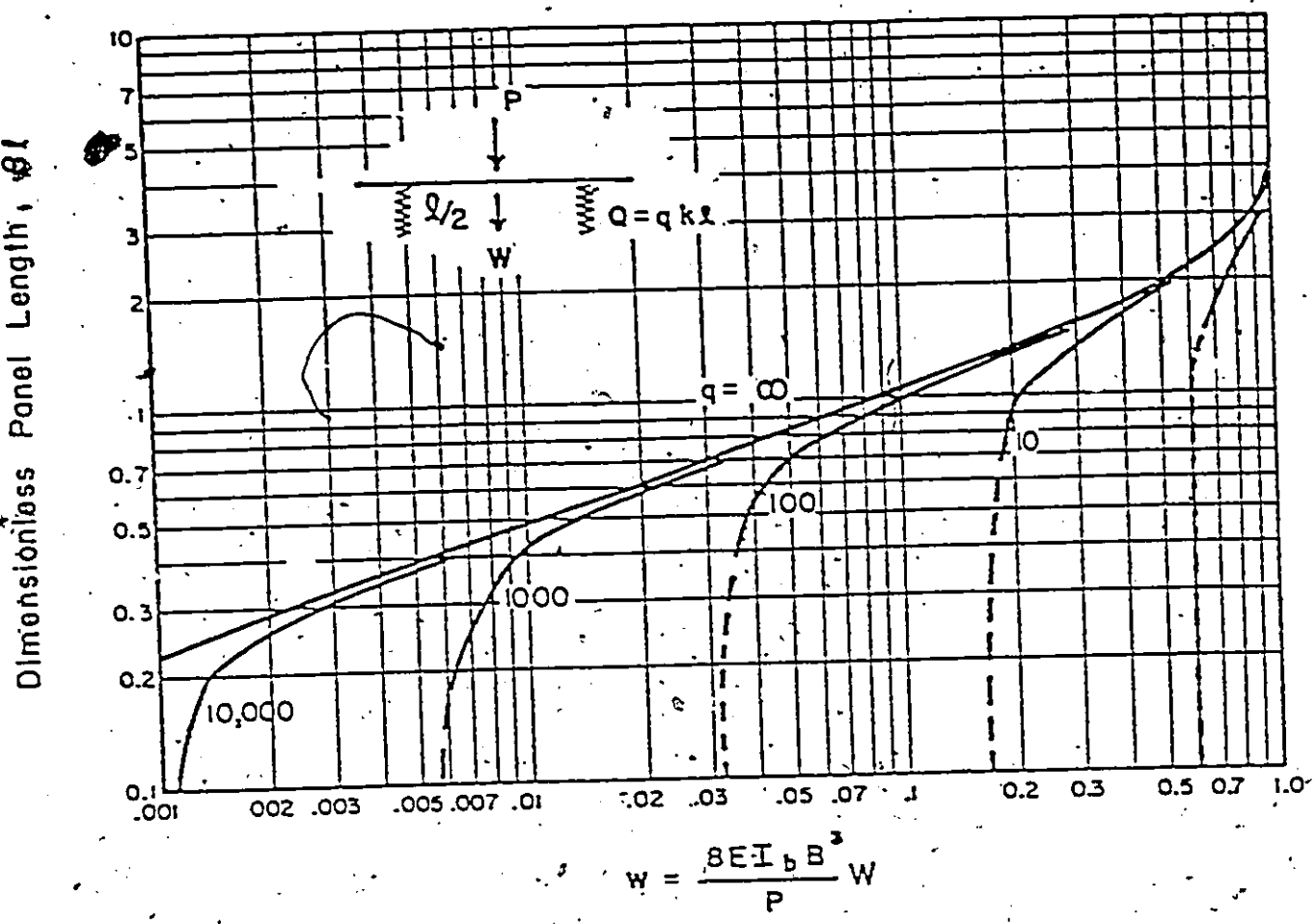

Figure 3.13 Midpanel Concentrated Load, Continuous BEF, Analogy for Distortion Stress at Load

*(REF: 25)

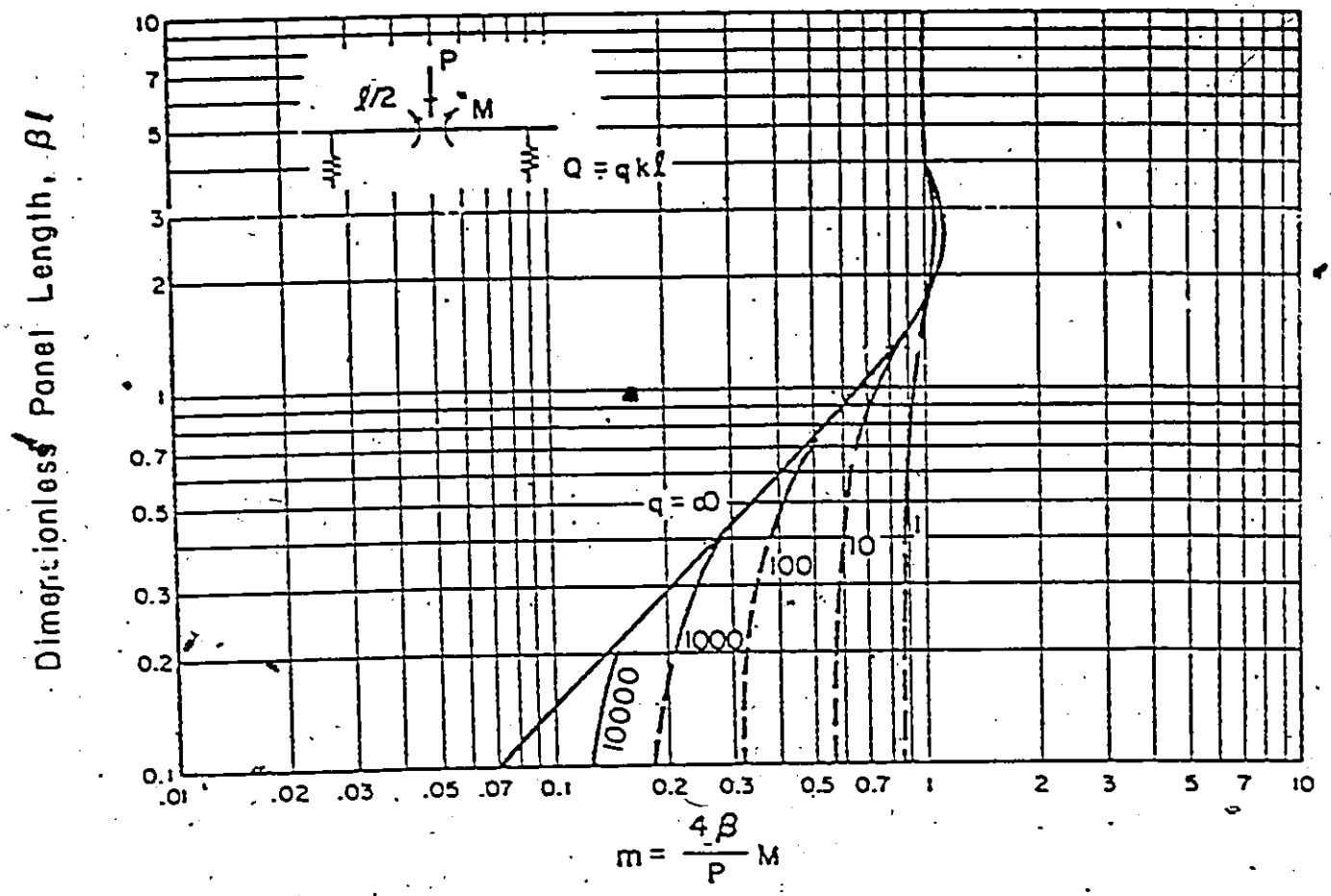

Figure 3.14* Midpanel Concentrated Load, Continuous BEF, Analogy for Warping Stress at Midpanel

* (REF. 25)

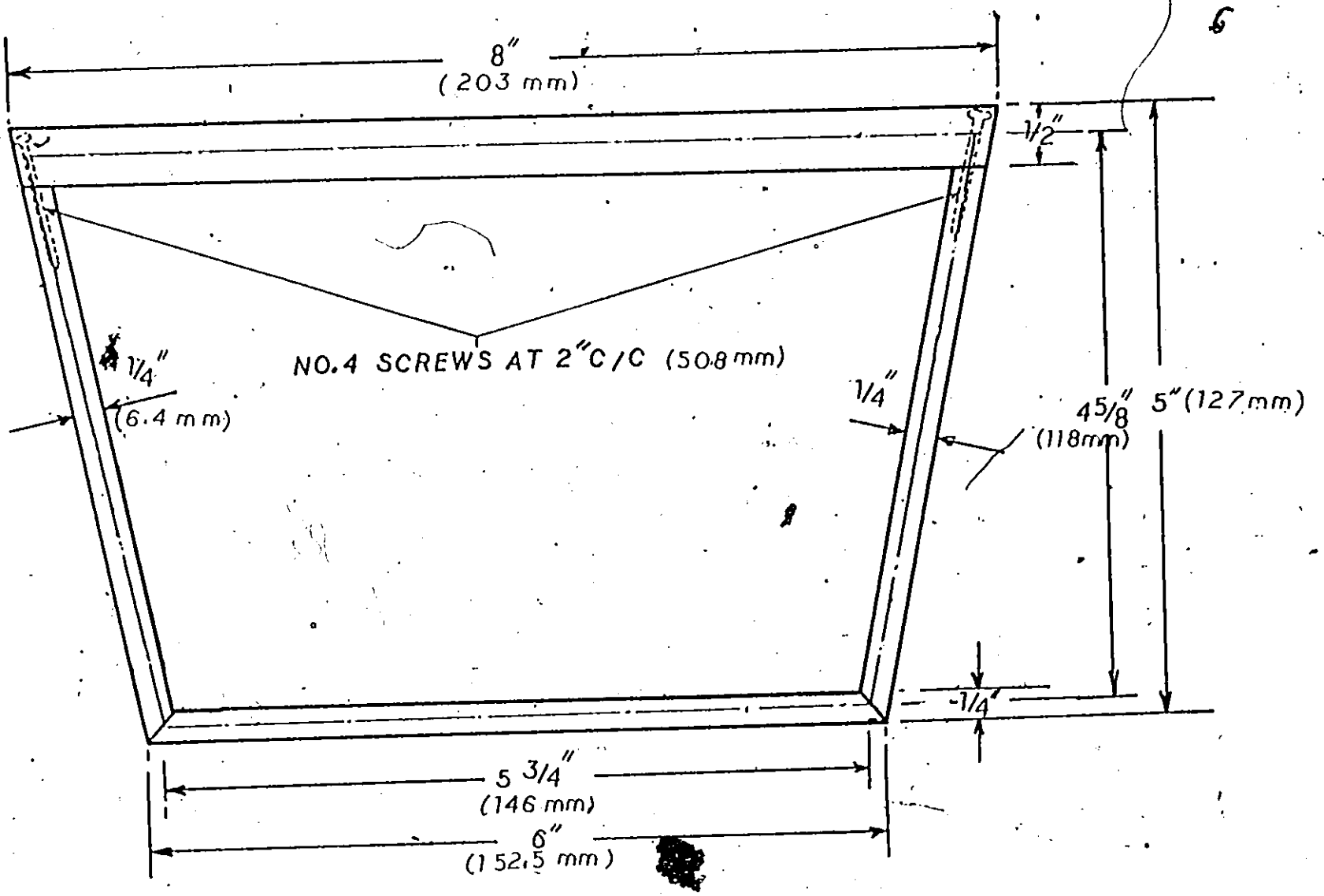

FIG.4.1 MODEL CROSS SECTION
(MODEL NO.1)

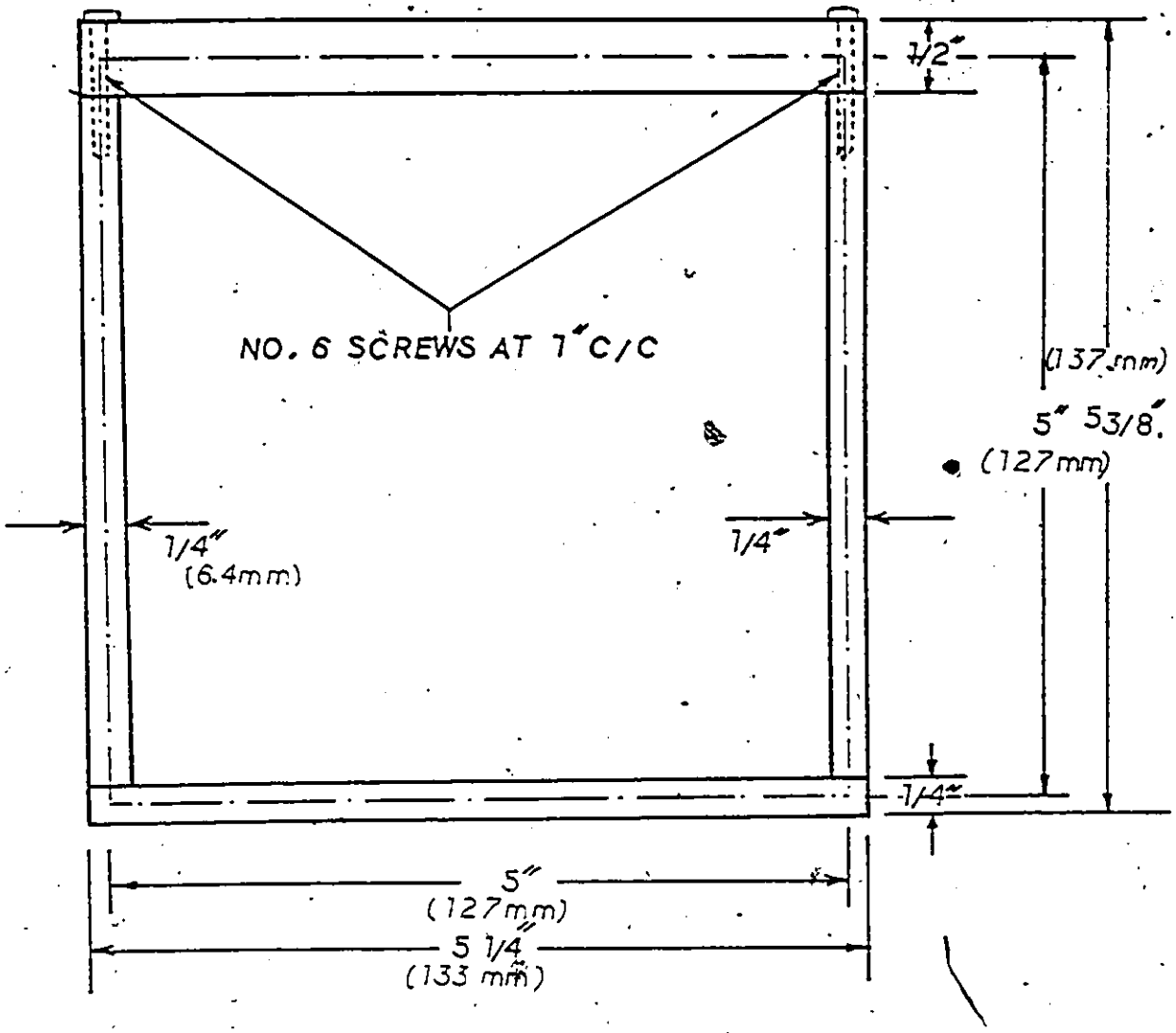

FIG.4.2 MODEL CROSS SECTION
(MODEL NO.2)

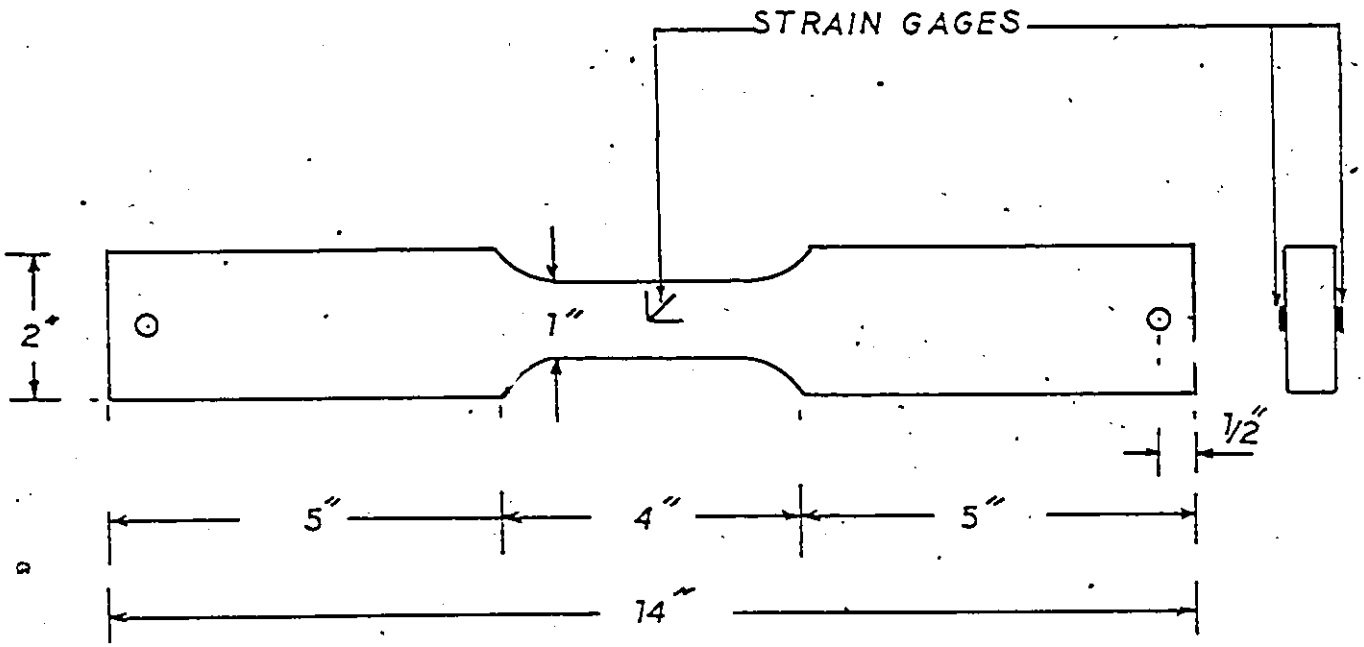

t = 1/2" for top flanges and 1/4" for bottom flanges and web coupons

FIG.4.3 TENSILE COUPON DIMENSIONS

COLOURED PICTURES
Images en couleur

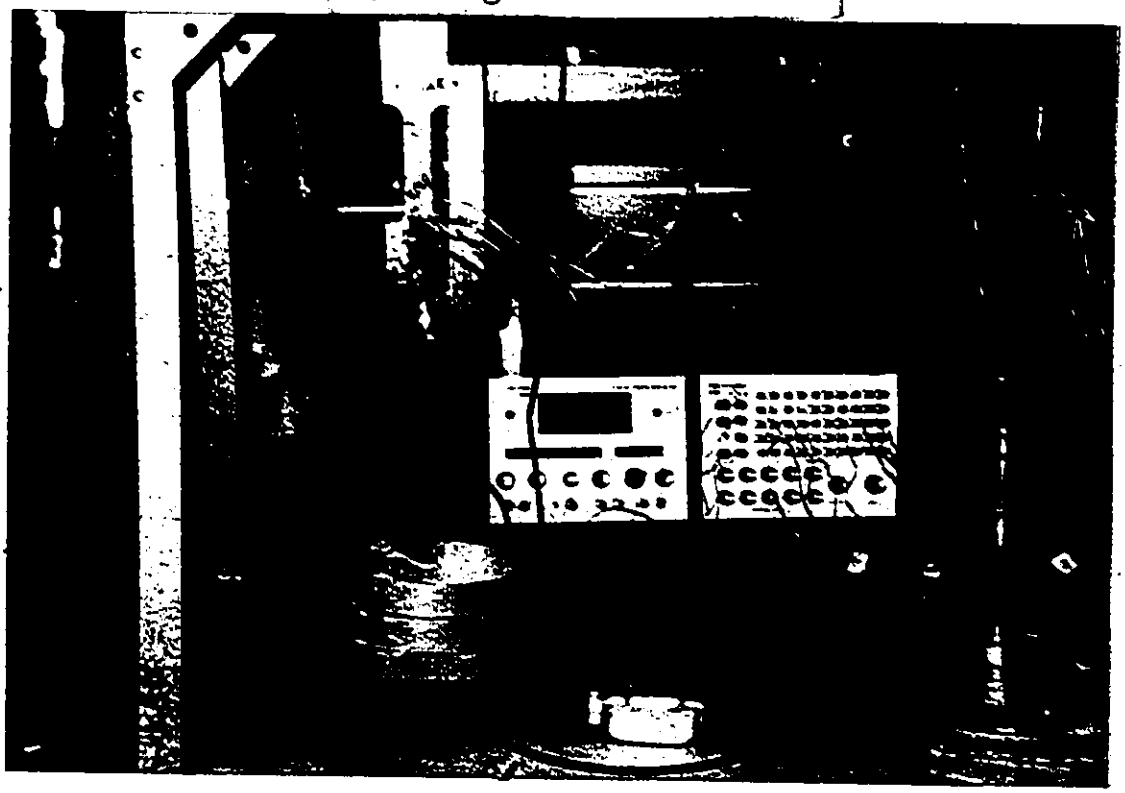

FIG.4.4 COUPON TEST

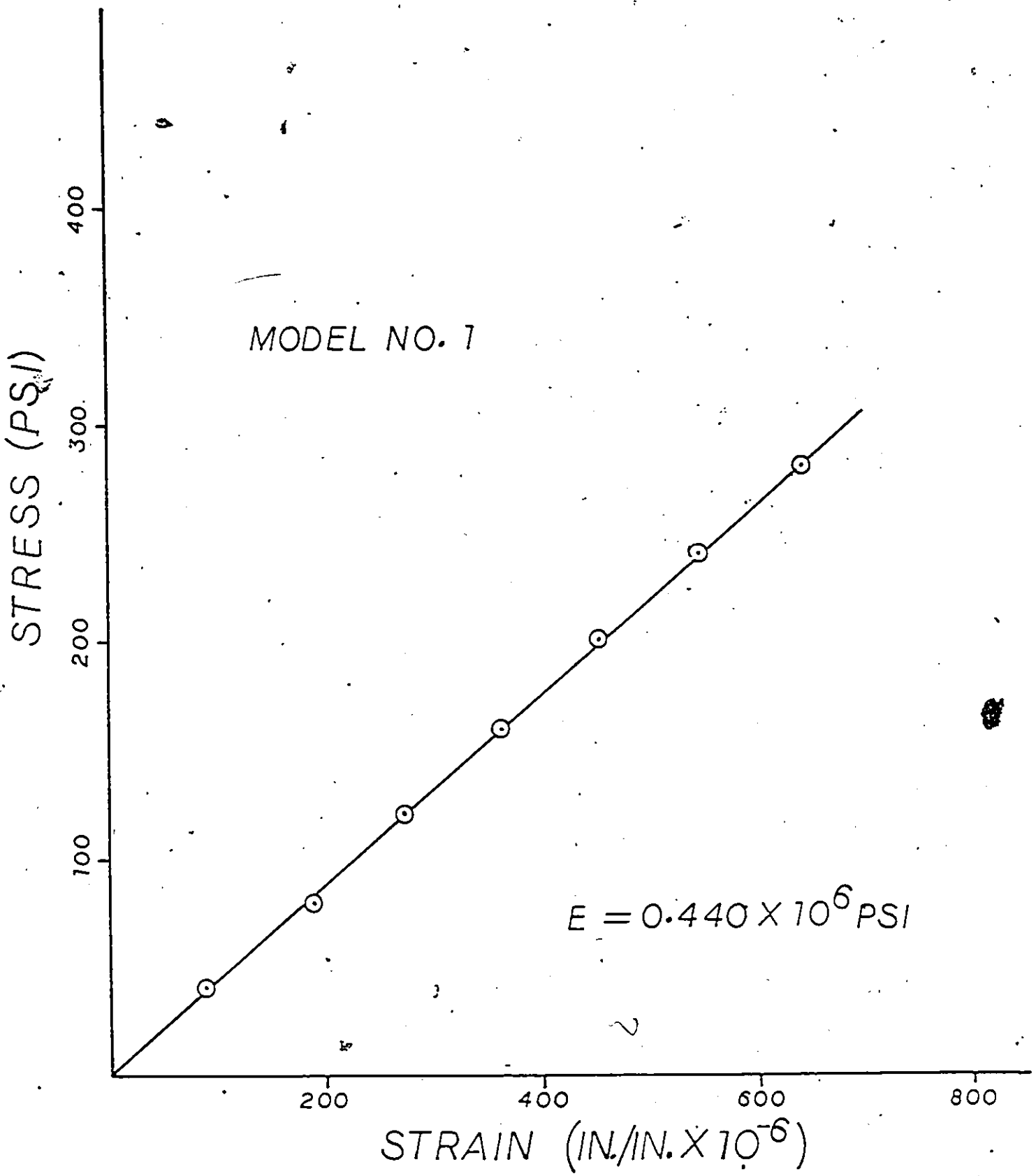

FIG.4.5 COUPON STRESS-STRAIN CURVE

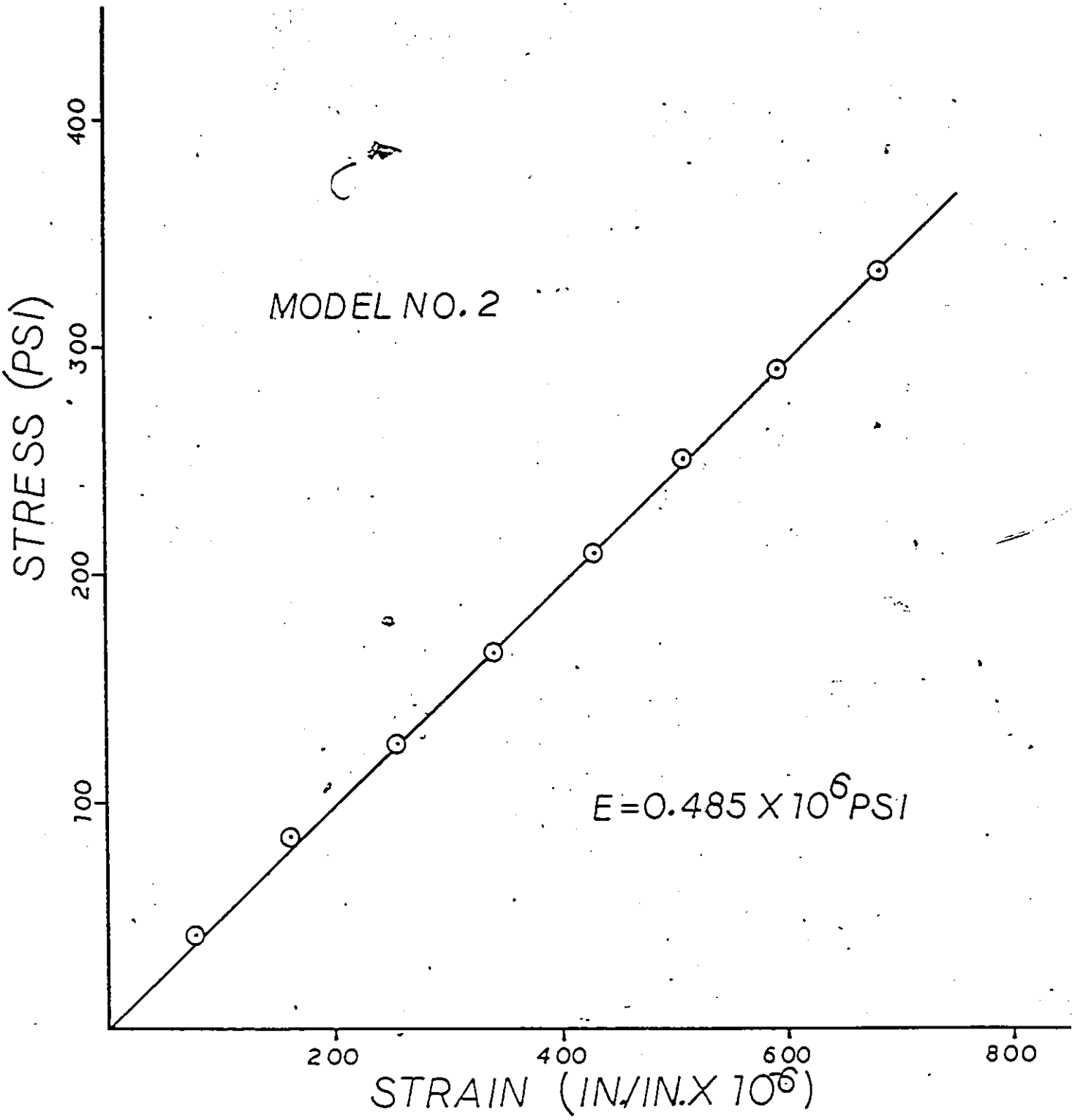

FIG.4.6 COUPON STRESS- STRAIN CURVE

COLOURED PICTURES
Images en couleur

FIG.4.7 MODEL CLOSE-UP (TRAPEZOIDAL SECTION)

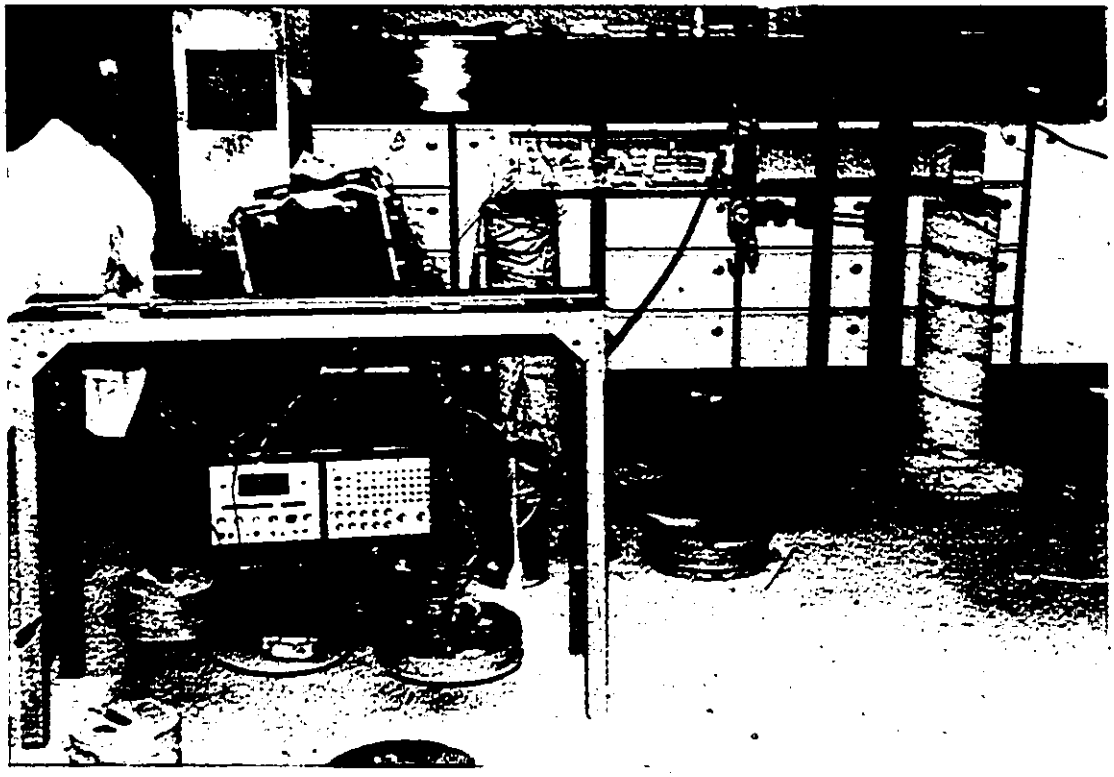

FIG.4.8 TEST SET-UP

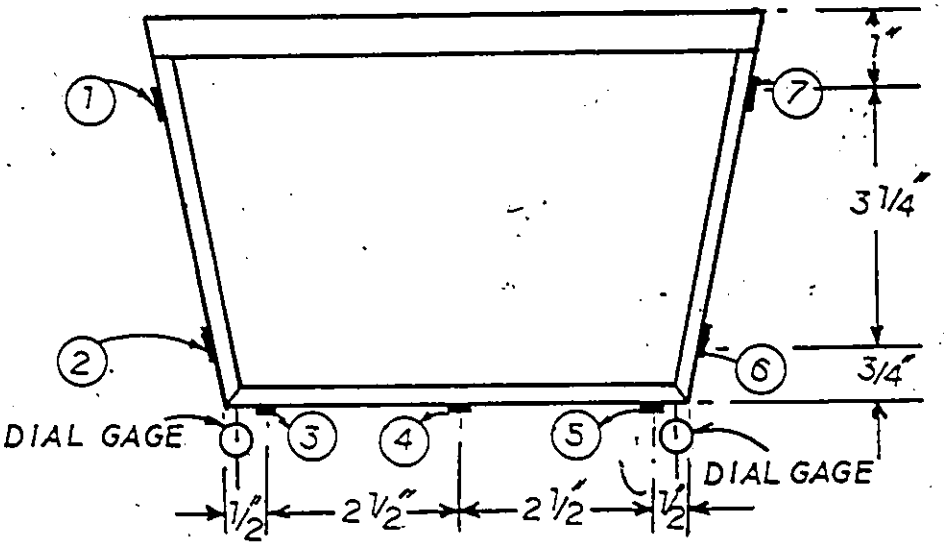

FIG.4.9 LOCATION OF STRAIN GAGES AND DIAL GAGES AT SECTION A (MIDSPAN)

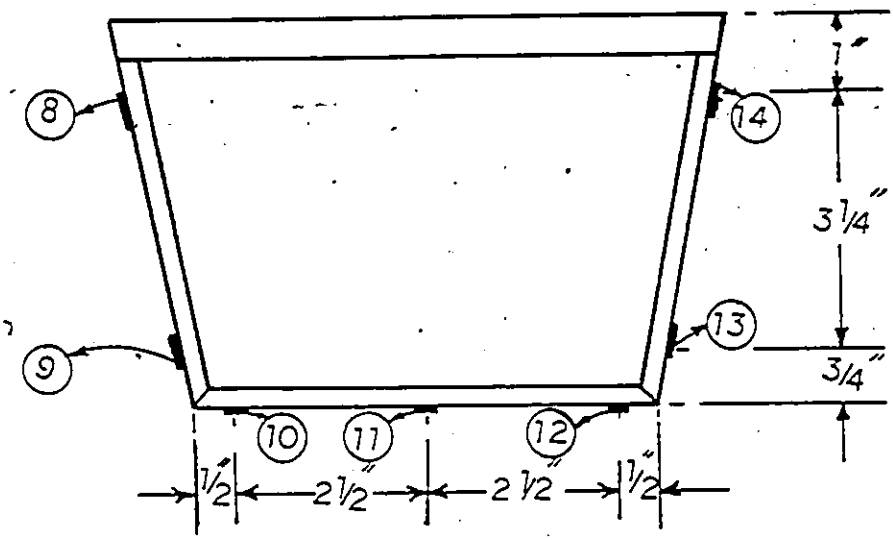

FIG.4.10 LOCATION OF STRAIN GAGES ON CROSS SECTION B

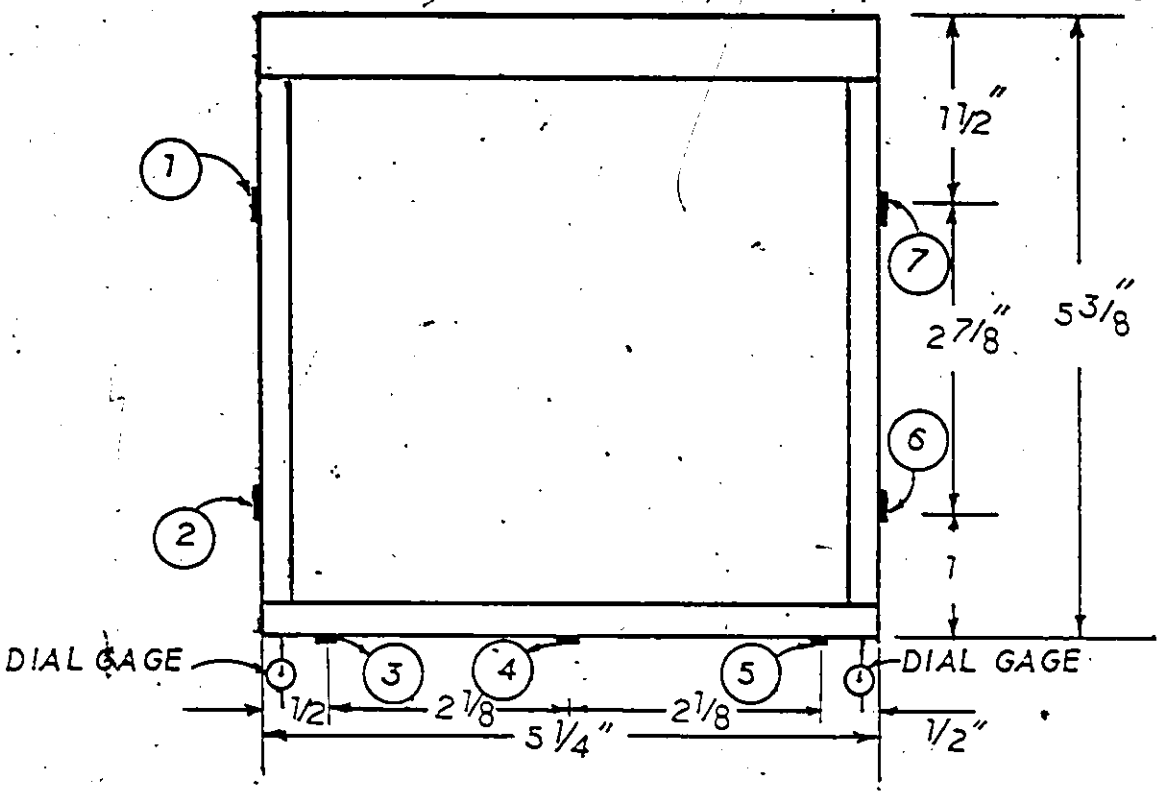

FIG.4.11 LOCATION OF STRAIN GAGES AND DIAL GAGES AT SECTION A (MIDSPAN)

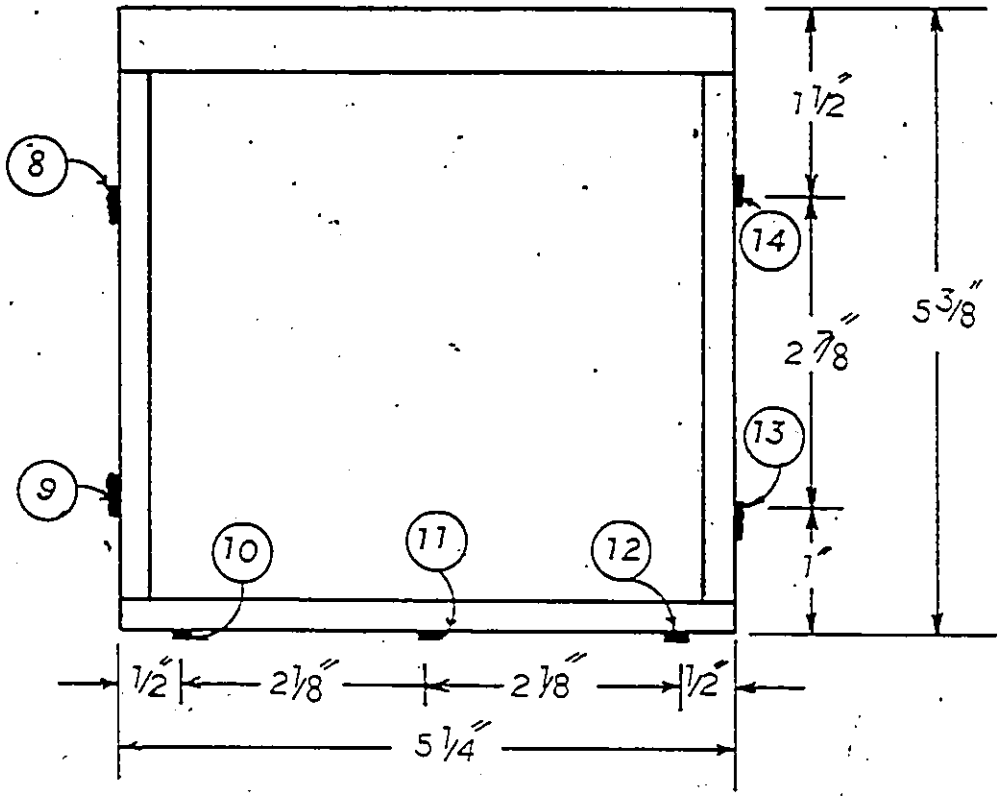

FIG.4.12 LOCATION OF STRAIN GAGES ON CROSS SECTION B

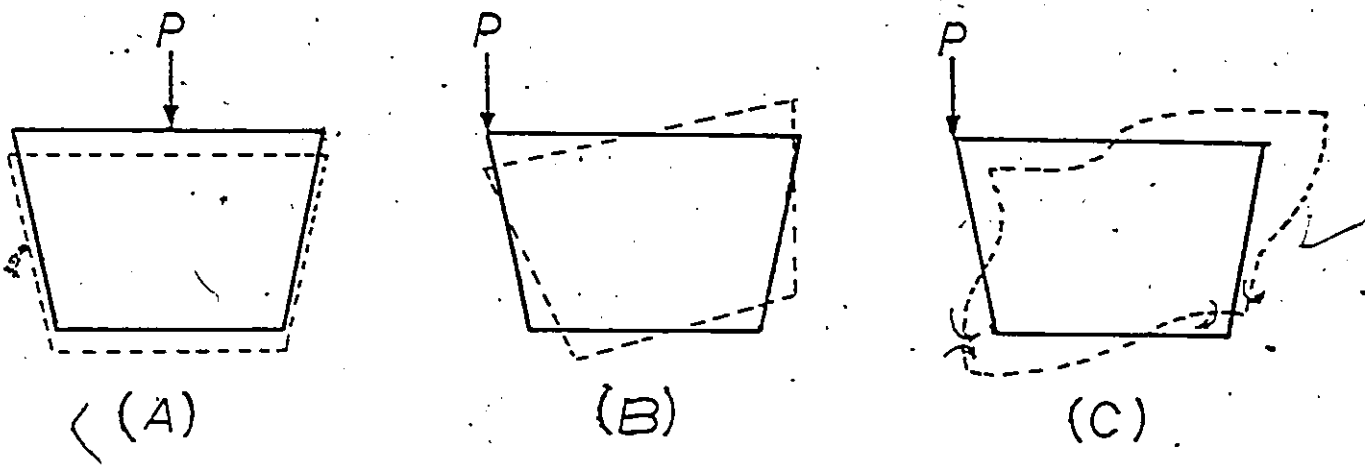

FIG.4.13 TYPES OF CROSS SECTION MOVEMENT

A) DEFLECTION DUE TO CONCENTRIC LOADING

B) RIGID SECTION DEFLECTION DUE TO ECCENTRIC LOADING

C) DEFORMATION OF CROSS SECTION

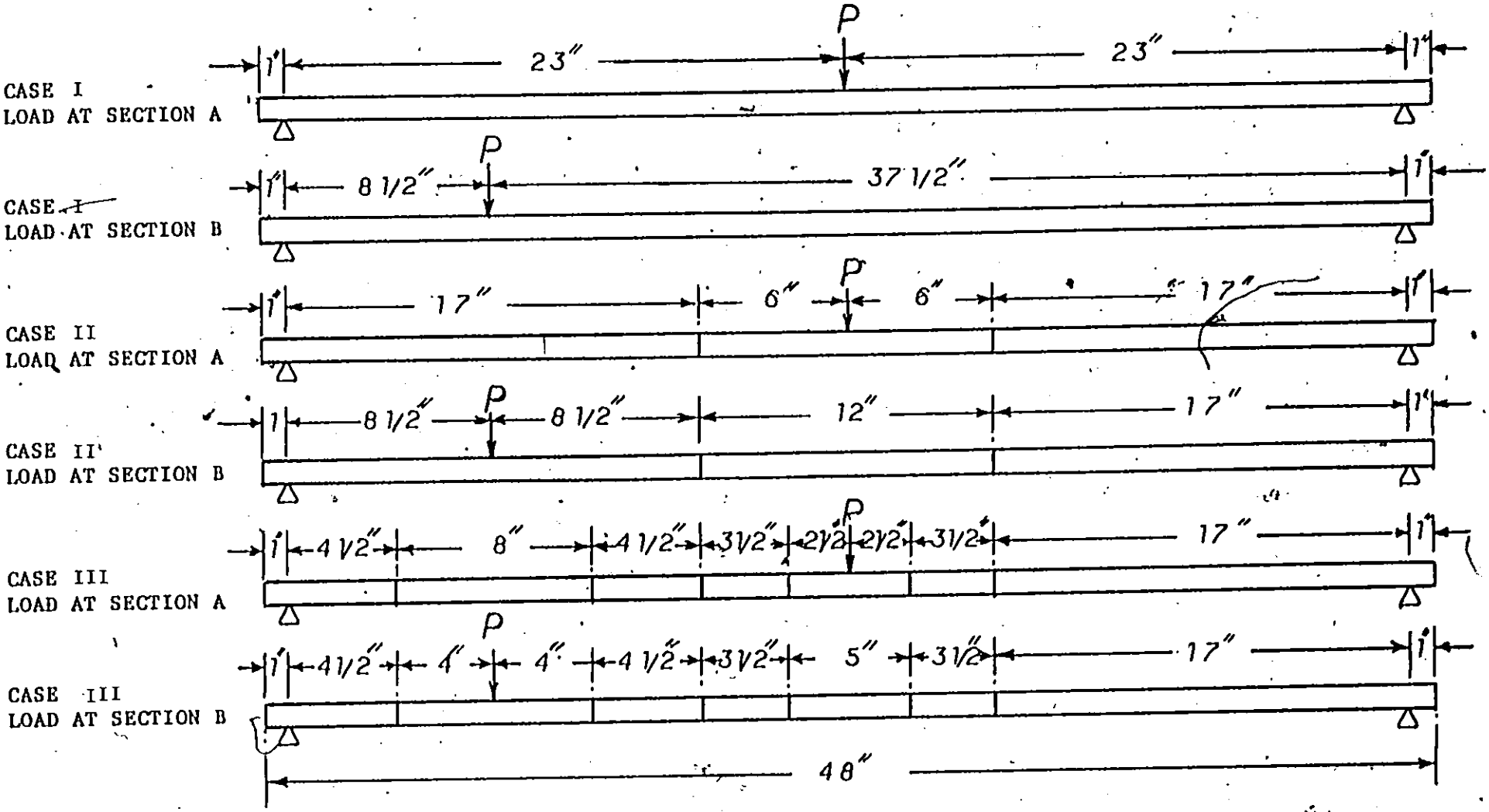

FIG.4.14 LOCATION OF DIAPHRAGMS AND TEST LOADS

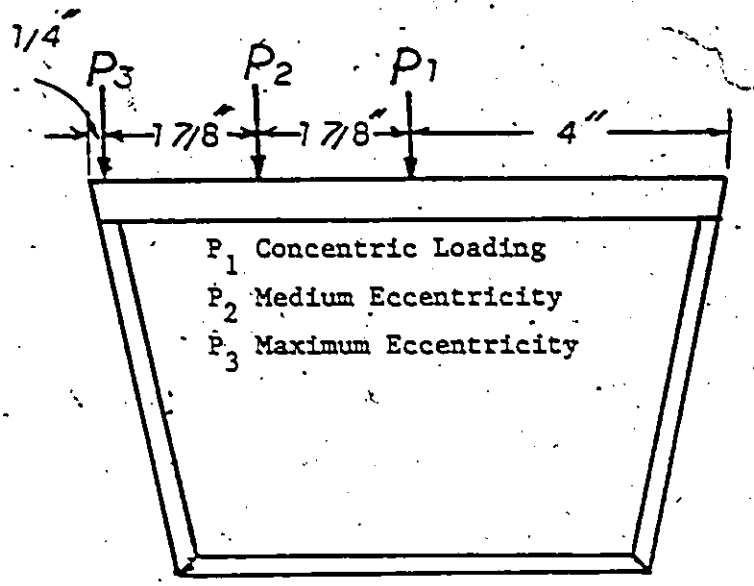

FIG.4.15 CROSS SECTION LOADING POINTS

COLOURED PICTURES
Images en couleur

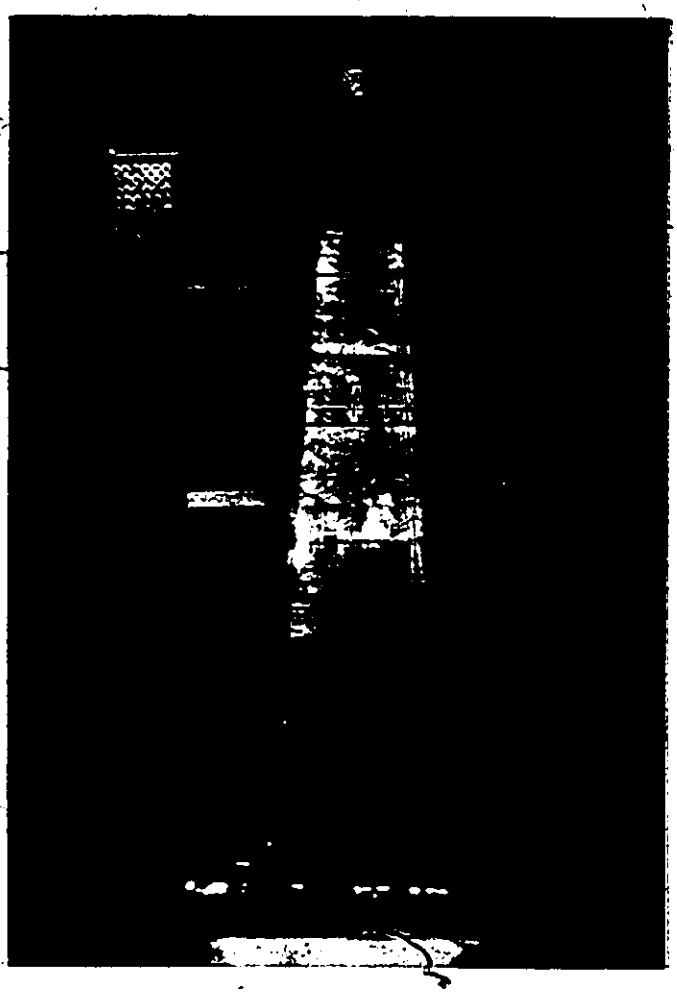

FIG.4.16 TWO DIAPHRAGMS WERE PLACED IN MODEL NO.2

COLOURED PICTURES
Images en couleur

FIG.4.17 SIX DIAPHRAGMS WERE PLACED IN MODEL NO.1

COLOURED PICTURES
Images en couleur

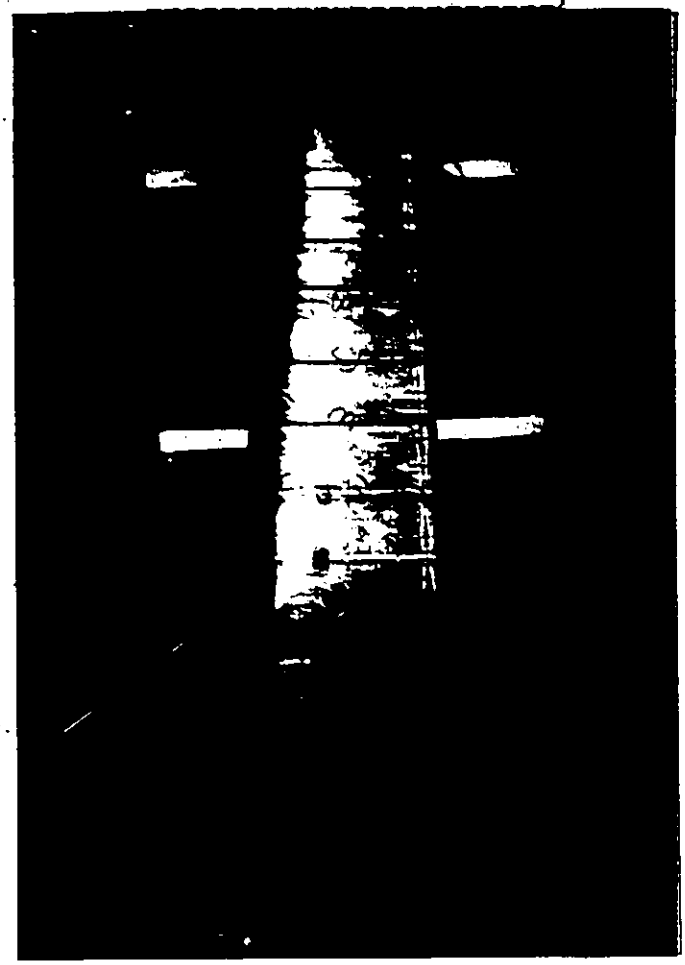

FIG.4.18 SIX DIAPHRAGMS WERE PLACED IN MODEL NO.2

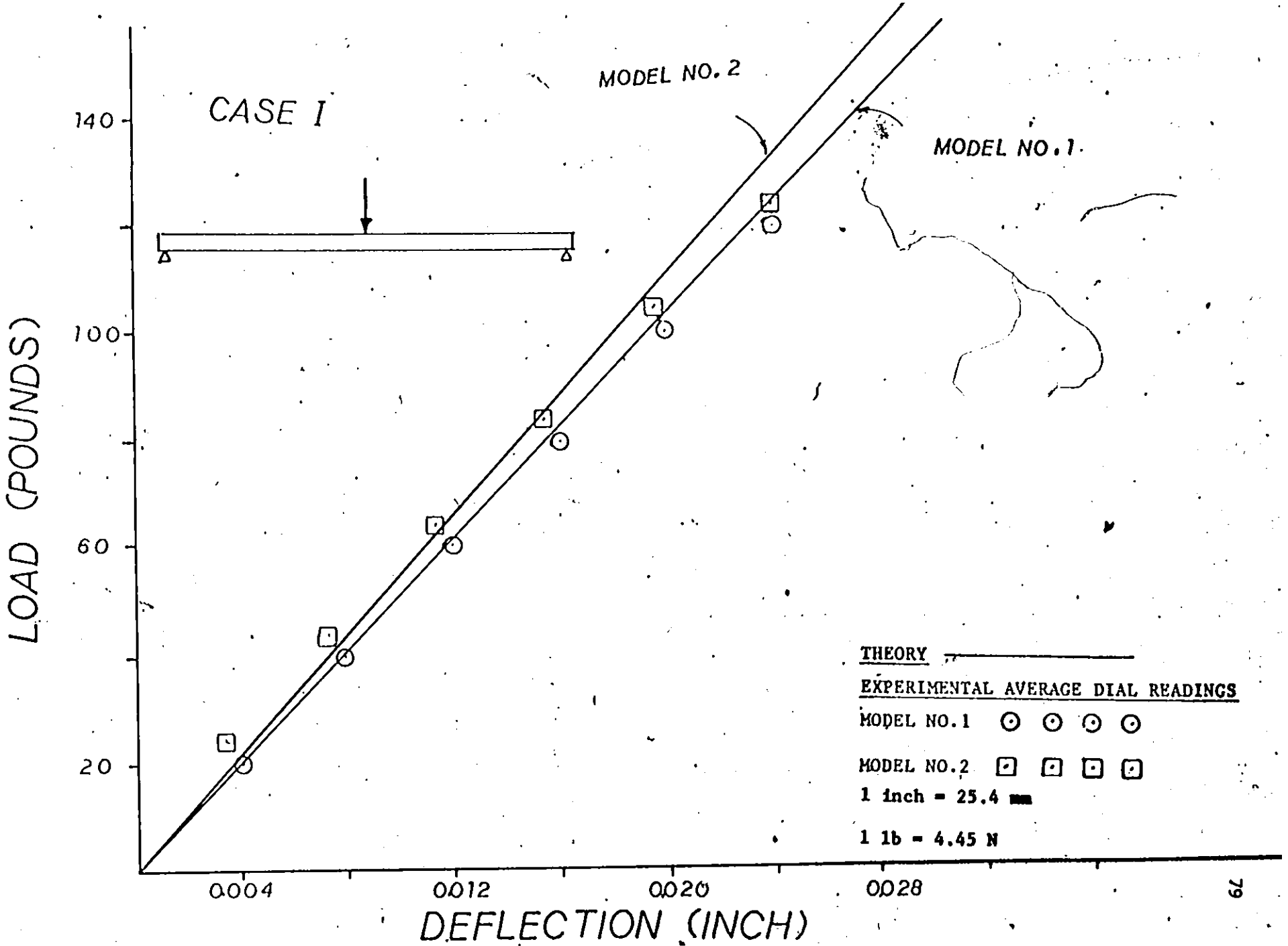

FIG.5.1 LOAD VS AVERAGE CENTERLINE DEFLECTION CONCENTRIC LOADING-CASE-I

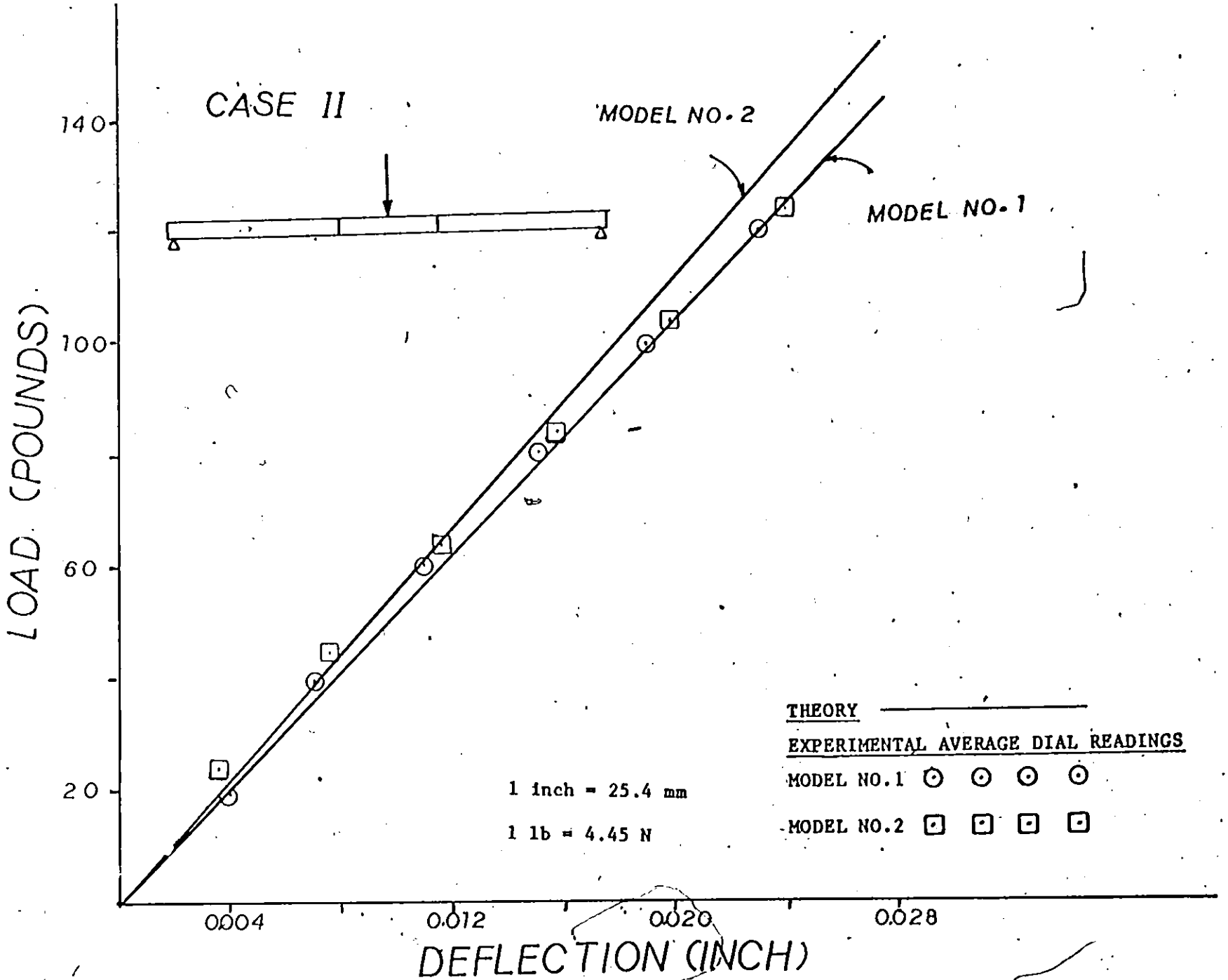

FIG.5.2 LOAD VS AVERAGE CENTERLINE DEFLECTION CONCENTRIC LOADING -CASE-II

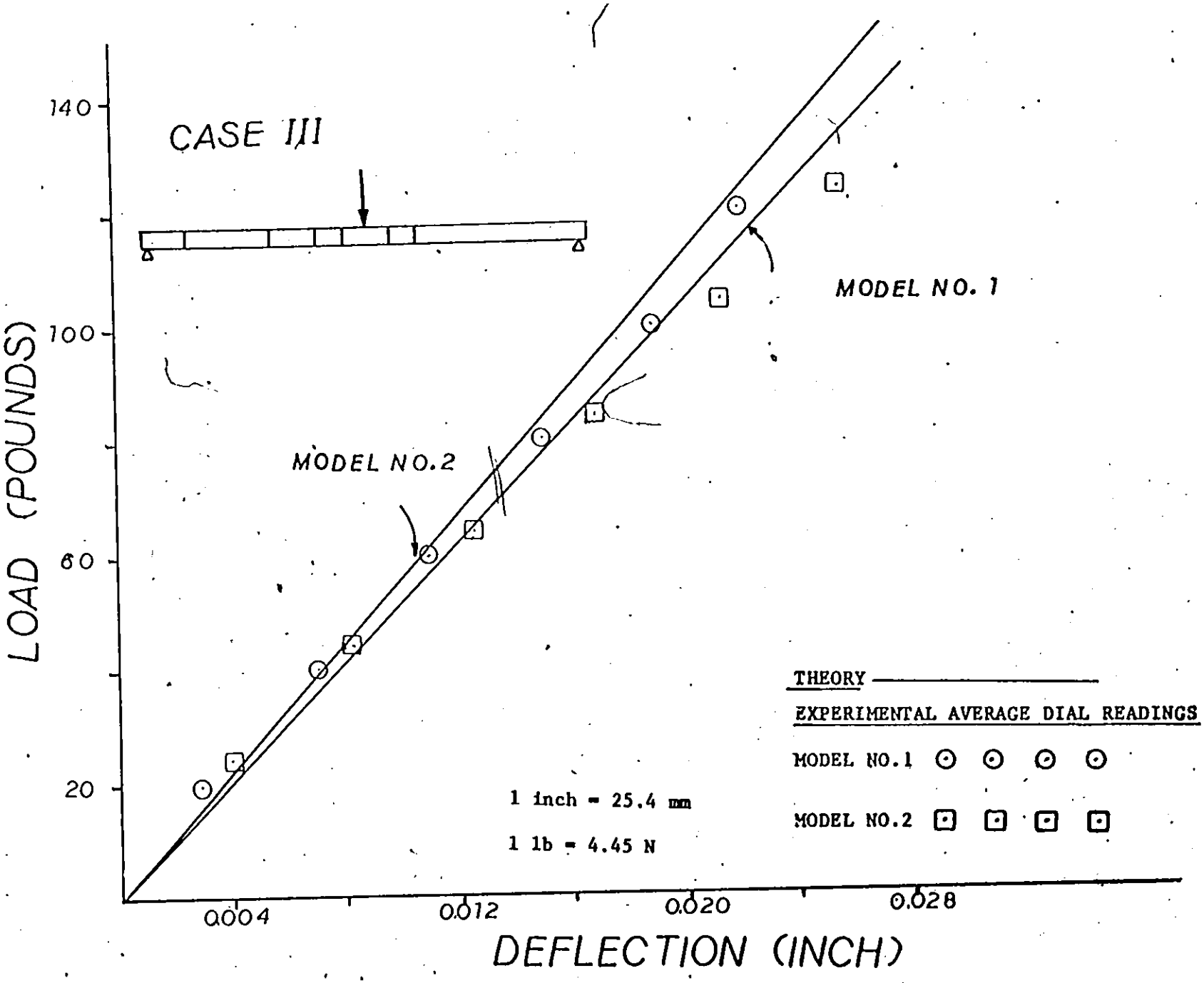

FIG.5.3 LOAD VS AVERAGE CENTERLINE DEFLECTION CONCENTRIC LOADING-CASE-III

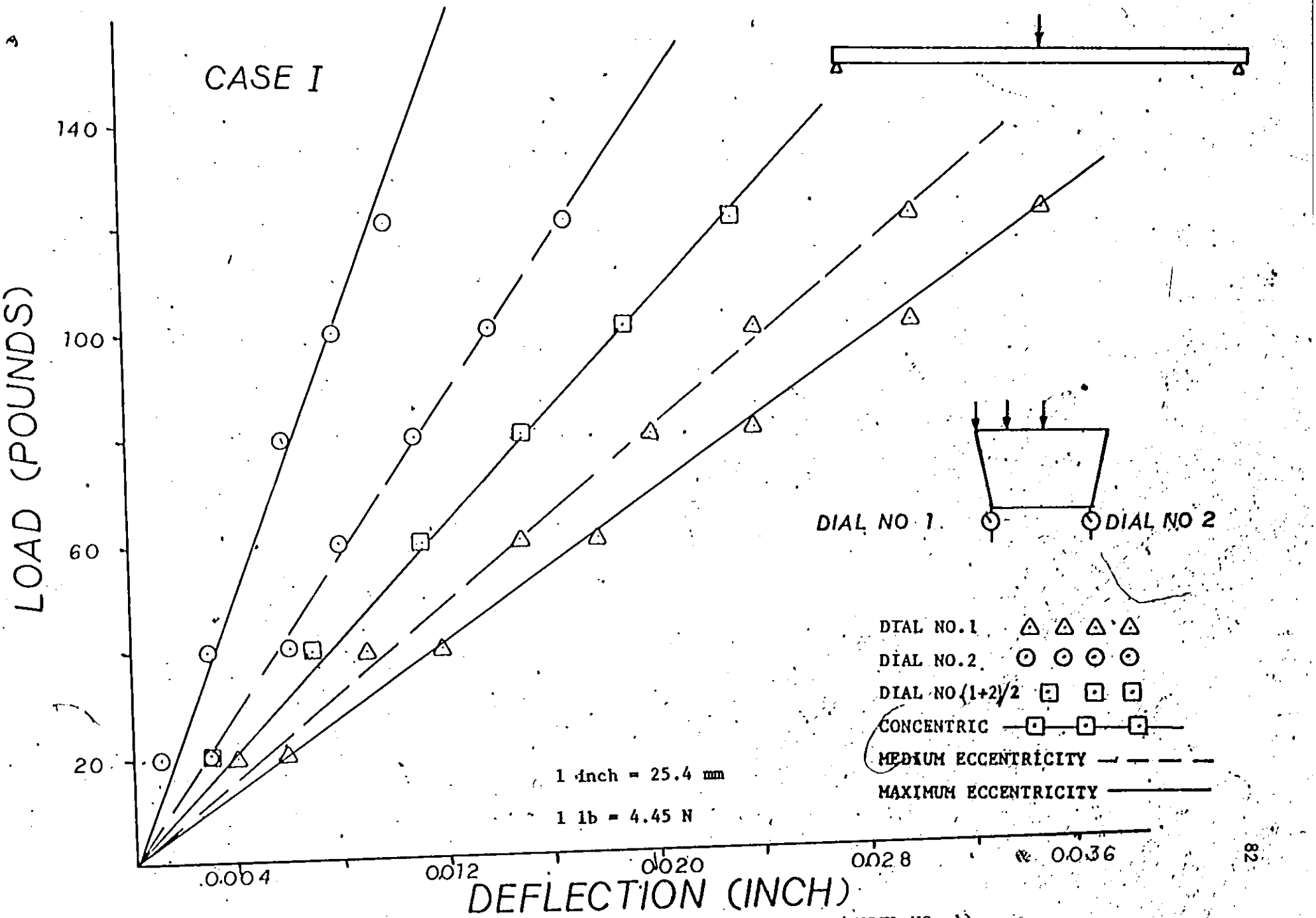

FIG.5.4 LOAD VS CENTERLINE DEFLECTION-CASE-I (MODEL NO. 1)

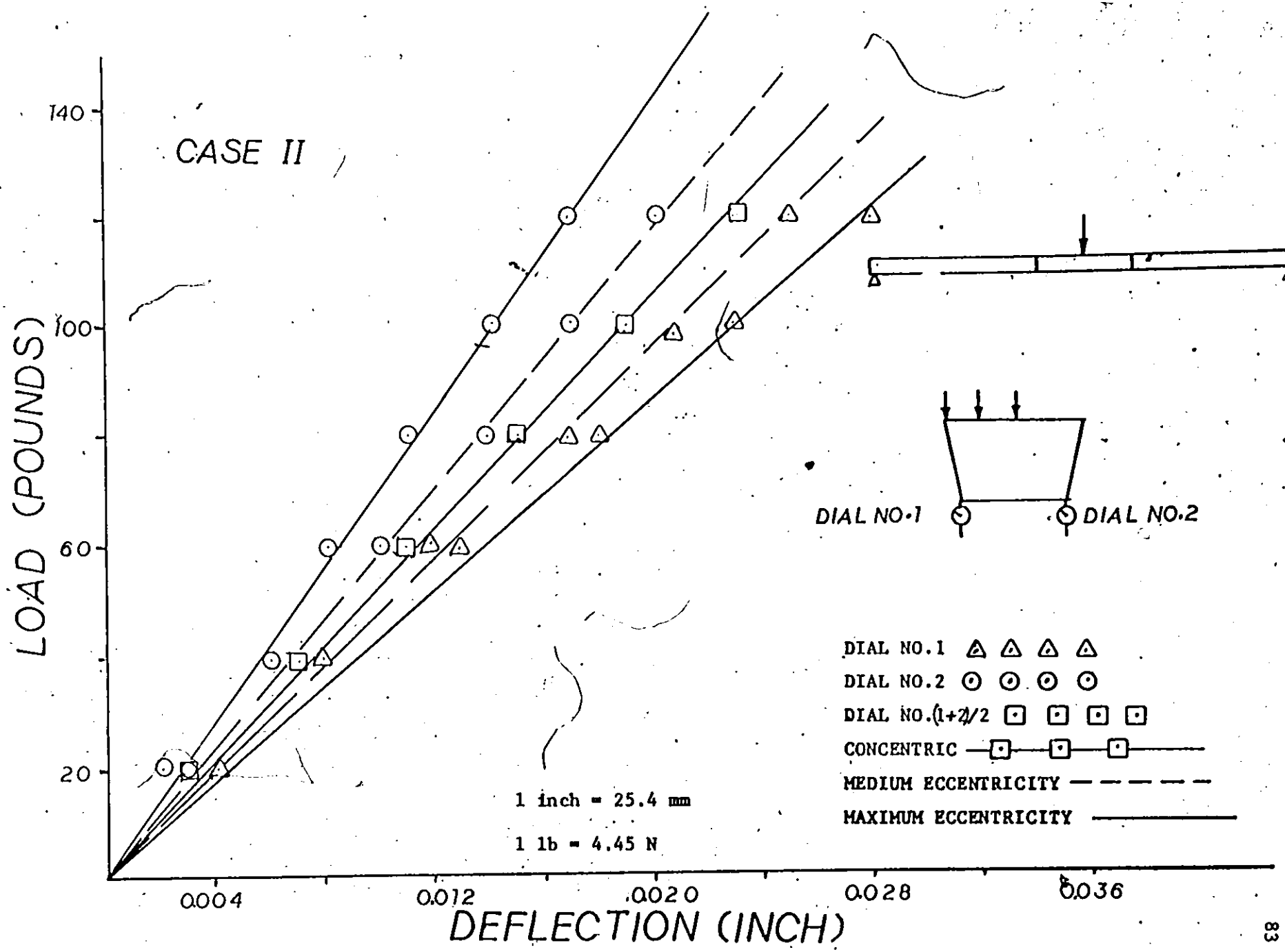

FIG.5.5 LOAD VS CENTERLINE DEFLECTION-CASE-II (MODEL NO.1)

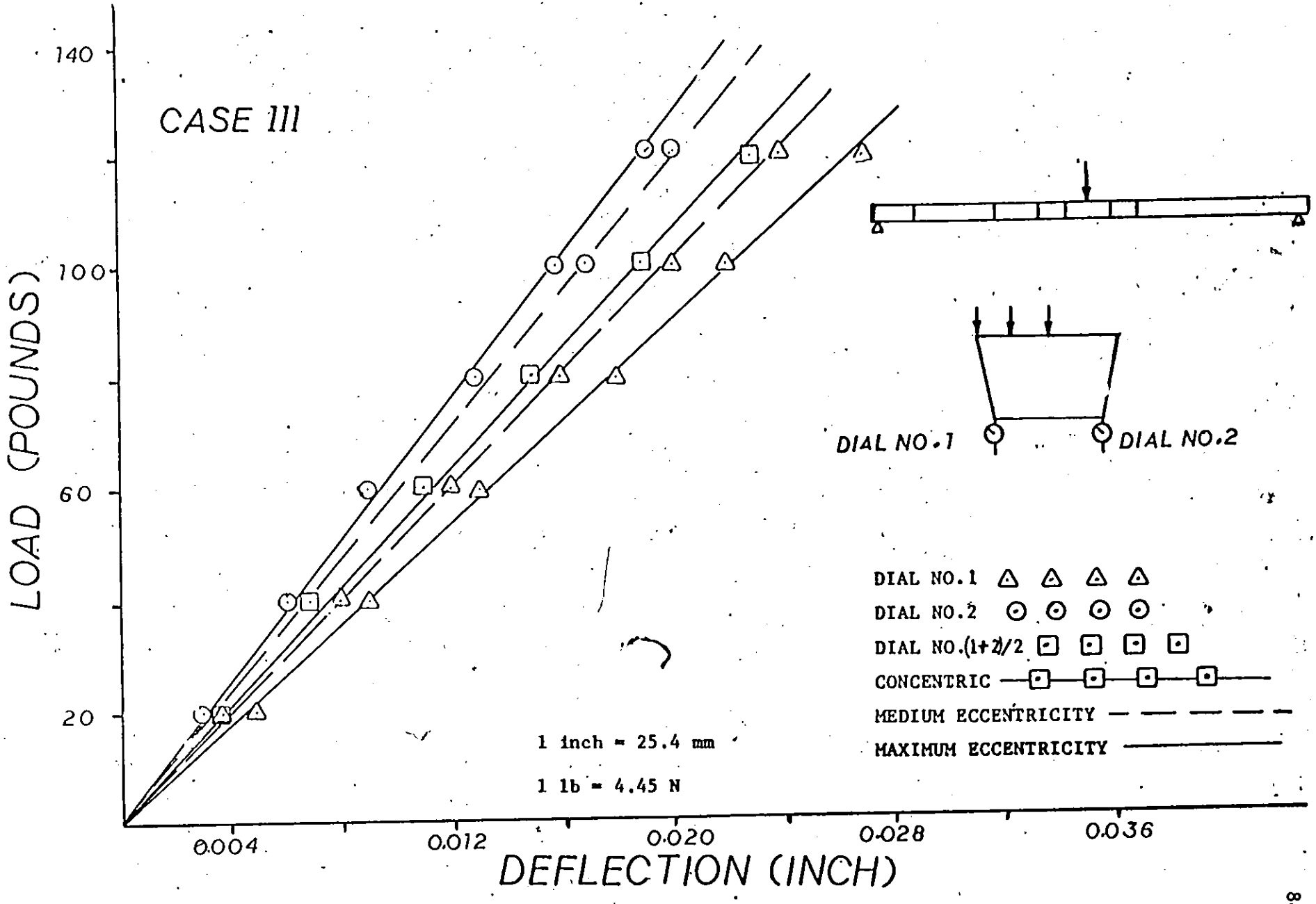

FIG.5.6 LOAD VS CENTERLINE DEFLECTION -CASE-III (MODEL NO.1)

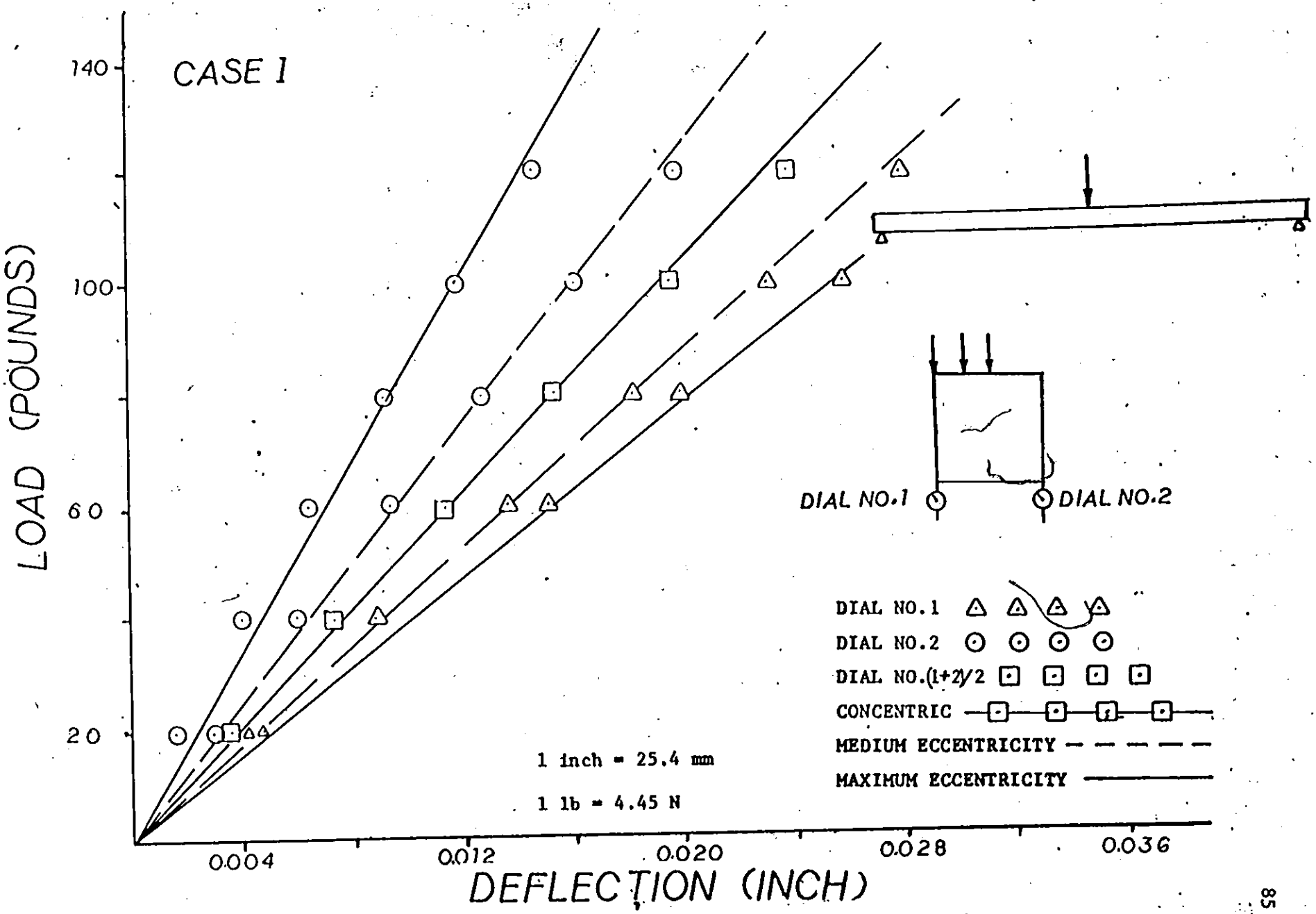

FIG.5.7 LOAD VS CENTERLINE DEFLECTION-CASE-I (MODEL NO.2)

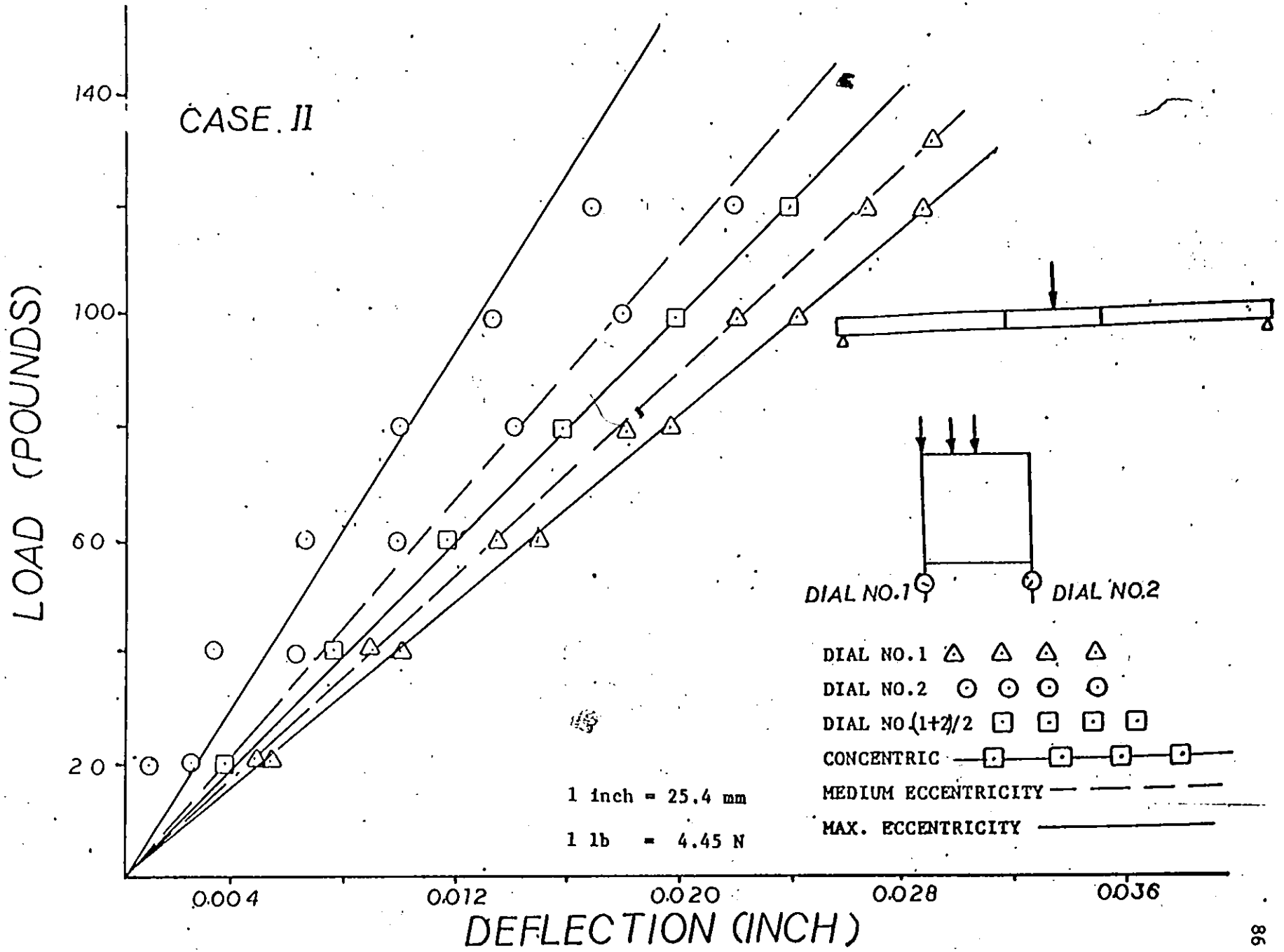

FIG.5.8 LOAD VS CENTERLINE DEFLECTION-CASE-II (MODEL NO.2)

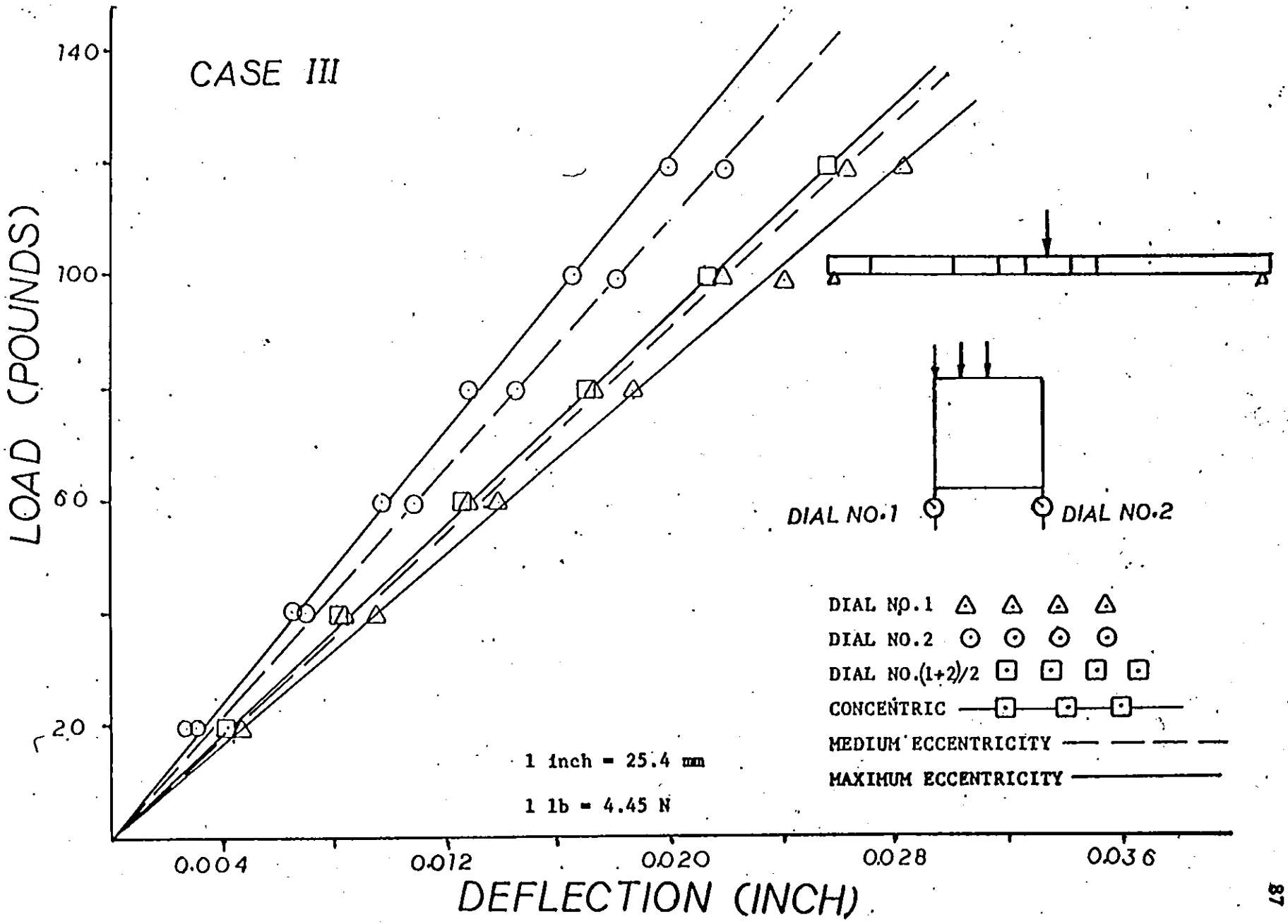

FIG.5.9 LOAD VS CENTERLINE DEFLECTION-CASE-III(MODEL NO.2)

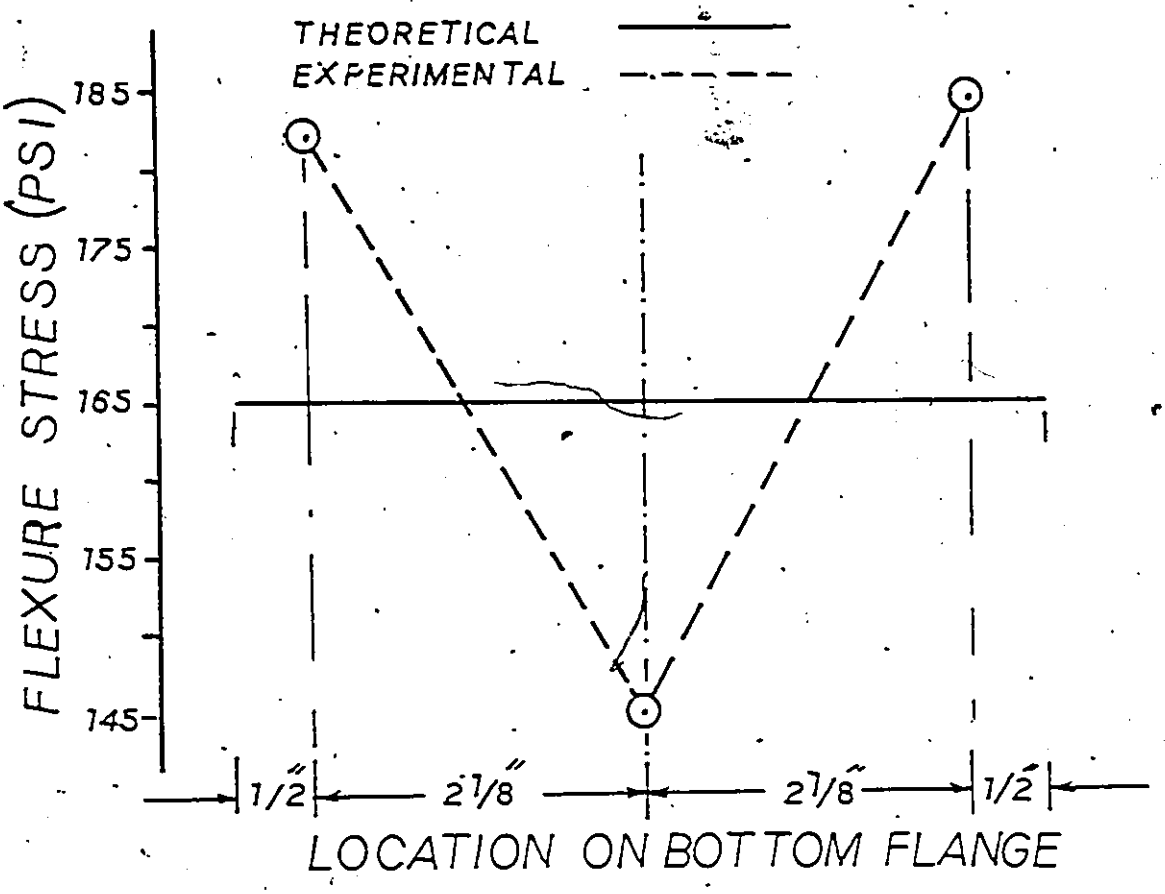

FIG.5.10 TYPICAL FLEXURAL STRESS PATTERN AT LOADED SECTION (MODEL NO.1)
(FOR LOAD 123.8 lbs.)

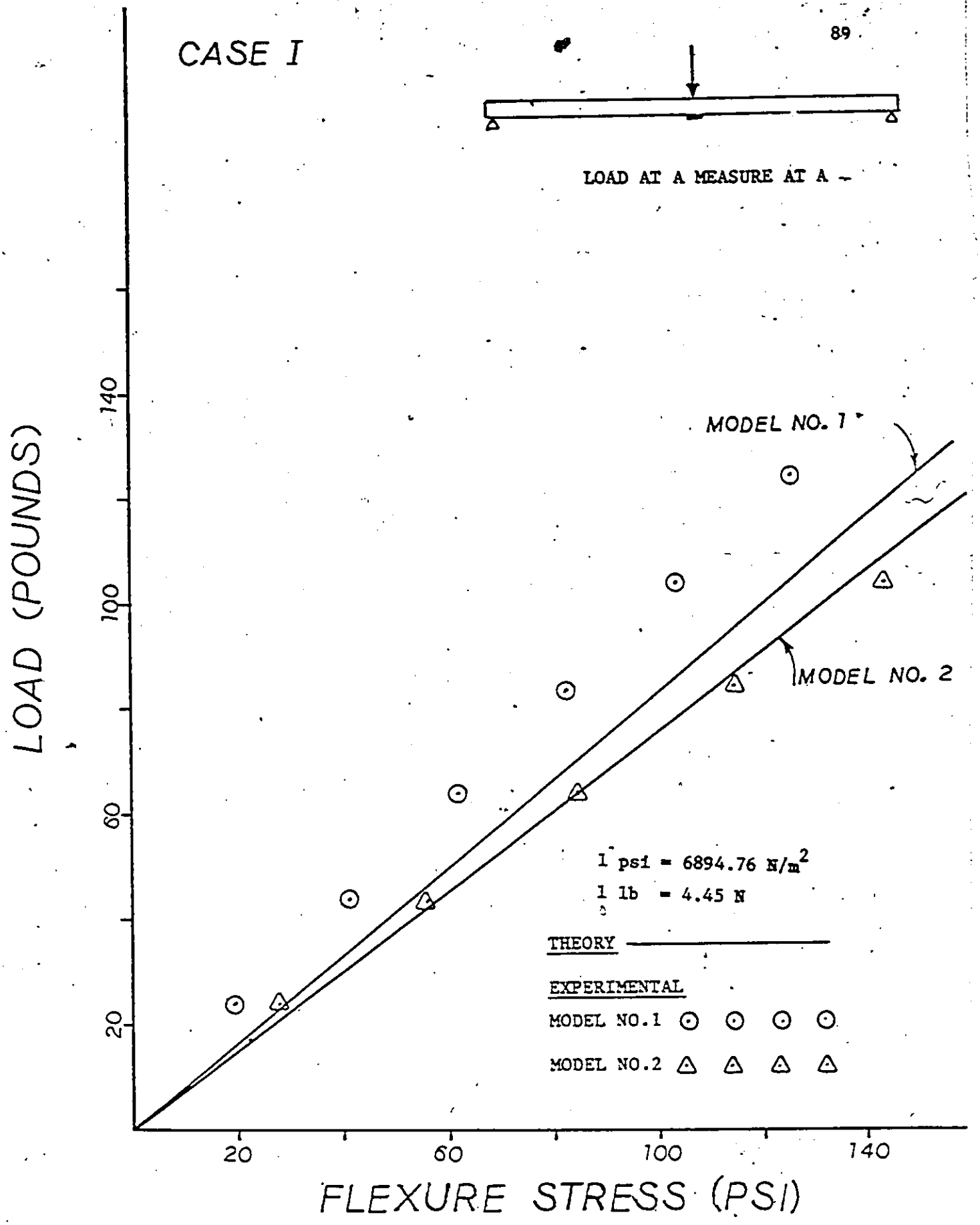

FIG.5.11 LOAD VS FLEXURE STRESS AT EXTREME SURFACE OF BOTTOM FLANGE

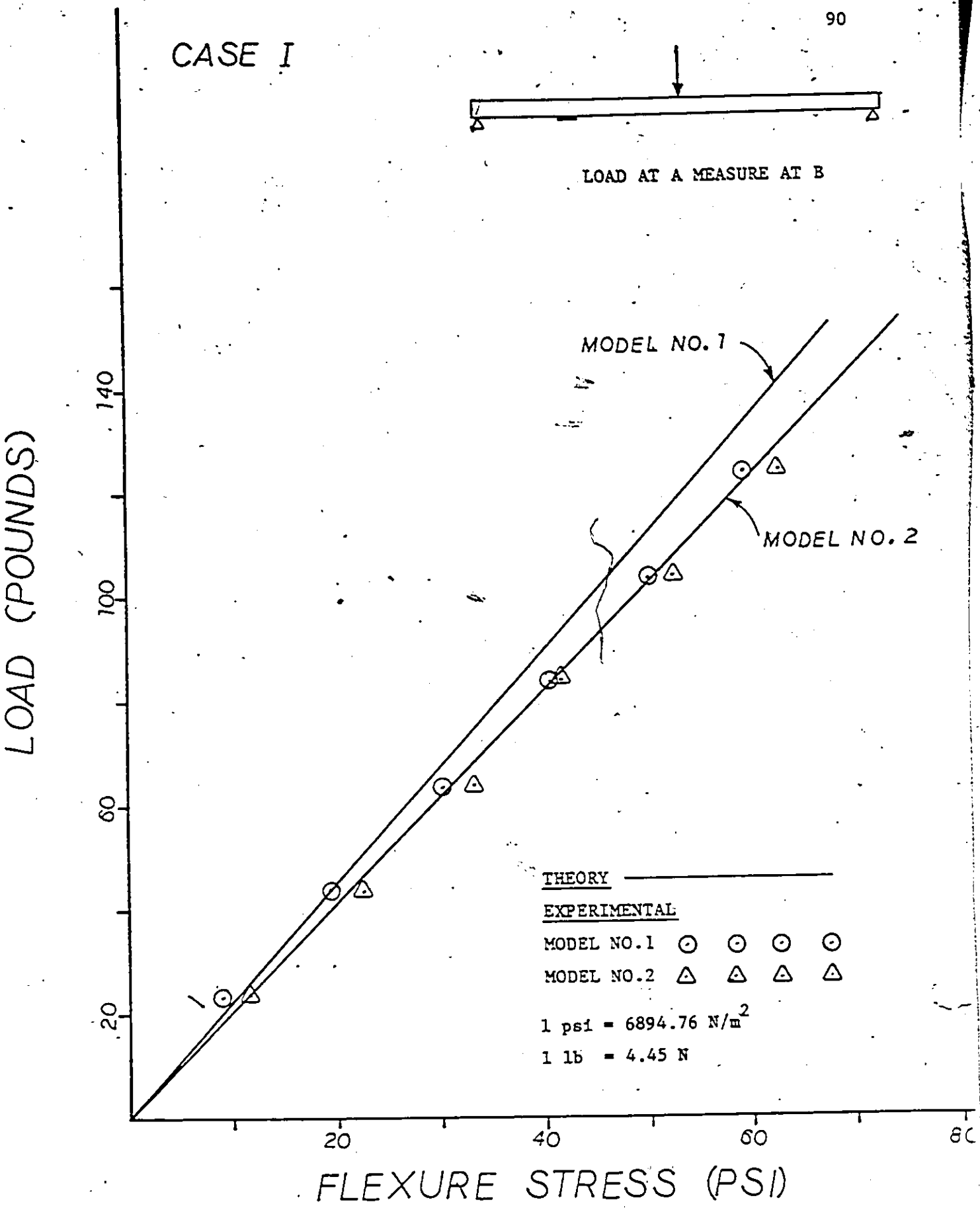

FIG.5.12 LOAD VS FLEXURE STRESS AT EXTREME SURFACE OF BOTTOM FLANGE

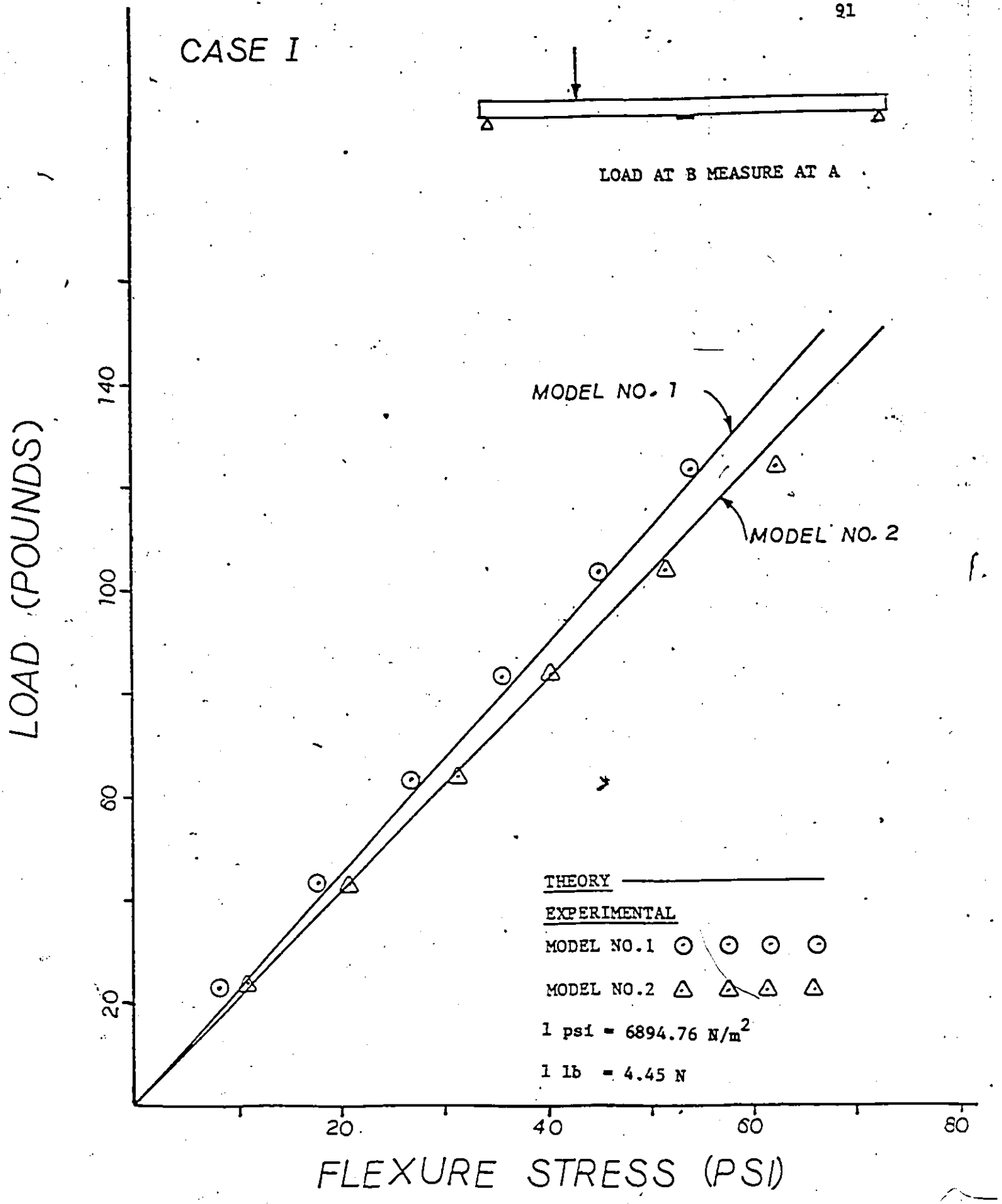

FIG.5.13 LOAD VS FLEXURE STRESS AT EXTREME SURFACE OF BOTTOM FLANGE

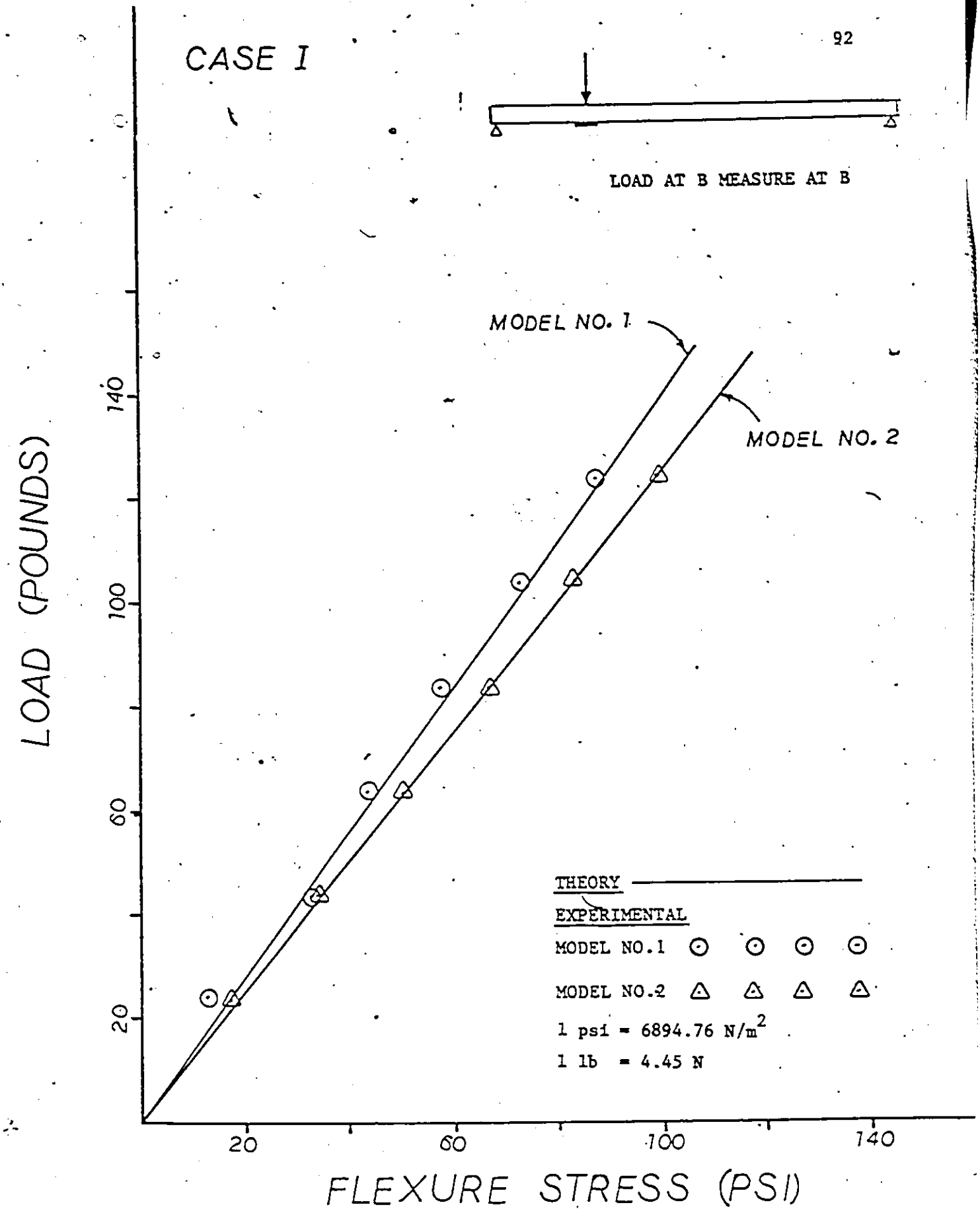

FIG.5.14 LOAD VS FLEXURE STRESS AT EXTREME SURFACE OF BOTTOM FLANGE

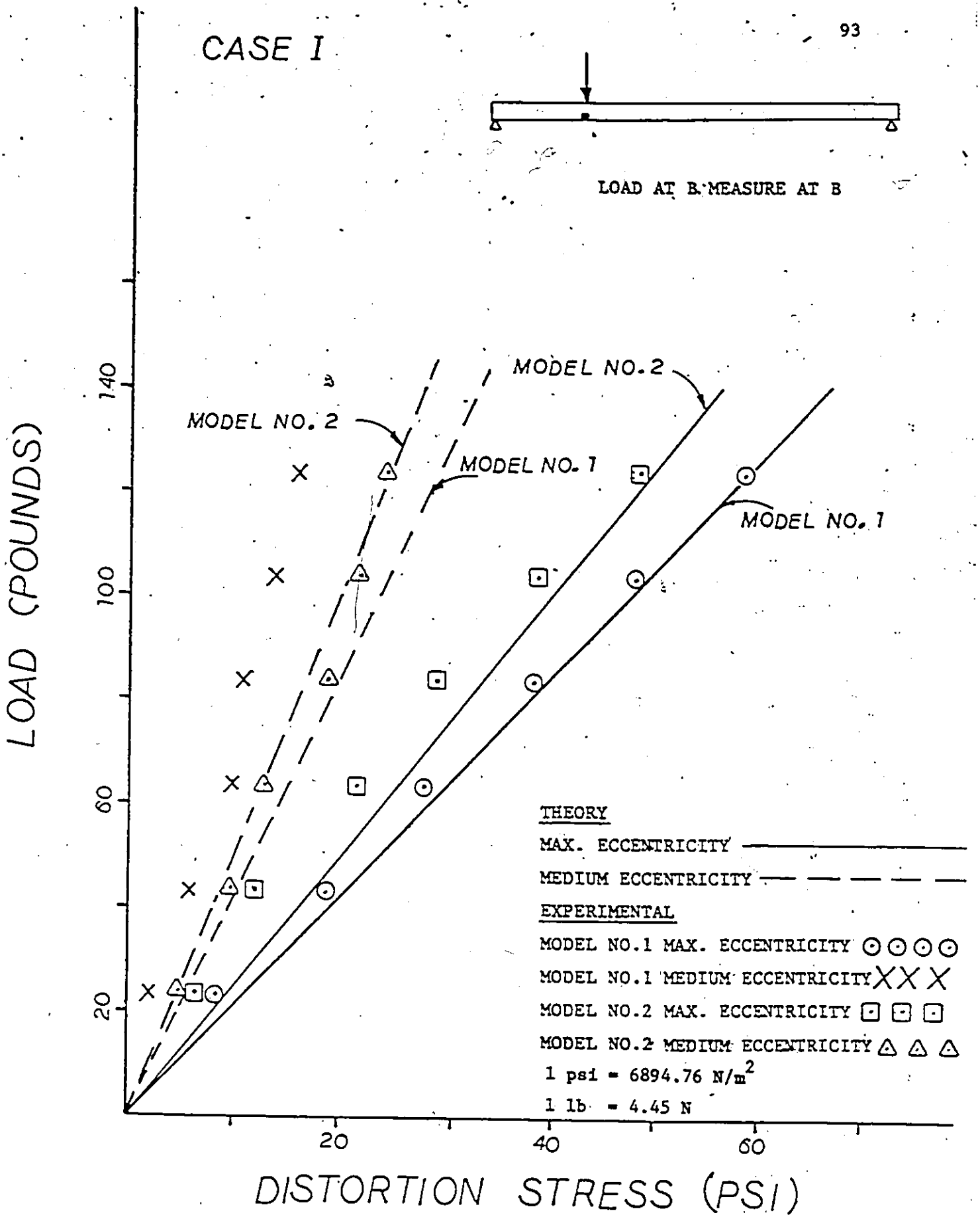

FIG.5.15 LOAD VS DISTORTION STRESS AT LOWER GAGE LOCATION

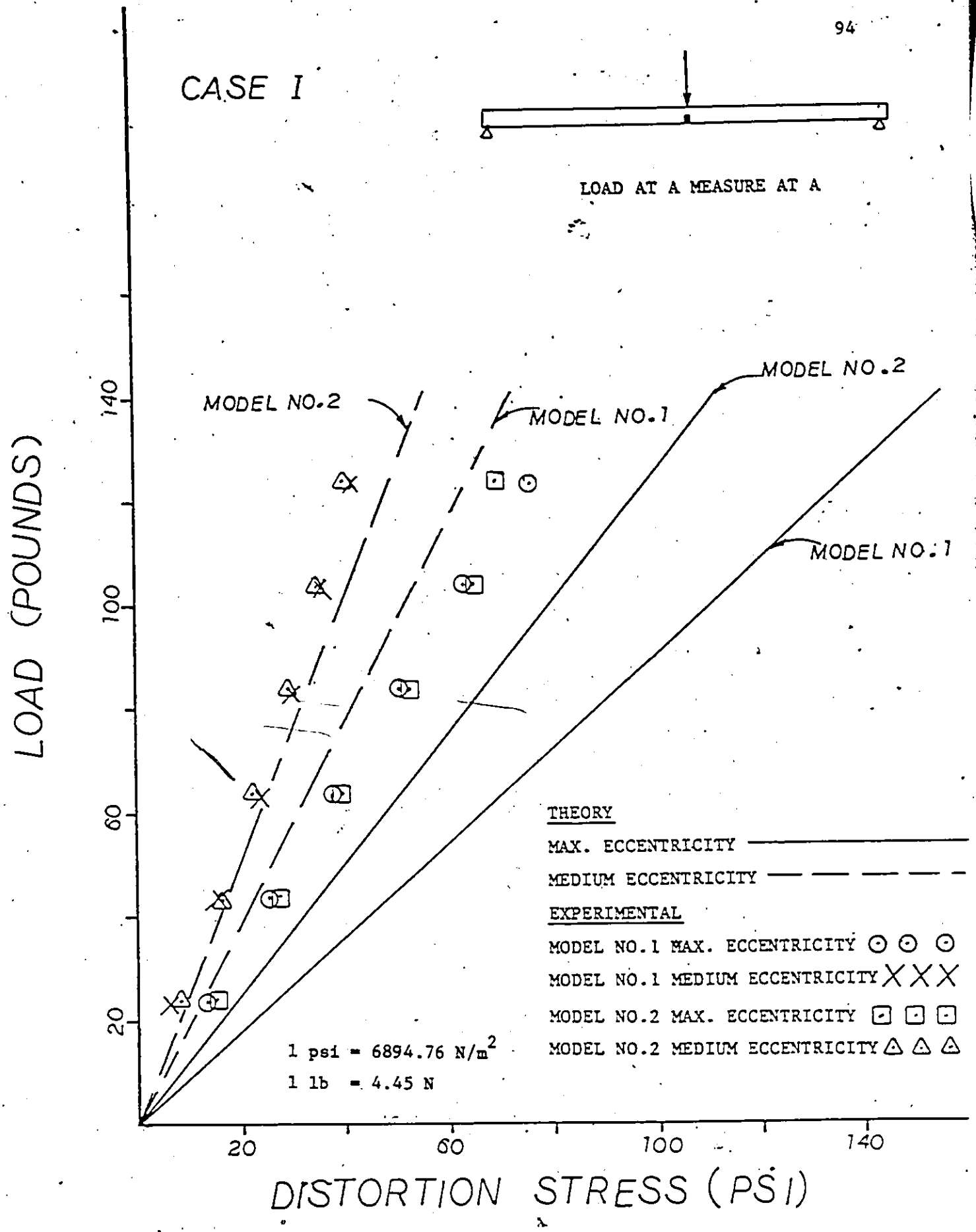

FIG.5.16 LOAD VS DISTORTION STRESS AT LOWER GAGE LOCATION

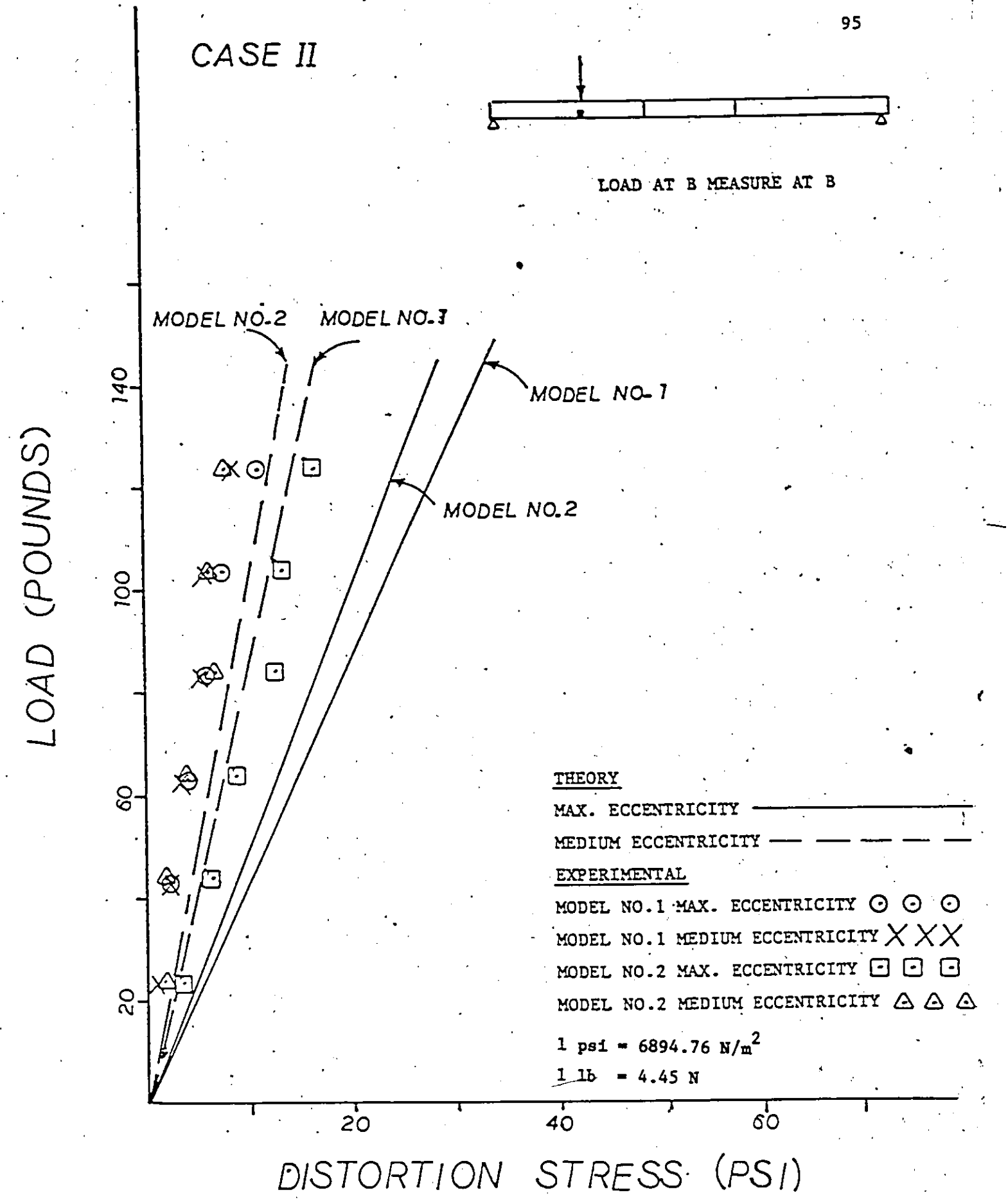

FIG.5.17 LOAD VS DISTORTION STRESS AT LOWER GAGE LOCATION

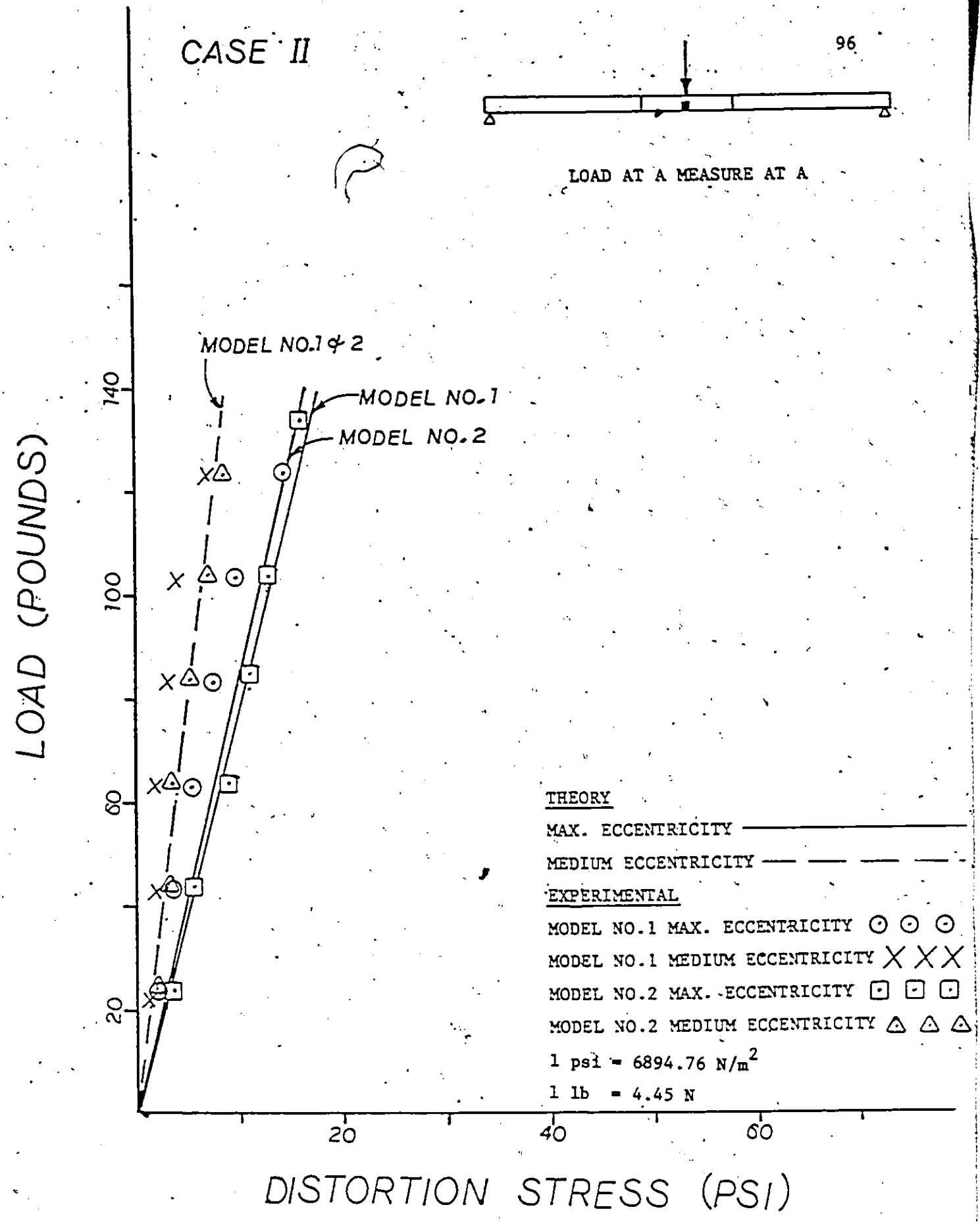

FIG.5.18 LOAD VS DISTORTION STRESS AT LOWER GAGE LOCATION

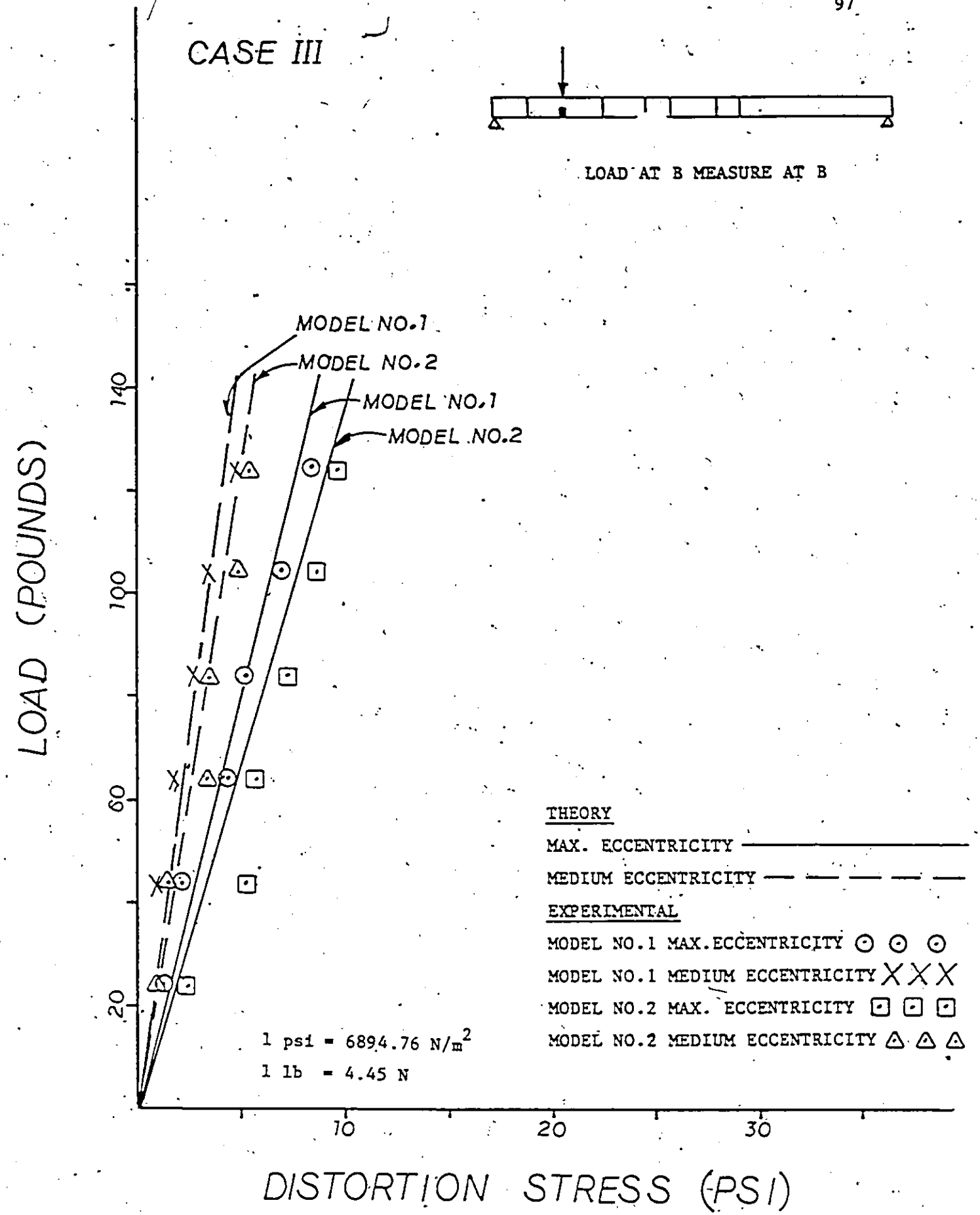

FIG.5.19 LOAD VS DISTORTION STRESS AT LOWER GAGE LOCATION

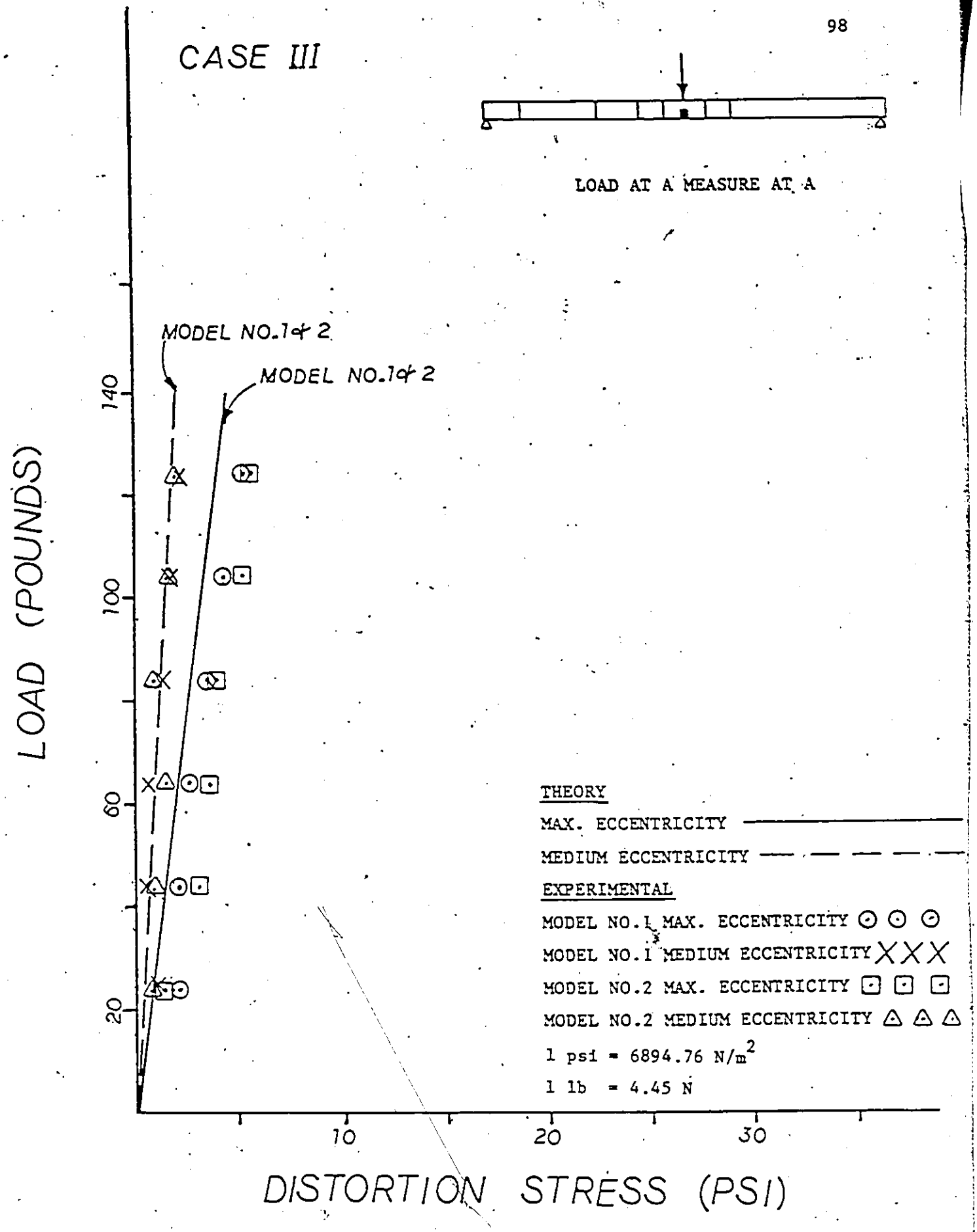

FIG.5.20 LOAD VS DISTORTION STRESS AT LOWER GAGE LOCATION

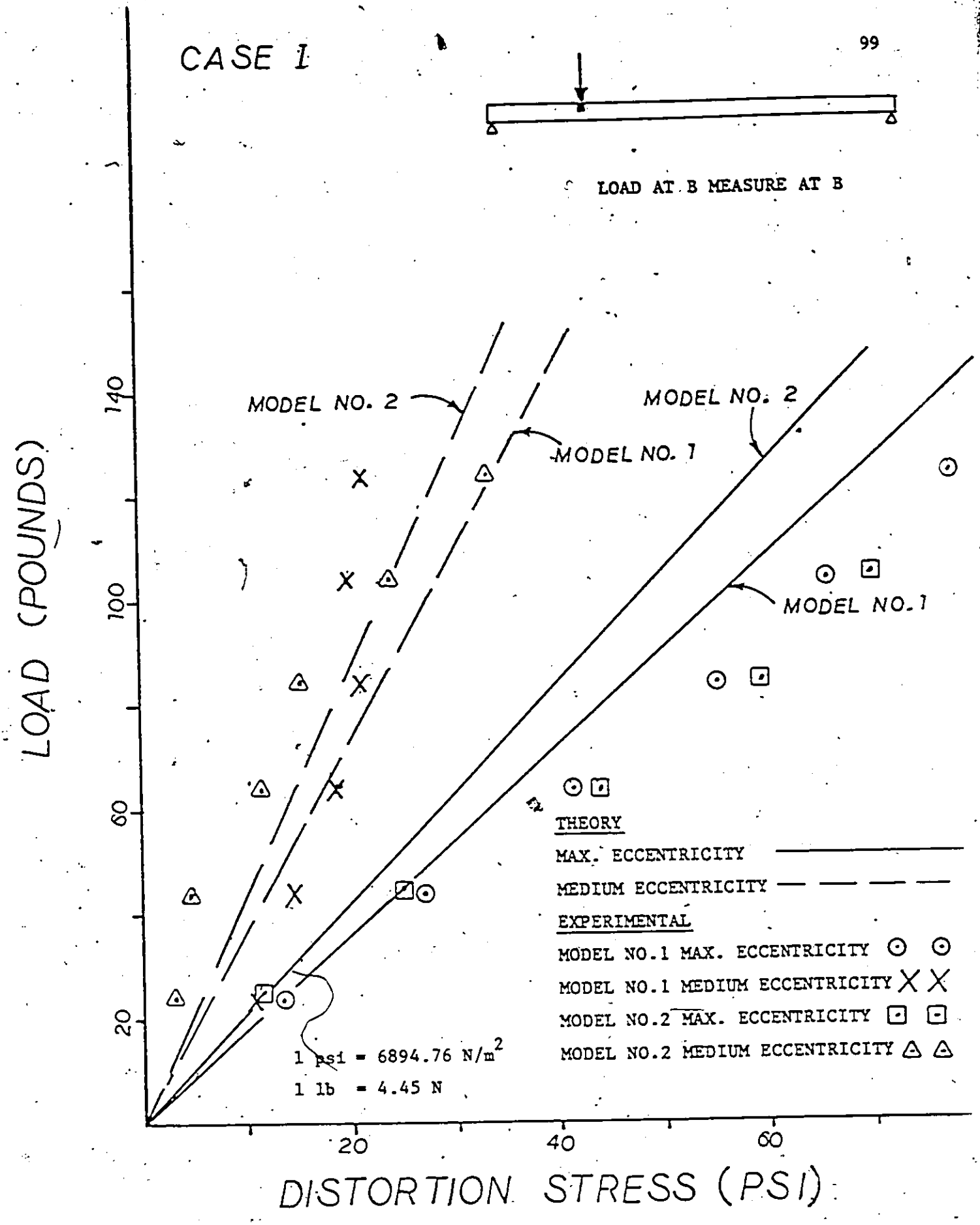

FIG.5.21 LOAD VS DISTORTION STRESS AT UPPER GAGE LOCATION

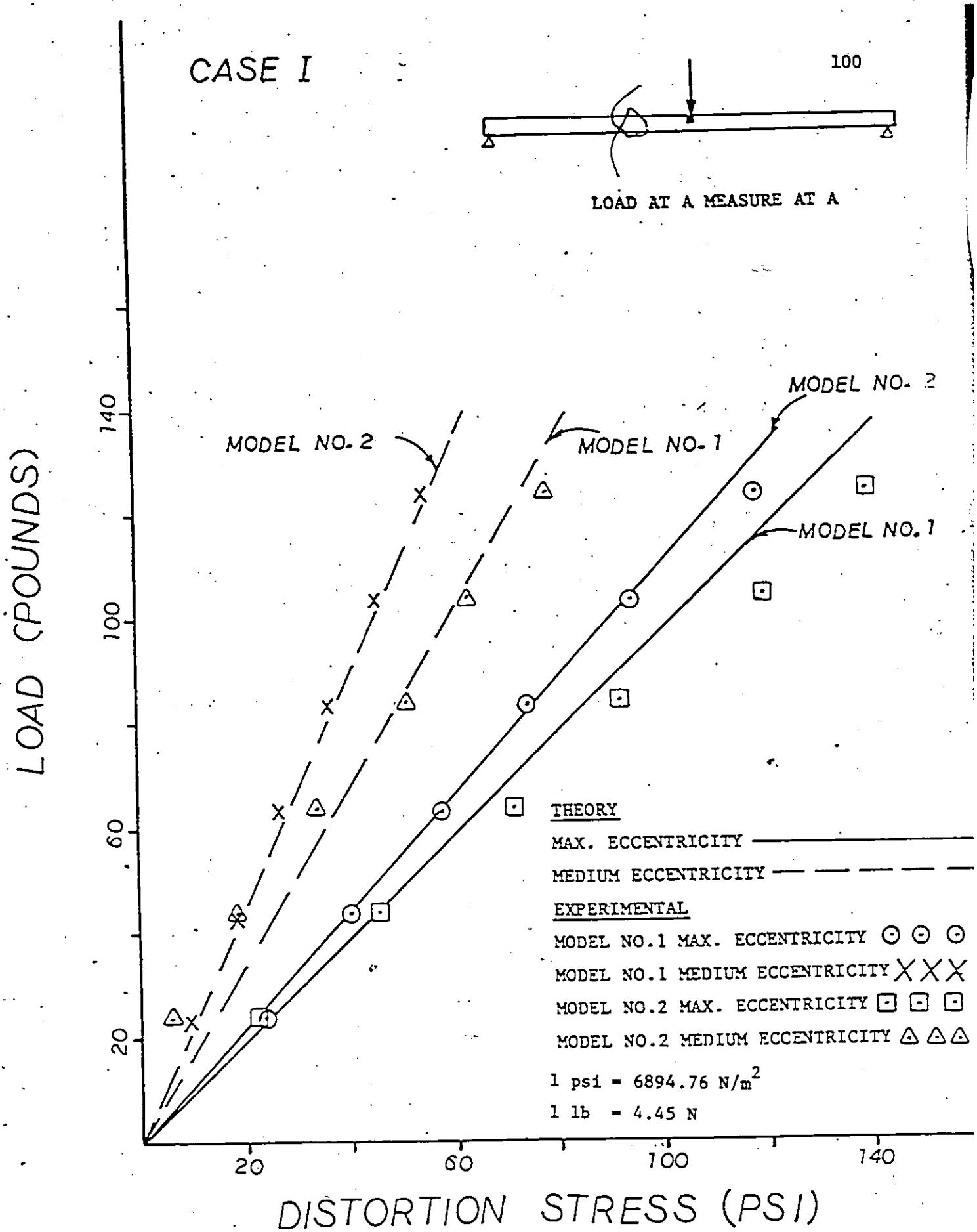

FIG.5.22 LOAD VS DISTORTION STRESS AT UPPER GAGE LOCATION

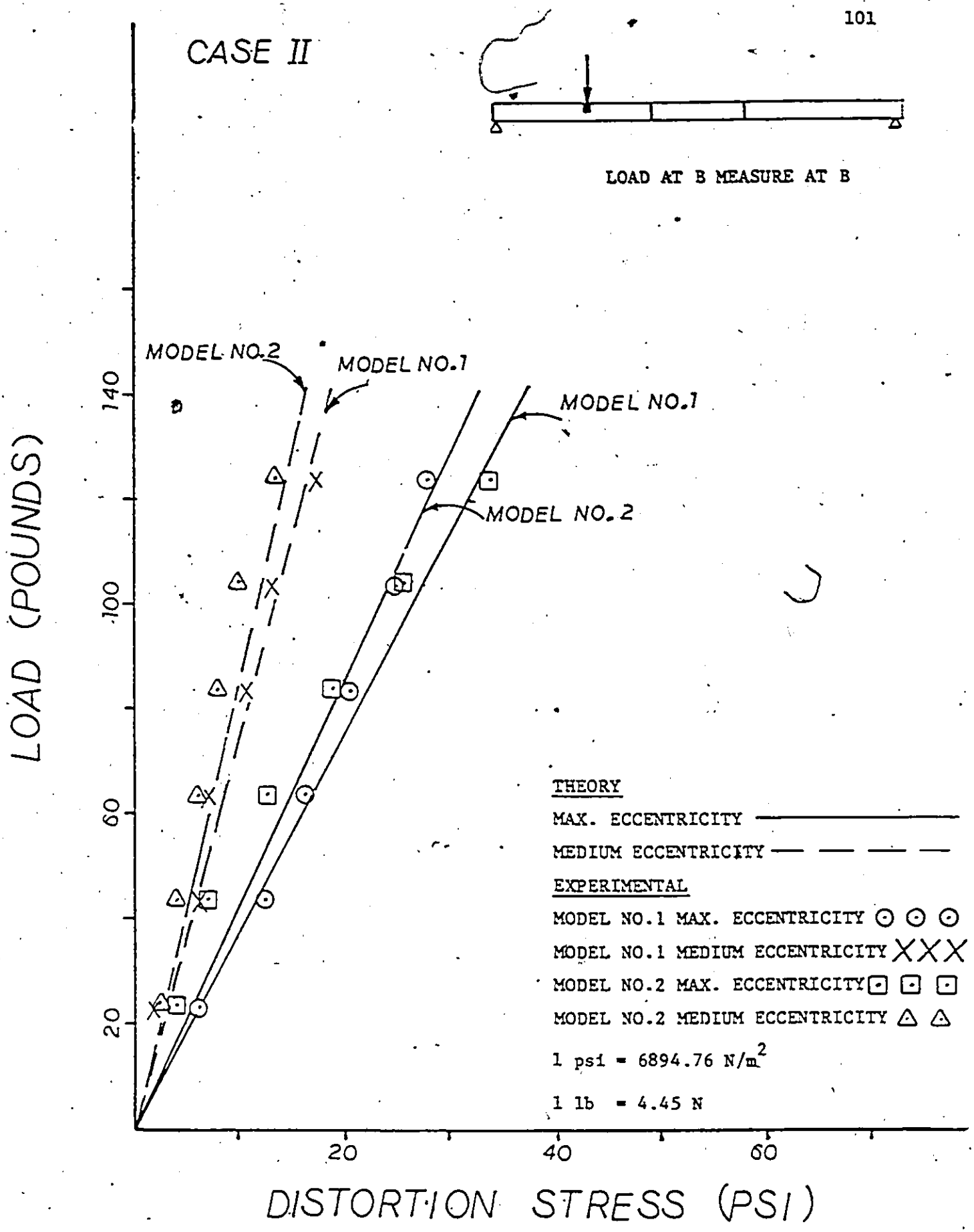

FIG.5.23 LOAD VS DISTORTION STRESS AT UPPER GAGE LOCATION

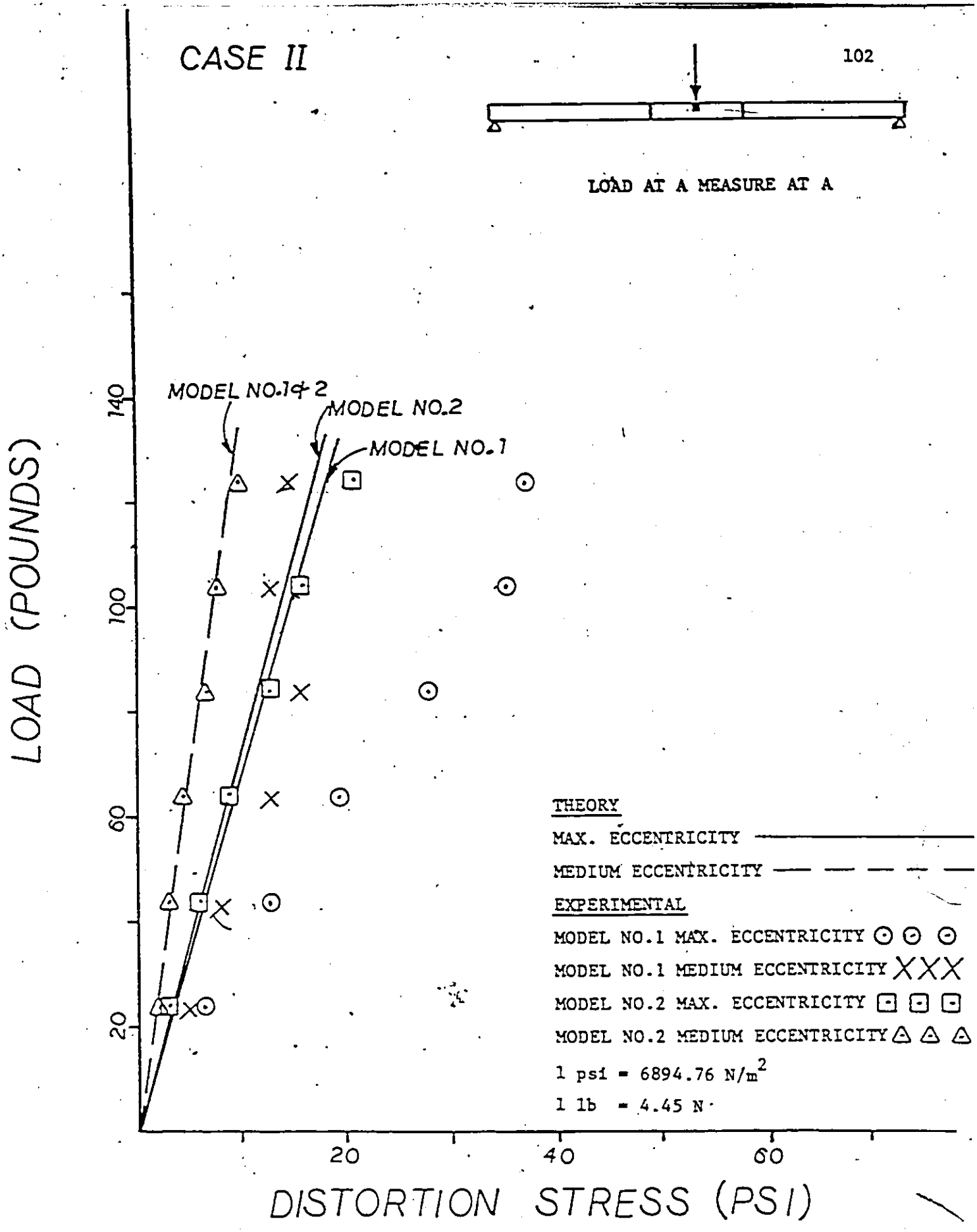

FIG.5.24 LOAD VS DISTORTION STRESS AT UPPER GAGE LOCATION

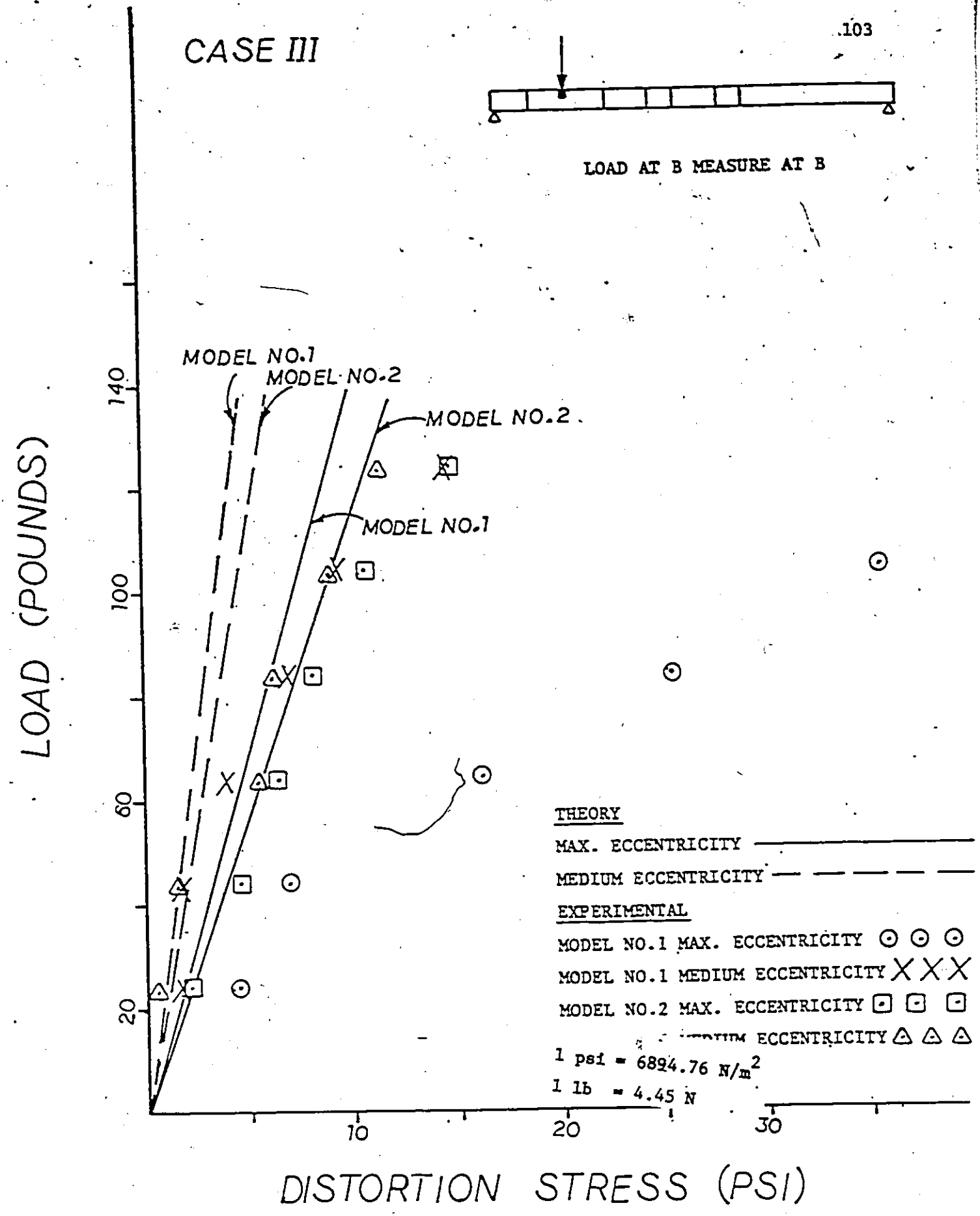

FIG.5.25 LOAD VS DISTORTION STRESS AT UPPER GAGE LOCATION

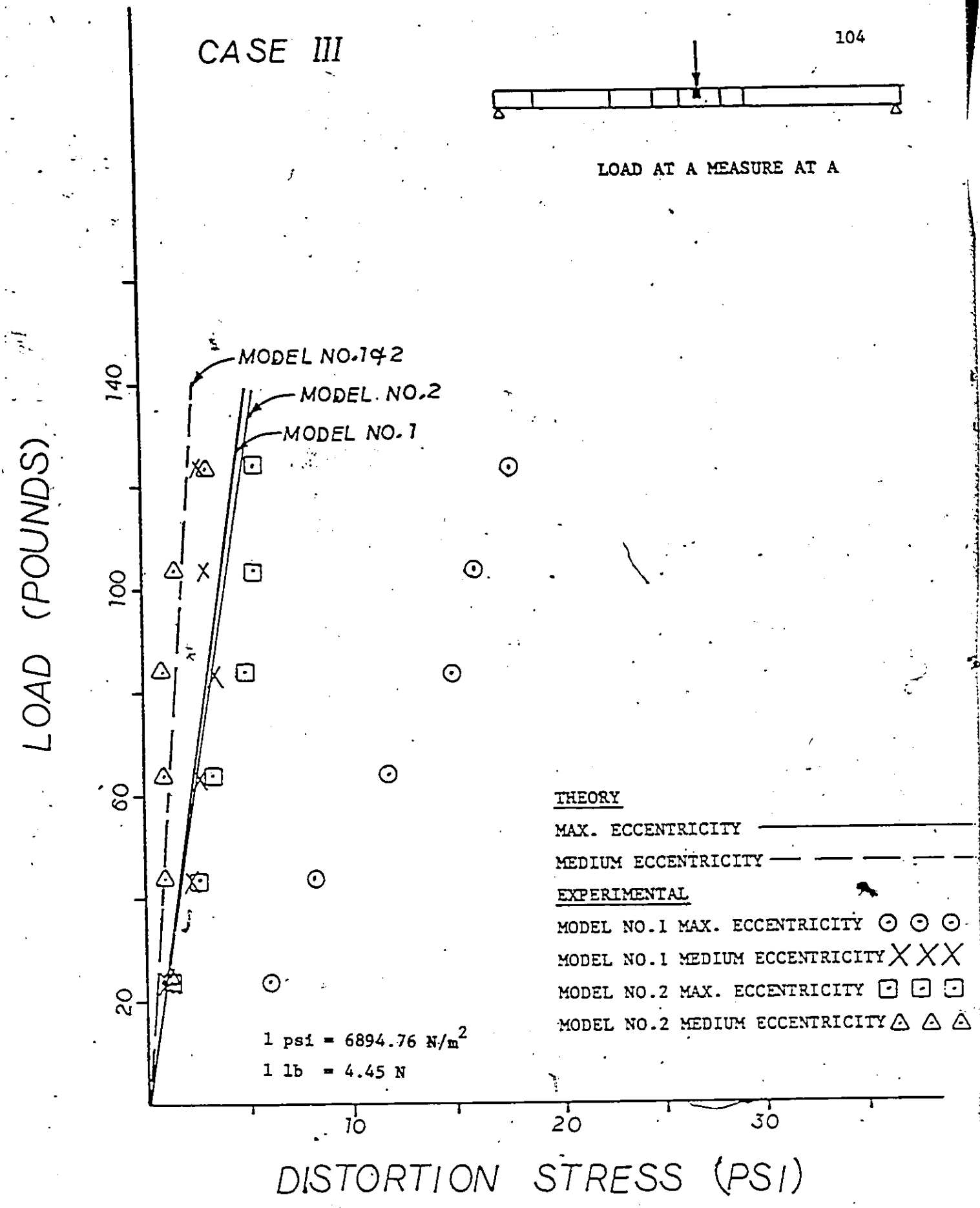

FIG.5.26 LOAD VS DISTORTION STRESS AT UPPER GAGE LOCATION

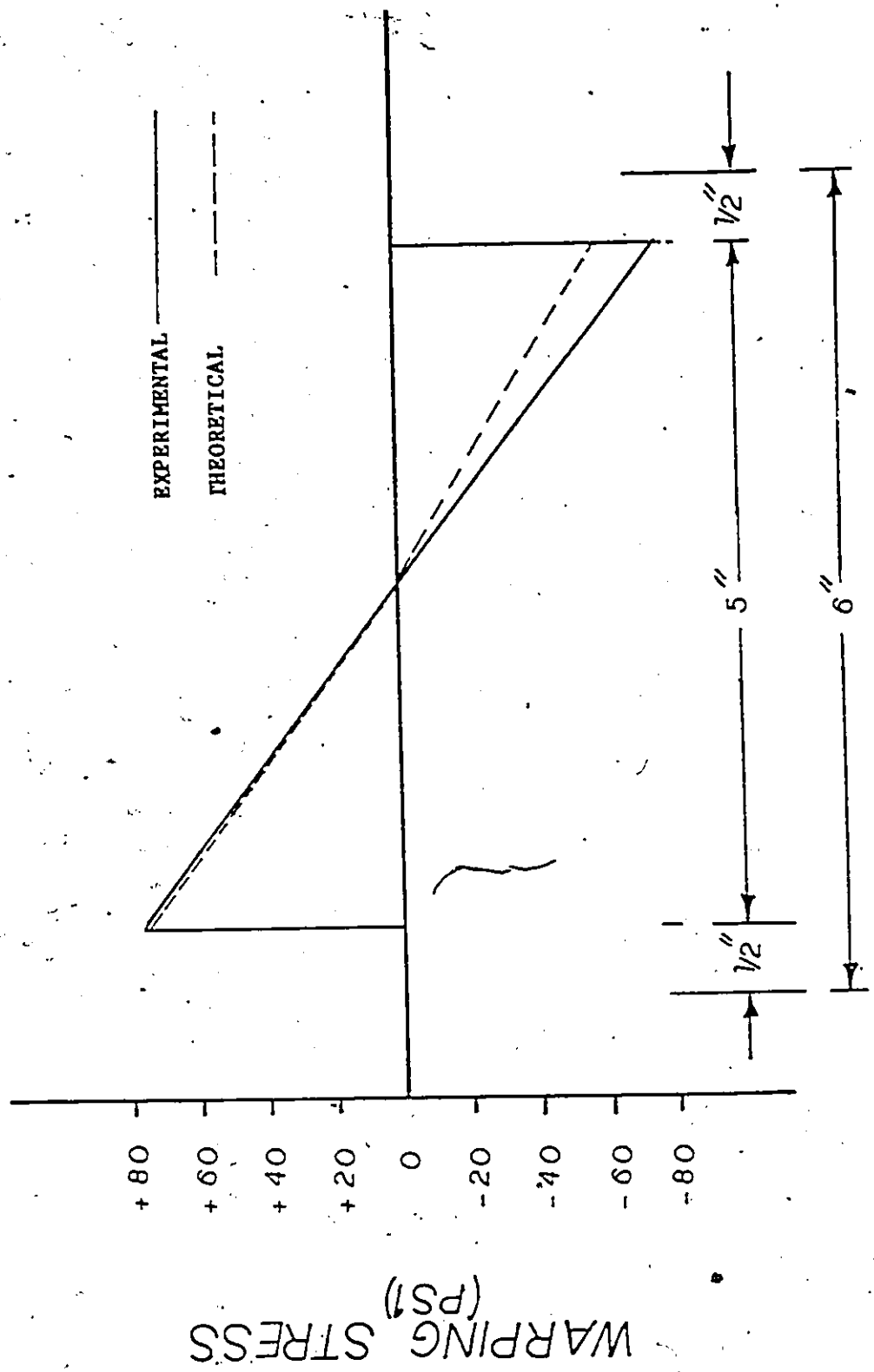

FIG.5.27 TYPICAL WARPING STRESS PATTERN AT LOADED SECTION
(MODEL NO.1- LOAD 123.8 lbs)

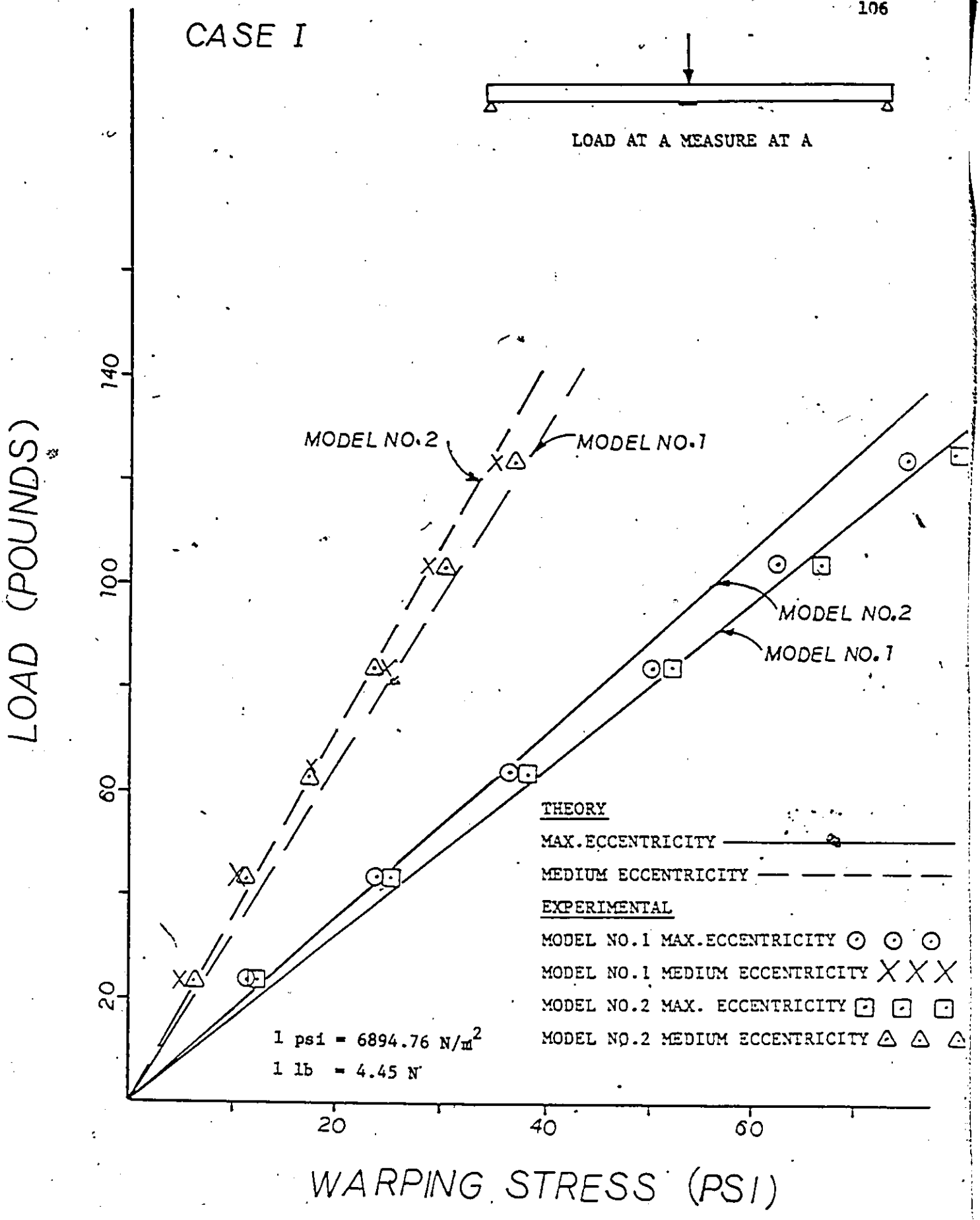

FIG.5.28 LOAD VS WARPING STRESS AT OUT SIDE GAGE LOCATION

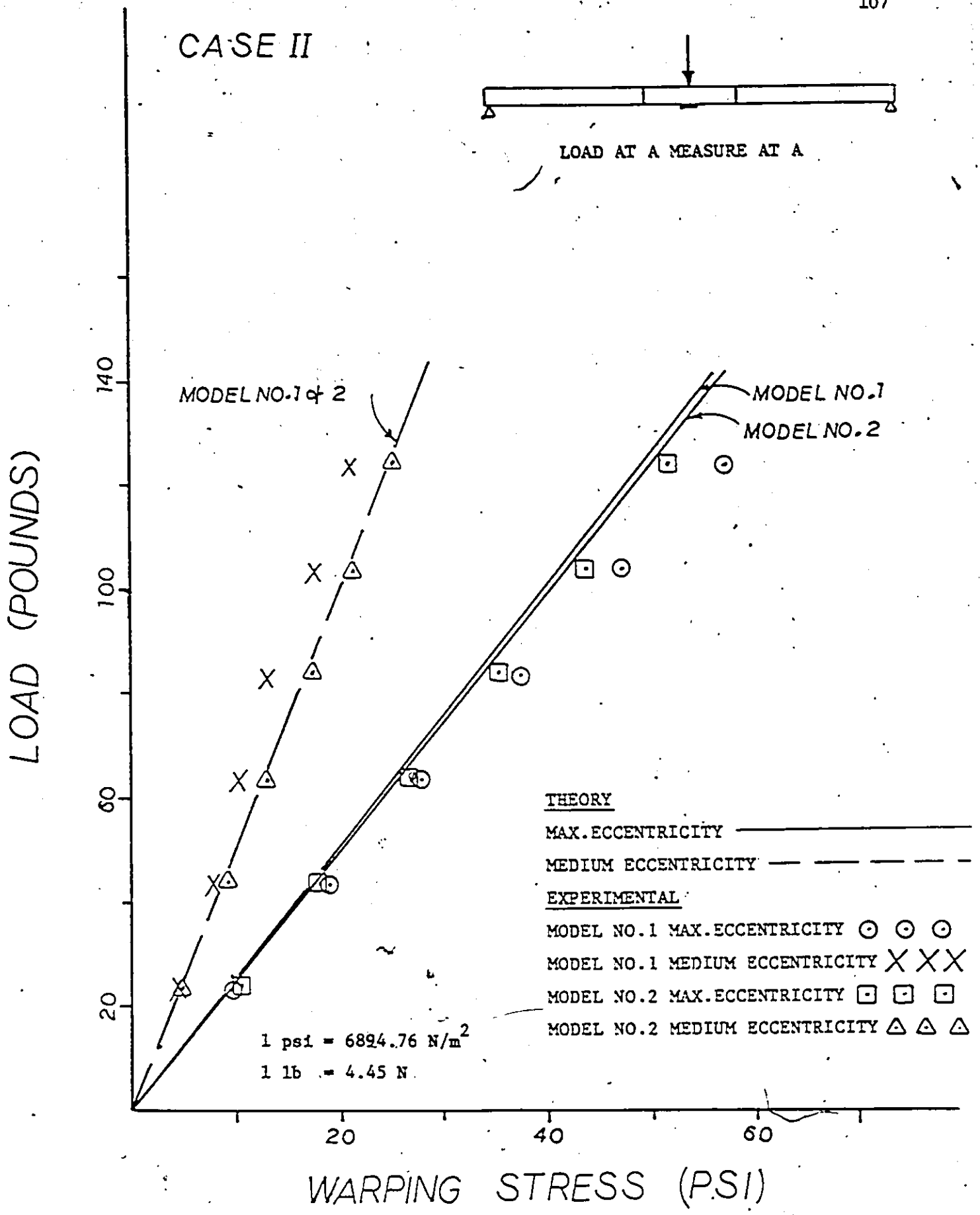

FIG.5.29 LOAD VS WARPING STRESS AT OUT SIDE GAGE LOCATION

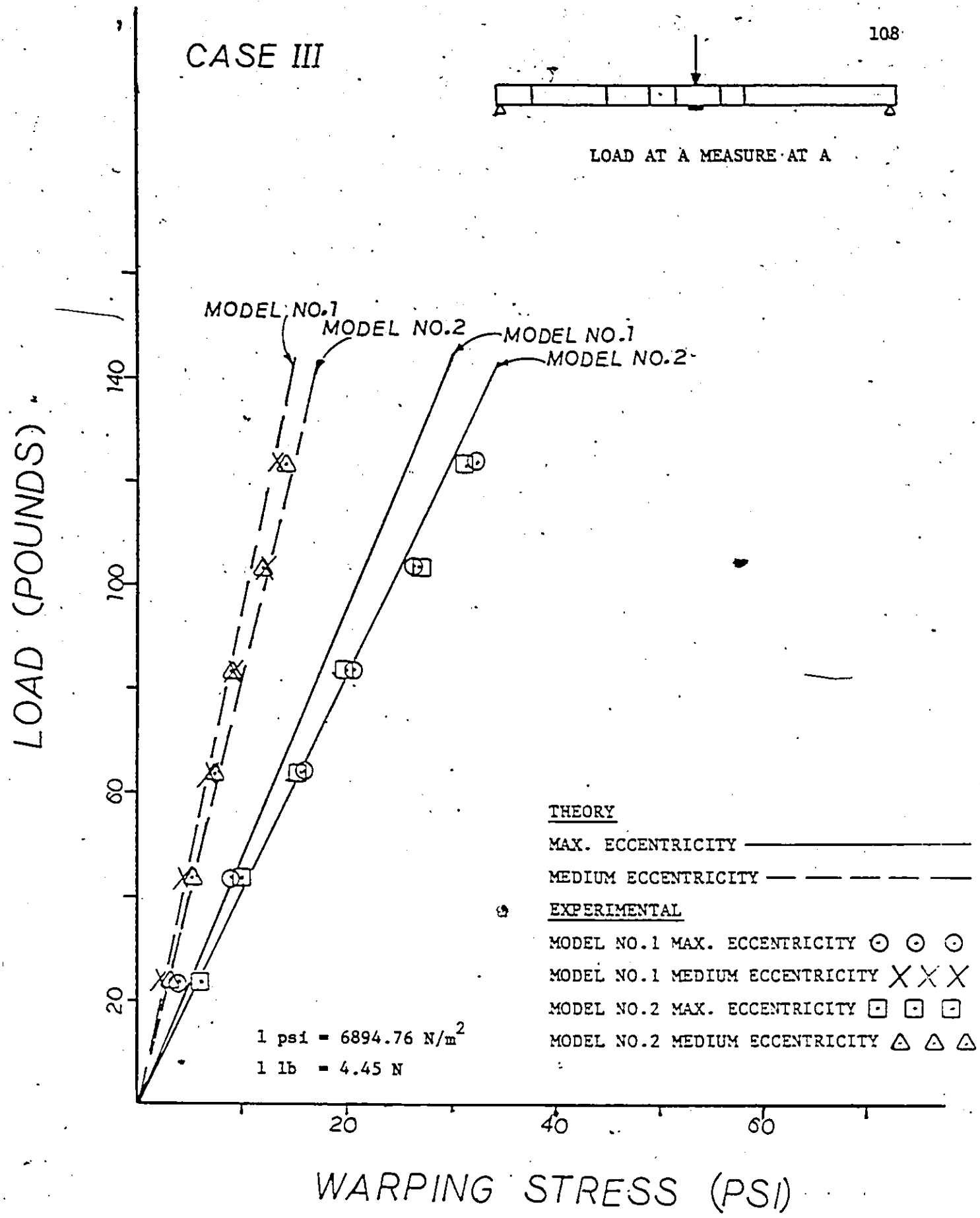

FIG.5.30 LOAD VS WARPING STRESS AT OUT SIDE GAGE LOCATION

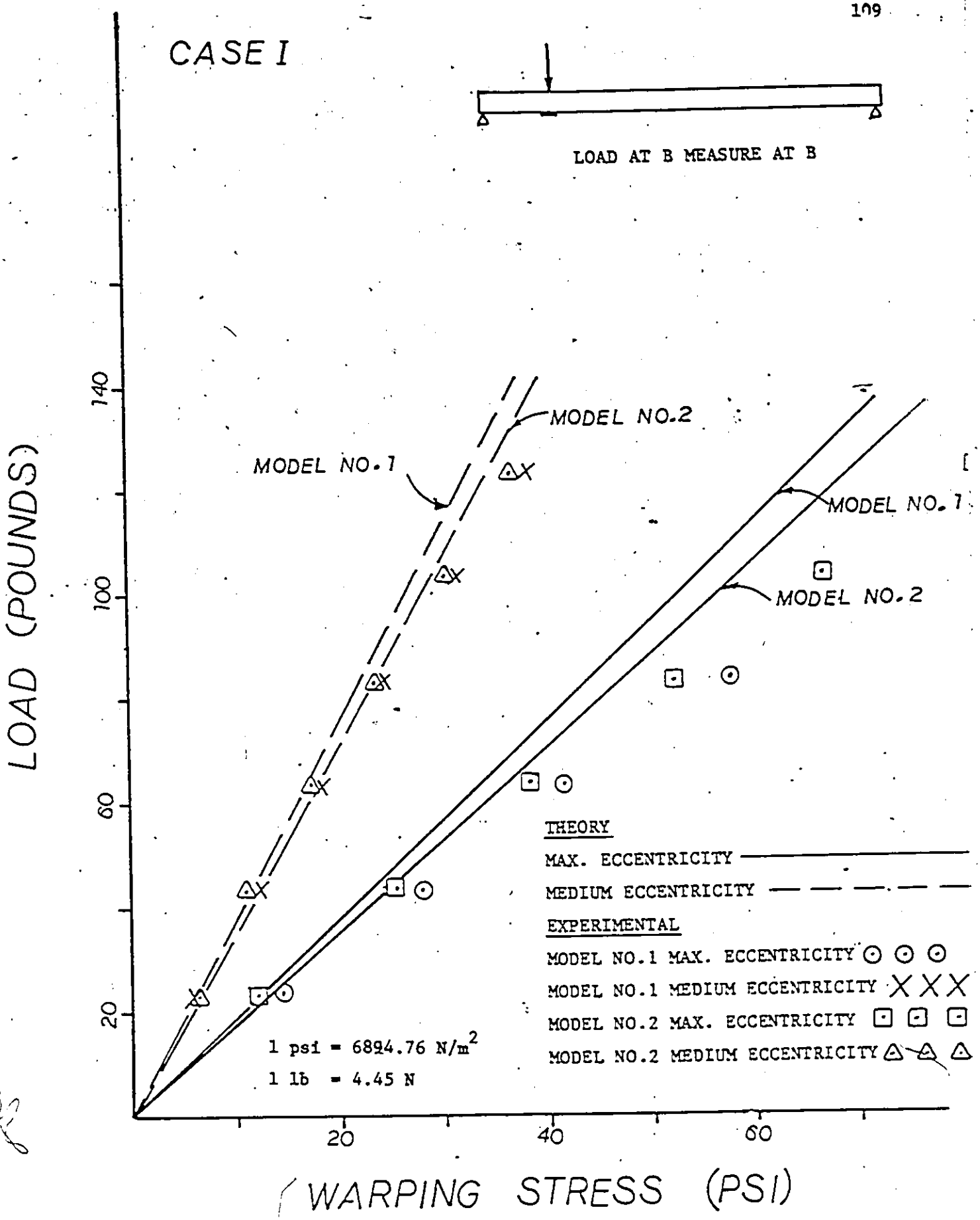

FIG.5.31 LOAD VS WARPING STRESS AT OUT SIDE GAGE LOCATION

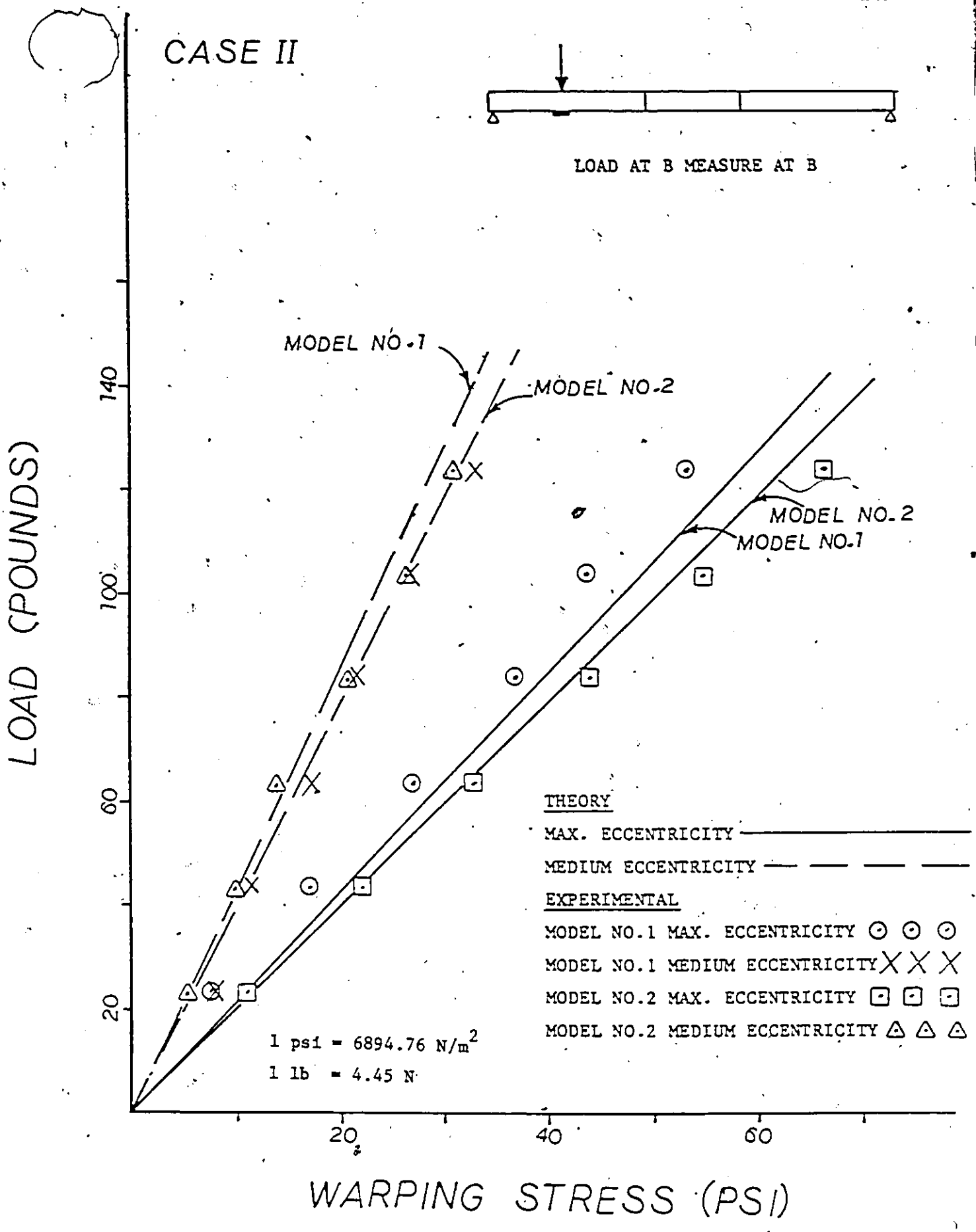

FIG.5.32 LOAD VS WARPING STRESS AT OUT SIDE GAGE LOCATION

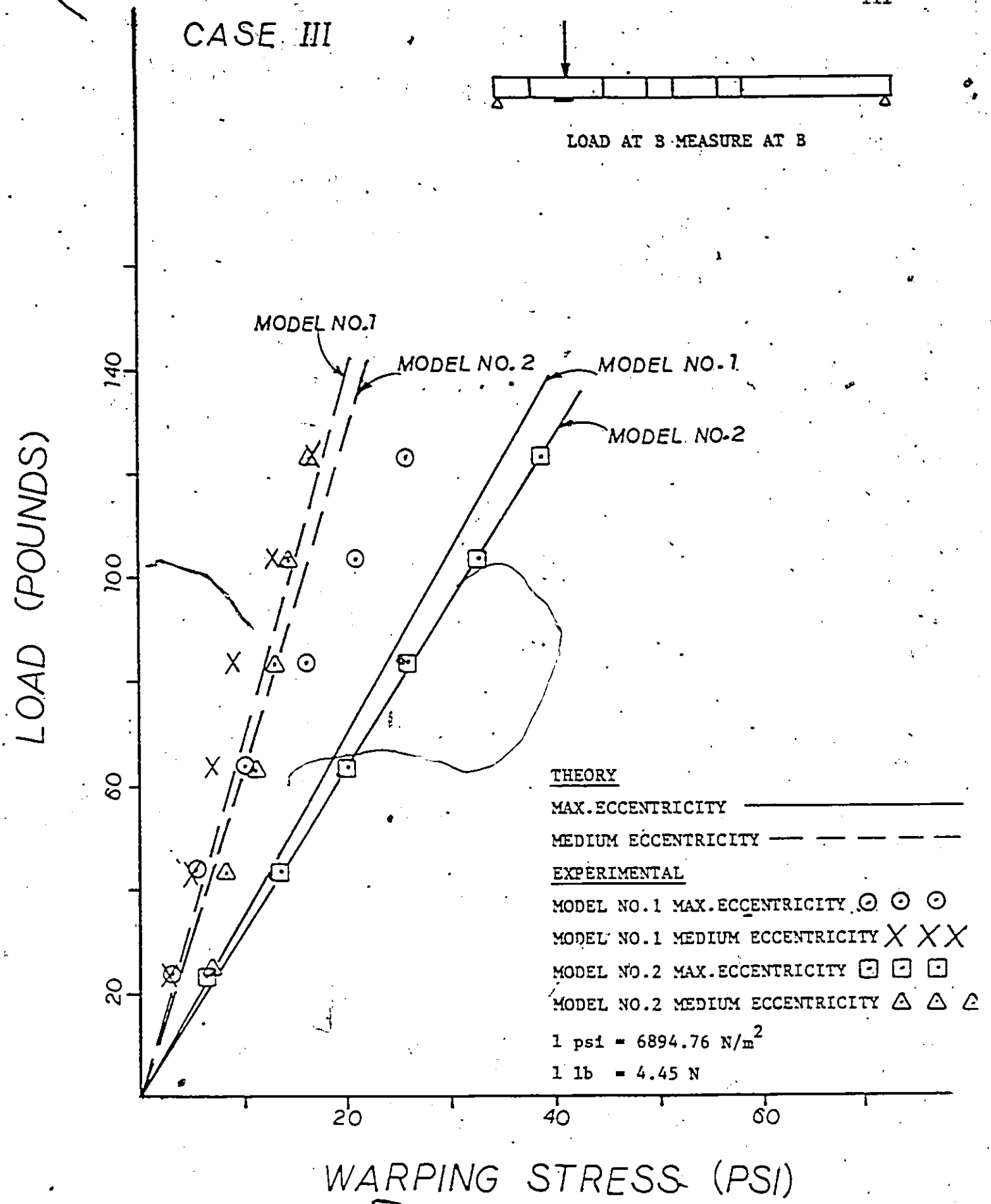

FIG.5.33 LOAD VS WARPING STRESS AT OUT SIDE GAGE LOCATION

REFERENCES

1. ASCE-AASHO Committee, "Curved Steel Box Girder Bridges-State of the Art" ASCE, J.of the Structural Division, Vol.104, No.ST11, November, 1978, pp.1719-1739.

2. Maisel,B.I. and Roll,F., "Method of Analysis and Design of Concrete Boxbeams with Side Cantilivers" Cement and Concrete Association, Technical Report 42.494, London, 1974.

3. Zienkiewicz,O.C., "The Finite Element Method in Engineering Science" McGraw-Hill, London,1971.

4. Desai,C.S.and Abel,J.F., "Introduction to the Finite Element Method", Van Nostrand Reinhold,New York.

5. Ghali,A.and Neville,A.M., "Structural Analysis " Intext, Scranton,1972.

6. Clough,R.W., "The Finite Element in Plane Stress Analysis" Proc. of the second ASCE Conference on Electronic Computation, Pittsburgh, Pennsylvania,1960.

7. Sisodiya,R.G., Ghali,A. and Cheung Y.K., "Diaphragms in Single and Double-Cell Box Girder Bridges with varing Angle of Skew", J. of ACI,Vol.29,No.7, pp415-419,July 1972.

8. Scordelis,A.C., "Analysis of Continuous Box Girder Bridges". Report No.SES 67-25, Dept. of Civil Engineering, University of California, Barkely,1967.

9. Cheung,Y.K., "Finite Strip Method in Structural Analysis", Pergamon Press,Oxford,1976.

10. Cheung,Y.K., "Folded Plate Structurs by Finite Strip Method", ASCE J. of the Structural Division,Vol.95,No.ST12, December 1969.

11. Cheung,Y.K., "Analysis of Box Girder Bridges by the Finite Strip Method", Proc. of the second Int.Symp. on Concrete Bridge Design, Chicago, April,1969, pp.357-378.

12. Loo,Y.C. and Cusens,A.R., "Development of the Finite Strip Method in the Analysis of Bridge Decks", Proc. of the Conf.on Development in Bridge Design and Construction, Crosby Lockwood, London,1971.

13. Branco, F.A., "Composite Box Girder Bridge Behaviour", thesis presented in partial fulfilment of degree of M.A.Sc, University of Waterloo, Ontario,1981.

14. Scordlis,A.C., "Analysis of Simply Supported Box Girder Bridges", Report No.SESM 66-17, Dept. of Civil Engineering, University of California, Barkeley, Calif.1966.

15. Swako,F., "Recent Developments in the Analysis of Steel Bridges using Electronic Computers", Proc.BCSA Conf. on Steel Bridges, 1963.

16. Pun,D., "Load Distribution of Composite Box Girder Bridges" M.A.Sc Thesis presented in partial fulfilment of the degree Dept. of Civil Engineering, University of Waterloo, 1979.

17. Hambly,E.C., "Bridge Deck Behaviour",Chapman and Hall,(J.W.S) London,1976.

18. Knittel,G., "Zur Berechnung des Dünnuandigen Kastentragers mit Gleichbleibendum Symmetrischen Querscmitt, (The Analysis of Thin Walled Box Girders of Constant Symmetrical Cross Section), Beton und Stahlbetonbau, September,1969.

19. Richmond,B., "Twisting of Thin-Walled Box Girder", Proc. Inst. of Civil Eng. April 1966.

20. Kupfer,H., "Kasbentrager mit Elastisch Ausgesteiftem Querschmitt unter Linien and Einzellasten,(Box Beam with Elastically Stiffened Cross Section under Live and Point Loads), H.W.Ernst und sohn, Berlin,1969.

21. Nimityongskul,P., "Influence of Intermediate Diaphragms on Load Distributionin Box Girder Bridges", Asian Institute of Technology, Bangkok, Thiland,1973,pp.208-216.

22. Abdel-Samad,S.R.,Wright,R.N.,and Robinson,A.R., "Analysis of Box Girders with Diaphragms" J. of Structural Division, ASCE, Vol.94, No.ST.10, Proc.Paper 6153, Oct. 1968, pp2231-2256.

23. V.Z. Vlasov, "Thin-Walled Elastic Beams", U.S. Dept. of Commarce, PST Cat.No.428, 1959.

24. Dalton,D.C. and Richmond,B., "Twisting of Thin Walled Box Girders of Trapezoidal Cross Section", Proceeding Institute of Civil Engineering, Vol.39, Jan.1968, pp.61-73.

25. Wright,R.N., Abdel-Samad, S.R. and Robinson,A.R., "B.E.F Anology for Analysis of Box Girder", J. of the Structural Division, ASCE, Vol.94, No.ST7, Proc.Paper 6025, July 1968, ppl719-1743.

26. Rajagopalan, N., Rajagoplan,B.K., "Distortional Analysis of Single Cell Prismatic Box Girders", Indian Roads Congress, Journal of Vol.41, No.2, Dec. 1980, pp.389-407.

27. The Subcommittee of Inquiry into the Basis of Design and Method of Erection of Steel Box Girder Bridges: Inerim Design and Workmanship Rule, Her Majesty's Stationery Office, 1973.

28. Sakai,F. and M. Nagai., "A Recommendation on the Design of Intermediate Diaphragms in Steel Box Girder Bridges", Proc. of JSCE, No.261, May 1977 (In Japanese)

29. Sakai,F. and M. Nagai, "A proposal for INtermediate Diaphragm Design in Curved Steel Box Girder Bridges", Proc. of JSCE,No.305, January,1981 (In Japanese)

30. Komatsu, Sadao., Nagai,Masatsugu., " Recommendation for design of Intermediate Diaphragms in Box Girders", Trans. JSCE, V14, March 1984, pp. 121-126

31. Myers,D.E. and Cooper,P.B. "BOX Girder Model Studies" J. of the Structural Division, ASCE, vol.95, No.ST12, Proc.Paper 6966, Dec.1969, pp.2845-2861

32. Godden, W.G., and Aslam,M., "Model Studies of Skew Multicell Girder Bridges", J. Eng. Mech. Div., ASCE, Vol.99, No.EMI, February 1973, pp.201-223

33. Mattock,A.H. and Johnstone, S.B., "Behaviour under Load of Composite Box Girder Bridges", J. Struc. Div.,ASCE, Vol.94, No. St10, October 1968, pp. 2351-2370

34. Goldberg,J.E and Leve, H.L., "Theory of Prismatic Folded Plate Structure ", Pub. IABSE, Vol.17, 1957. pp.59-86

35. Maggard,S.P and Parr, D.H., "Primary Stress in Thin Walled Flexural Members", Technical Report No. 43, Engineering Experimental Station, New Mexico State University, Las Cruces, Max, Feb.1968.

36. Pama, R.P., Pribadi, D.Z., Lee, S.L and Nimityongskul,P., "Model Studies of Double Cell Box Girder Bridges with Intermediate Diaphragms", Transp. Res. Board, Bridge Engineering , Proc. of a Conf. St. Louis, Mo, Sept.1978, pp. 53-64.

37. Green, R., "Composite Box Girder Bridges- The Construction Phase", Canadian Conf. on Structural Engineering, CISC, Toronto, Ontario, 1978.

38. Zanoni,Edward, "Model Studies of Folded Plate Structure", M.S. Thesis, Lehigh University, Bethlemham, Pa.1962.

39. S. Timoshenko and J.N.Goodier, "Theory of Elasticity",McGraw-Hill Book Company, Inc.pp.177.

Appendix A

TABLE

TABLE- 1 SUMMARY OF TESTING PROGRAM

LOCATION OF DIAPHRAGMS FIG. 4.14	SECTION	LOADING POINT
CASE I 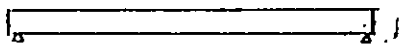 WITHOUT DIAPHRAGM	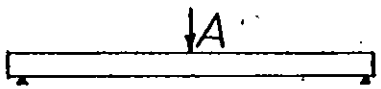 FOR DETAIL SEE FIG. 4.9 & 4.11 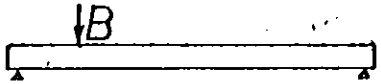 FOR DETAIL SEE FIG. 4.10 & 4.12	P_1 = CONCENTRIC LOADING P_2 = MEDIUM ECCENTRICITY P_3 = MAX. ECCENTRICITY
CASE II 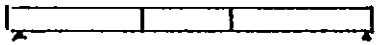 TWO DIAPHRAGMS	SAME AS ABOVE	SAME AS ABOVE
CASE III 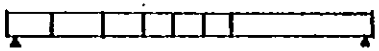 SIX DIAPHRAGMS	SAME AS ABOVE	SAME AS ABOVE

TABLE-2

REDUCTION OF DISTORTION AND WARPING STRESSES

DUE TO DIAPHRAGMS

(FOR LOADING 123.81bs-550.66N)

LOCATION OF DIAPHRAGMS	THEORY % OF BENDING STRESS		EXPERIMENTAL % OF BENDING STRESS	
	SECTION A	SECTION B	SECTION A	SECTION B
MODEL NO. 1				
Case-I				
Distortion Stress at Bottom of Web	85	65	60	67
Distortin Stress at Top of Web	98	75	94	89
Warping Stress	50	98	61	78
Case-II				
Distortion Stress at Bottom of Web	10	31	11	12
Distortion Stress at Top of Web	12	36	29	31
Warping Stress	32	64	45	58
Case-111				
Distortion Stress at Bottom of Web	2.5	8.6	4	9
Distortion Stress at Top of Web	3	10	14	60
Warping Stress	17	39	26	29

TABLE-3

REDUCTION OF DISTORTION AND WARPING STRESSES

DUE TO DIAPHRAGMS

(FOR LOADING 123.81bs-550.66N)

LOCATION OF DIAPHRAGMS	THEORY % OF BENDING STRESS		EXPERIMENTAL % OF BENDING STRESS	
	SECTION A	SECTION B	SECTION A	SECTION B
MODEL NO. 2				
Case-I				
Distortion Stress at Bottom of Web	58	51	41	49
Distortin Stress at Top of Web	69	60	80	84
Warping Stress	43	71	41	83
Case-II				
Distortion Stress at Bottom of Web	9	25	9	17
Distortion Stress at Top of Web	11	30	12	34
Warping Stress	30	64	30	66
Case-III				
Distortion Stress at Bottom of Web	2	9	3	10
Distortion Stress at Top of Web	3	11	3	15
Warping Stress	18	39	18	39

Appendix B

EXPERIMENTAL READINGS

TABLE- 1
EXPERIMENTAL STRAIN READINGS AND STRESSES FOR CASE- I
(MODEL NO.1, MEDIUM ECCENTRICITY)

SECTION	TYPE OF STRESS	LOCATION	GAGE NO.	LOADS (lb)	STRAIN GAGE READING (10^{-6} IN/IN)		DIFFERENCE (10^{-6} IN/IN)	E (PSI) 10^6	STRESS (PSI)
					P_1	P_2			
A	Distortion	Upper gage	1	23.8	33	12	21	0.440	9.24
				43.8	75	33	42		18.48
				63.8	117	56	61		26.84
				83.8	160	77	83		36.52
				103.8	203	99	104		45.52
				123.8	245	121	124		54.56
		Lower gage	6	23.8	- 15	- 28	13		5.72
				43.8	- 24	- 60	36		15.84
				63.8	- 36	- 90	54		23.76
				83.8	- 49	- 118	69		30.36
				103.8	- 63	- 144	81		35.64
				123.8	- 77	- 172	95		41.80
B	Distortion	Upper gage	8	23.8	60	35	25		11.00
				43.8	108	75	33		14.52
				63.8	160	118	42		18.48
				83.8	210	162	48		21.12
				103.8	250	205	45		19.80
				123.8	301	252	49		21.56
		Lower gage	13	23.8	- 19	- 15	6		2.64
				43.8	- 16	- 30	14		6.16
				63.8	- 23	- 46	23		10.12
				83.8	- 37	- 62	25		11.00
				103.8	- 46	- 78	32		14.08
				123.8	- 56	- 94	38		16.72

TABLE - 2
EXPERIMENTAL STRAIN READINGS AND STRESSES FOR CASE - I
(MODEL NO.1, MEDIUM ECCENTRICITY)

SECTION	TYPE OF STRESS	LOCATION	GAGE NO.	LOADS (lb)	STRAIN GAGE READING (10^{-6} IN/IN)		DIFFERENCE (10^{-6} IN/IN)	E (PSI) 10^6	STRESS (PSI)
					P_1	P_2			
A	Warping	Bottom flange	3	23.8	42	53	11	0.440	4.84
				43.8	90	114	24		10.56
				63.8	135	176	41		18.04
				83.8	180	236	56		24.64
				103.8	227	293	66		29.04
				123.8	275	356	81		35.64
B	Warping	Bottom flange	10	23.8	30	43	13		5.72
				43.8	65	93	28		12.32
				63.8	100	142	42		18.48
				83.8	134	190	56		24.64
				103.8	169	242	73		32.12
				123.8	205	293	88		38.72

TABLE - 3
EXPERIMENTAL STRAIN READINGS AND STRESSES FOR CASE- II
(MODEL NO.1, MEDIUM ECCENTRICITY)

SECTION	TYPE OF STRESS	LOCATION	GAGE NO.	LOADS (lb)	STRAIN GAGE READING (10^{-6} IN/IN)		DIFFERENCE (10^{-6} IN/IN)	E (PSI) 10^6	STRESS (PSI)
					P_1	P_2			
A	Distortion	Upper gage	1	23.8	23	11	12	0.440	5.28
				43.8	48	30	18		7.92
				63.8	78	48	30		13.20
				83.8	102	65	37		16.28
				103.8	135	96	29		12.76
				123.8	164	128	36		15.84
		Lower gage	6	23.8	- 19	- 15	4		1.76
				43.8	- 35	- 31	4		1.76
				63.8	- 49	- 45	4		1.76
				83.8	- 66	- 59	7		3.08
				103.8	- 84	- 75	9		3.96
				123.8	-106	- 90	16		7.04
B	Distortion	Upper gage	8	23.8	34	38	4		1.76
				43.8	68	82	14		6.16
				63.8	107	123	16		7.04
				83.8	145	169	24		10.56
				103.8	182	212	30		13.20
				123.8	220	260	40		17.60
		Lower gage	9	23.8	- 10	- 12	2		0.88
				43.8	- 18	- 24	6		2.64
				63.8	- 27	- 35	8		3.52
				83.8	- 36	- 48	12		5.28
				103.8	- 46	- 60	14		6.16
				123.8	- 55	- 75	20		8.80

TABLE - 4

EXPERIMENTAL STRAIN READINGS AND STRESSES FOR CASE - II

(MODEL NO.1, MEDIUM ECCENTRICITY)

SECTION	TYPE OF STRESS	LOCATION	GAGE NO.	LOADS (lb)	STRAIN GAGE READING (10^{-6} IN/IN)		DIFFERENCE (10^{-6} IN/IN)	E (PSI) 10^6	STRESS (PSI)
					P_1	P_2			
A	Warping	Bottom flange	3	23.8	39	50	11	0.440	4.84
				43,8	80	98	18		7.92
				63.8	124	147	23		10.12
				83.8	168	197	29		12.76
				103,8	210	250	40		17.60
				123.8	254	302	48		21.12
B	Warping	Bottom flange	10	23.8	26	44	18		7.92
				43.8	55	81	26		11.44
				63.8	85	125	40		17.60
				83.8	119	169	50		22.00
				103.8	153	215	62		27.28
				123.8	182	258	76		33.44

TABLE - 5

EXPERIMENTAL STRAIN READINGS AND STRESSES FOR CASE - III

(MODEL NO.1, MEDIUM ECCENTRICITY)

SECTION	TYPE OF STRESS	LOCATION	GAGE NO.	LOADS (lb)	STRAIN GAGE READING (10^{-6} IN/IN)		DIFFERENCE (10^{-6} IN/IN)	E (PSI) 10^6	STRESS (PSI)
					P_1	P_2			
A	Distortion	Upper gage	1	23.8	23	21	2	0.440	0.88
				43.8	48	43	5		2.20
				63.8	72	66	6		2.64
				83.8	93	85	8		3.52
				103.8	113	106	7		3.08
				123,8	132	126	6		2.64
		Lower gage	6	23.8	- 19	- 19	0		0.00
				43.8	- 32	- 33	1		0.44
				63.8	- 47	- 46	1		0.44
				83.8	- 62	- 59	3		1.32
				103.8	- 78	- 74	4		1.76
				123.8	- 95	- 90	5		2.20
B	Distortion	Upper gage	8	23.8	44	48	4		1.76
				43.8	88	92	4		1.76
				63.8	123	132	9		3.96
				83.8	156	172	16		7.04
				103.8	190	212	22		9.68
				123.8	218	253	35		15.40
		Lower gage	9	23.8	- 10	- 10	0		0.00
				43.8	- 20	- 22	2		0.88
				63.8	- 30	- 34	4		1.76
				83.8	- 40	- 46	6		2.64
				103.8	- 49	- 57	8		3.52
				123.8	- 58	- 69	11		4.84

TABLE - 6
EXPERIMENTAL STRAIN READINGS AND STRESSES FOR CASE - III
(MODEL NO.1, MEDIUM ECCENTRICITY)

SECTION	TYPE OF STRESS	LOCATION	GAGE NO.	LOADS (lb)	STRAIN GAGE READING (10^{-6} IN/IN)		DIFFERENCE (10^{-6} IN/IN)	E (PSI) 10^6	STRESS (PSI)
					P_1	P_2			
A	Warping	Bottom flange	3	23.8	39	45	6	0.440	2.64
				43.8	82	92	10		4.40
				63.8	124	140	16		7.04
				83.8	166	188	22		9.68
				103.8	209	236	27		11.88
				123.8	253	284	31		13.64
B	Warping	Bottom flange	10	23.8	29	35	6		2.64
				43.8	62	74	12		5.28
				63.8	93	109	16		7.04
				83.8	125	145	20		8.80
				103.8	153	182	29		12.76
				123.8	185	223	38		16.72

TABLE - 7
EXPERIMENTAL STRAIN READINGS AND STRESSES FOR CASE - I
(MODEL NO.1, MAX.- ECCENTRICITY)

SECTION	TYPE OF STRESS	LOCATION	GAGE NO.	LOADS (lb)	STRAIN GAGE READING (10^{-6} IN/IN)		DIFFERENCE (10^{-6} IN/IN)	E (PSI) 10^{6}	STRESS (PSI)
					P_1	P_3			
A	Distortion	Upper gage	1	23.8	32	- 85	53	0.440	23.32
				43.8	74	-166	92		40.48
				63.8	116	-248	132		58.08
				83.8	160	-330	170		74.80
				103.8	202	-420	218		95.92
				123.8	244	-515	271		119.24
		Lower gage	6	23.8	- 14	- 44	30		13.20
				43.8	- 25	- 82	57		25.08
				63.8	- 39	-126	87		38.28
				83.8	- 54	-169	115		50.60
				103.8	- 68	-213	145		63.80
				123.8	- 82	-257	175		77.00
B	Distortion	Upper gage	14	23.8	41	10	31		13.64
				43.8	86	25	61		26.84
				63.8	133	39	94		41.36
				83.8	176	50	126		55.44
				103.8	215	65	150		66.00
				123.8	256	77	179		78.76
		Lower gage	13	23.8	- 20	- 9	11		4.84
				43.8	- 40	- 16	24		10.56
				63.8	- 64	- 23	41		18.04
				83.8	- 88	- 37	51		22.44
				103.8	-114	- 46	68		29.92
				123.8	-140	- 56	84		36.96

TABLE - 8
EXPERIMENTAL STRAIN READINGS AND STRESSES FOR CASE - I
(MODEL NO.1, MAX. ECCENTRICITY)

SECTION	TYPE OF STRESS	LOCATION	GAGE NO.	LOADS (lb)	STRAIN GAGE READING (10^{-6} IN/IN)		DIFFERENCE (10^{-6} IN/IN)	E (PSI) 10^6	STRESS (PSI)
					P_1	P_3			
A	Warping	Bottom flange	3	23.8	43	70	27	0.440	11.88
				43.8	91	145	54		23.76
				63.8	137	221	84		36.96
				83.8	182	297	115		50.60
				103.8	228	372	144		63.36
				123.8	277	449	172		75.68
B	Warping	Bottom flange	10	23.8	30	64	34		14.96
				43.8	64	128	64		28.16
				63.8	100	196	96		42.24
				83.8	134	265	131		57.64
				103.8	170	340	170		74.80
				123.8	206	410	204		89.76

TABLE - 9
EXPERIMENTAL STRAIN READINGS AND STRESSES FOR CASE - II
(MODEL NO.1, MAX. ECCENTRICITY)

SECTION	TYPE OF STRESS	LOCATION	GAGE NO.	LOADS (lb)	STRAIN GAGE READING (10^{-6} IN/IN) P_1	STRAIN GAGE READING (10^{-6} IN/IN) P_3	DIFFERENCE (10^{-6} IN/IN)	E (PSI) 10^6	STRESS (PSI)
A	Distortion	Upper gage	7	23.8	19	4	15	0.440	6.60
				43.8	40	10	30		13.20
				63.8	64	20	44		19.36
				83.8	88	24	64		28.16
				103.8	112	30	82		36.08
				123.8	130	45	85		37.40
		Lower gage	6	23.8	- 19	- 13	6		2.64
				43.8	- 34	- 26	8		3.52
				63.8	- 52	- 40	12		5.28
				83.8	- 72	- 55	17		7.48
				103.8	- 92	- 70	22		9.68
				123.8	-118	- 85	33		14.52
B	Distortion	Upper gage	8	23.8	35	- 48	13		5.72
				43.8	68	- 96	28		12.32
				63.8	107	-144	37		16.28
				83.8	145	-192	47		20.68
				103.8	183	-240	57		25.08
				123.8	220	-285	65		28.60
		Lower gage	9	23.8	- 10	- 10	0		0.00
				43.8	- 18	- 23	5		2.20
				63.8	- 27	- 36	9		3.96
				83.8	- 36	- 49	13		5.72
				103.8	- 46	- 63	17		7.48
				123.8	- 55	- 80	25		11.00

TABLE -10
EXPERIMENTAL STRAIN READINGS AND STRESSES FOR CASE - II
(MODEL NO.1, MAX. ECCENTRICITY)

SECTION	TYPE OF STRESS	LOCATION	GAGE NO.	LOADS (lb)	STRAIN GAGE READING (10^{-6} IN/IN)		DIFFERENCE (10^{-6} IN/IN)	E (PSI) 10^6	STRESS (PSI)
					P_1	P_3			
A	Warping	Bottom flange	3	23.8	40	62	22	0.440	9.68
				43.8	80	123	43		18.92
				63.8	124	188	64		28.16
				83.8	170	255	85		37.40
				103.8	210	318	108		47.52
				123.8	254	385	131		57.64
B	Warping	Bottom flange	12	23.8	29	12	17		7.48
				43.8	60	22	38		16.72
				63.8	95	33	62		27.28
				83.8	129	45	84		36.96
				103.8	157	57	100		44.00
				123.8	190	68	122		53.68

TABLE -11
EXPERIMENTAL STRAIN READINGS AND STRESSES FOR CASE - III
(MODEL NO.1, MAX. ECCENTRICITY)

SECTION	TYPE OF STRESS	LOCATION	GAGE NO.	LOADS (lb)	STRAIN GAGE READING (10^{-6} IN/IN)		DIFFERENCE (10^{-6} IN/IN)	E (PSI) 10^6	STRESS (PSI)
					P_1	P_3			
A	Distortion	Upper gage	7	23.8	17	3	14	0.440	6.16
				43.8	32	13	19		8.36
				63.8	48	21	27		11.88
				83.8	64	30	34		14.96
				103.8	80	43	37		16.28
				123.8	95	54	41		18.04
		Lower gage	6	23.8	- 20	- 15	5		2.20
				43.8	- 33	- 28	5		2.20
				63.8	- 48	- 42	6		2.64
				83.8	- 64	- 56	8		3.52
				103.8	- 79	- 69	10		4.40
				123.8	- 96	- 84	12		5.28
B	Distortion	Upper gage	8	23.8	30	- 40	10		4.40
				43.8	66	- 50	16		7.04
				63.8	95	- 58	37		16.28
				83.8	128	- 70	58		25.52
				103.8	161	- 80	81		35.64
				123.8	191	- 90	101		44.44
		Lower gage	9	23.8	- 9	- 12	3		1.32
				43.8	- 18	- 23	5		2.20
				63.8	- 27	- 37	10		4.40
				83.8	- 40	- 52	12		5.28
				103.8	- 48	- 64	16		7.04
				123.8	- 58	- 77	19		8.36

TABLE - 12

EXPERIMENTAL STRAIN READINGS AND STRESSES FOR CASE - III
(MODEL NO.1, MAX. ECCENTRICITY)

SECTION	TYPE OF STRESS	LOCATION	GAGE NO.	LOADS (lb)	STRAIN GAGE READING (10^{-6} IN/IN)		DIFFERENCE (10^{-6} IN/IN)	E (PSI) 10^{6}	STRESS (PSI)
					P_1	P_3			
A	Warping	Bottom Flange	3	23.8	41	50	9	0.440	3.96
				43.8	84	104	20		8.80
				63.8	126	162	36		15.84
				83.8	170	217	47		20.68
				103.8	213	273	60		26.40
				123.8	256	330	74		32.56
B	Warping	Bottom flange	10	23.8	29	22	7		3.08
				43.8	62	50	12		5.28
				63.8	93	70	23		10.12
				83.8	125	89	36		15.84
				103.8	153	106	47		20.68
				123.8	185	126	59		25.96

TABLE - 13
EXPERIMENTAL STRAIN READINGS AND STRESSES FOR CASE- I
(MODEL NO.2, MEDIUM ECCENTRICITY)

SECTION	TYPE OF STRESS	LOCATION	GAGE NO.	LOADS (lb)	STRAIN GAGE READING (10^{-6} IN/IN)		DIFFERENCE (10^{-6} IN/IN)	E (PSI) 10^{6}	STRESS (PSI)
					P_1	P_2			
A	Warping	Bottom flange	3	23.8	58	68	10	0.485	4.85
				43.8	116	140	24		11.64
				63.8	179	210	31		15.04
				83.8	238	283	45		21.83
				103.8	298	355	57		27.65
				123.8	358	428	70		33.95
B	Warping	Bottom flange	10	23.8	37	50	13		6.30
				43.8	71	94	23		11.16
				63.8	106	142	36		17.46
				83.8	140	189	49		23.77
				103.8	174	237	63		30.56
				123.8	208	284	76		36.86

TABLE - 14
EXPERIMENTAL STRAIN READINGS AND STRESSES FOR CASE - I
(MODEL NO.2, MEDIUM ECCENTRICITY)

SECTION	TYPE OF STRESS	LOCATION	GAGE NO.	LOADS (lb)	STRAIN GAGE READING (10^{-6} IN/IN)		DIFFERENCE (10^{-6} IN/IN)	E (PSI) 10^6	STRESS (PSI)
					P_1	P_2			
A	Distortion	Upper gage	1	23.8	28	- 15	13	0.485	6.31
				43.8	62	- 24	38		18.43
				63.8	97	- 27	70		33.95
				83.8	137	- 31	106		51.41
				103.8	167	- 36	131		63.53
				123.8	206	- 42	164		79.54
		Lower gage	6	23.8	- 12	- 28	16		7.76
				43.8	- 23	- 56	33		16.00
				63.8	- 38	- 84	46		22.31
				83.8	- 53	-114	61		29.59
				103.8	- 69	-142	73		35.40
				123.8	- 87	-170	83		40.26
B	Distortion	Upper gage	14	23.8	37	43	6		2.91
				43.8	72	81	9		4.37
				63.8	105	129	24		11.64
				83.8	137	169	32		15.52
				103.8	172	222	50		24.25
				123.8	207	276	69		33.47
		Lower gage	13	23.8	- 7	- 18	11		5.34
				43.8	- 15	- 35	20		9.70
				63.8	- 25	- 52	27		13.10
				83.8	- 34	- 71	37		17.95
				103.8	- 44	- 89	45		21.83
				123.8	- 55	-106	51		24.74

TABLE - 15
EXPERIMENTAL STRAIN READINGS AND STRESSES FOR CASE- II
(MODEL NO.2, MEDIUM ECCENTRICITY)

SECTION	TYPE OF STRESS	LOCATION	GAGE NO.	LOADS (lb)	STRAIN GAGE READING (10^{-6} IN/IN)		DIFFERENCE (10^{-6} IN/IN)	E (PSI)	STRESS (PSI)
					P_1	P_2		10^6	
A	Warping	Bottom flange	3	23.8	54	64	10	0.485	4.85
				43.8	112	130	18		8.73
				63.8	169	196	27		13.10
				83.8	228	264	36		17.46
				103.8	288	332	44		21.34
				123.8	348	400	52		25.22
B	Warping	Bottom flange	10	23.8	38	49	11		5.34
				43.8	75	95	20		9.70
				63.8	113	142	29		14.07
				83.8	149	192	43		20.86
				103.8	186	241	55		26.68
				123.8	223	287	64		31.04

TABLE - 16
EXPERIMENTAL STRAIN READINGS AND STRESSES FOR CASE - II
(MODEL NO.2, MEDIUM ECCENTRICITY)

SECTION	TYPE OF STRESS	LOCATION	GAGE NO.	LOADS (lb)	STRAIN GAGE READING (10^{-6} IN/IN)		DIFFERENCE (10^{-6} IN/IN)	E (PSI) 10^6	STRESS (PSI)
					P_1	P_2			
A	Distortion	Upper gage	1	23.8	14	10	4	0.485	1.94
				43.8	28	22	6		2.91
				63.8	42	33	9		4.37
				83.8	58	44	14		6.79
				103.8	74	58	16		7.76
				123.8	91	71	20		9.70
		Lower gage	6	23.8	- 14	- 18	4		1.94
				43.8	- 28	- 35	7		3.40
				63.8	- 47	- 53	6		2.91
				83.8	- 63	- 73	10		4.85
				103.8	- 78	- 93	15		7.28
				123.8	- 97	-114	17		8.24
B	Distortion	Upper gage	14	23.8	37	33	4		1.94
				43.8	69	61	8		3.88
				63.8	104	92	12		5.82
				83.8	140	124	16		7.76
				103.8	176	156	20		9.70
				123.8	216	188	28		13.58
		Lower gage	13	23.8	- 7	- 10	3		1.45
				43.8	- 15	- 20	5		2.43
				63.8	- 23	- 31	8		3.88
				83.8	- 31	- 42	11		5.34
				103.8	- 40	- 53	13		6.31
				123.8	- 48	- 64	16		7.76

TABLE -17
EXPERIMENTAL STRAIN READINGS AND STRESSES FOR CASE- III
(MODEL NO.2, MEDIUM ECCENTRICITY)

SECTION	TYPE OF STRESS	LOCATION	GAGE NO.	LOADS (lb)	STRAIN GAGE READING (10^{-6} IN/IN)		DIFFERENCE (10^{-6} IN/IN)	E (PSI) 10^{6}	STRESS (PSI)
					P_1	P_2			
A	Warping	Bottom flange	3	23.8	55	62	7	0.485	3.40
				43.8	112	122	10		4.85
				63.8	168	183	15		7.28
				83.8	225	243	18		8.73
				103.8	281	306	25		12.13
				123.8	339	368	29		14.07
B	Warping	Bottom flange	10	23.8	36	50	14		6.79
				43.8	71	88	17		8.25
				63.8	106	129	23		11.16
				83.8	143	170	27		13.10
				103.8	179	209	30		14.55
				123.8	216	250	34		16.49

TABLE - 18
EXPERIMENTAL STRAIN READINGS AND STRESSES FOR CASE - III
(MODEL NO.2, MEDIUM ECCENTRICITY)

SECTION	TYPE OF STRESS	LOCATION	GAGE NO.	LOADS (lb)	STRAIN GAGE READING (10^{-6} IN/IN)		DIFFERENCE (10^{-6} IN/IN)	E (PSI) 10^6	STRESS (PSI)
					P_1	P_2			
A	Distortion	Upper gage	7	23.8	7	9	2	0.485	0.97
				43.8	17	19	2		0.97
				63.8	25	27	2		0.97
				83.8	34	36	2		0.97
				103.8	41	44	3		1.46
				123.8	47	53	6		2.91
		Lower gage	2	23.8	- 20	- 18	2		0.97
				43.8	- 45	- 43	2		0.97
				63.8	- 66	- 63	3		1.46
				83.8	- 89	- 87	2		0.97
				103.8	-109	-112	3		1.46
				123.8	-130	-134	4		1.94
B	Distortion	Upper gage	8	23.8	23	24	1		0.49
				43.8	49	46	3		1.46
				63.8	75	66	9		4.37
				83.8	102	89	13		6.30
				103.8	129	110	19		9.22
				123.8	157	133	24		11.64
		Lower gage	9	23.8	- 11	- 13	2		0.97
				43.8	- 24	- 27	3		1.46
				63.8	- 37	- 44	7		3.40
				83.8	- 51	- 58	7		3.40
				103.8	- 65	- 75	10		4.85
				123.8	- 78	- 89	11		5.34

TABLE - 19

EXPERIMENTAL STRAIN READINGS AND STRESSES FOR CASE- I

(MODEL NO.2, MAX. ECCENTRICITY)

SECTION	TYPE OF STRESS	LOCATION	GAGE NO.	LOADS (lb)	STRAIN GAGE READING (10^{-6} IN/IN)		DIFFERENCE (10^{-6} IN/IN)	E (PSI) 10^6	STRESS (PSI)
					P_1	P_3			
A	Warping	Bottom flange	3	23.8	58	85	27	0.485	13.10
				43.8	116	165	49		23.77
				63.8	176	247	71		34.44
				83.8	238	332	94		45.59
				103.8	298	416	118		57.23
				123.8	358	503	145		70.33
B	Warping	Bottom flange	10.	23.8	37	62	25		12.13
				43.8	71	123	52		25.22
				63.8	106	185	79		38.32
				83.8	140	248	108		52.38
				103.8	174	312	138		66.93
				123.8	208	378	170		82.45

TABLE - 20

EXPERIMENTAL STRAIN READINGS AND STRESSES FOR CASE - I

(MODEL NO.2, MAX. ECCENTRICITY)

SECTION	TYPE OF STRESS	LOCATION	GAGE NO.	LOADS (lb)	STRAIN GAGE READING (10^{-6} IN/IN)		DIFFERENCE (10^{-6} IN/IN)	E (PSI) 10^6	STRESS (PSI)
					P_1	P_3			
A	Distortion	Upper gage	1	23.8	28	- 74	46	0.485	22.31
				43.8	62	-156	94		45.59
				63.8	97	-246	149		72.27
				83.8	137	-328	191		92.64
				103.8	167	-414	247		119.80
				123.8	206	-494	288		139.68
		Lower gage	6	23.8	- 12	- 40	28		13.58
				43.8	- 23	- 78	55		26.68
				63.8	- 38	-116	78		37.83
				83.8	- 53	-156	103		49.96
				103.8	- 69	-194	125		60.63
				123.8	- 87	-232	145		70.33
B	Distortion	Upper gage	8	23.8	37	- 60	23		11.16
				43.8	72	-123	51		24.74
				63.8	105	-196	91		44.14
				83.8	137	-260	123		59.66
				103.8	172	-316	144		69.84
				123.8	207	-380	173		83.90
		Lower gage	13	23.8	- 11	- 24	13		6.30
				43.8	- 23	- 48	25		12.13
				63.8	- 35	- 80	45		21.83
				83.8	- 47	-108	61		29.59
				103.8	- 59	-140	81		39.29
				123.8	- 72	-173	101		48.99

TABLE - 21
EXPERIMENTAL STRAIN READINGS AND STRESSES FOR CASE- II
(MODEL NO.2, MAX. ECCENTRICITY)

SECTION	TYPE OF STRESS	LOCATION	GAGE NO.	LOADS (lb)	STRAIN GAGE READING (10^{-6} IN/IN)		DIFFERENCE (10^{-6} IN/IN)	E (PSI) 10^6	STRESS (PSI)
					P_1	P_3			
A	Warping	Bottom flange	3	23.8	54	75	21	0.485	10.19
				43.8	112	149	37		17.95
				63.8	169	225	56		27.16
				83.8	228	301	73		35.40
				103.8	288	379	91		44.14
				123.8	348	457	109		52.87
B	Warping	Bottom flange	10	23.8	38	61	23		11.16
				43.8	75	121	46		22.31
				63.8	113	181	68		32.98
				83.8	149	240	91		44.14
				103.8	186	299	113		54.80
				123.8	223	360	137		66.44

TABLE - 22
EXPERIMENTAL STRAIN READINGS AND STRESSES FOR CASE - II
(MODEL NO.2, MAX. ECCENTRICITY)

SECTION	TYPE OF STRESS	LOCATION	GAGE NO.	LOADS (lb)	STRAIN GAGE READING (10^{-6} IN/IN)		DIFFERENCE (10^{-6} IN/IN)	E (PSI) 10^6	STRESS (PSI)
					P_1	P_3			
A	Distortion	Upper gage	7	23.8	14	8	6	0.485	2.91
				43.8	28	15	13		6.30
				63.8	42	23	19		9.22
				83.8	58	31	27		13.10
				103.8	74	40	34		16.49
				123.8	91	47	44		21.34
		Lower gage	6	23.8	- 14	- 7	7		3.40
				43.8	- 28	- 17	11		5.34
				63.8	- 47	- 29	18		8.73
				83.8	- 63	- 40	23		11.15
				103.8	- 78	- 51	27		13.10
				123.8	- 97	- 64	33		16.00
B	Distortion	Upper gage	14	23.8	35	27	8		3.88
				43.8	65	51	14		6.79
				63.8	101	75	26		12.61
				83.8	136	97	39		18.92
				103.8	172	120	52		25.22
				123.8	211	140	71		34.44
		Lower gage	9	23.8	- 12	- 5	7		3.40
				43.8	- 23	- 10	13		6.30
				63.8	- 35	- 17	18		8.73
				83.8	- 48	- 24	26		12.61
				103.8	- 59	- 31	28		13.58
				123.8	- 72	- 38	34		16.49

TABLE - 23
EXPERIMENTAL STRAIN READINGS AND STRESSES FOR CASE -III
(MODEL NO.2, MAX. ECCENTRICITY)

SECTION	TYPE OF STRESS	LOCATION	GAGE NO.	LOADS (lb)	STRAIN GAGE READING (10^{-6} IN/IN)		DIFFERENCE (10^{-6} IN/IN)	E (PSI) 10^{6}	STRESS (PSI)
					P_1	P_3			
A	Warping	Bottom flange	3	23.8	55	68	13	0.485	6.30
				43.8	112	132	20		9.70
				63.8	168	200	32		15.52
				83.8	225	266	41		19.89
				103.8	281	336	55		26.68
				123.8	339	404	65		31.53
B	Warping	Bottom flange	10	23.8	36	49	13		6.30
				43.8	71	99	28		13.58
				63.8	106	147	41		19.89
				83.8	143	197	54		26.19
				103.8	179	247	68		32.98
				123.8	216	296	80		38.80

TABLE -24
EXPERIMENTAL STRAIN READINGS AND STRESSES FOR CASE-III
(MODEL NO.2, MAX. ECCENTRICITY)

SECTION	TYPE OF STRESS	LOCATION	GAGE NO.	LOADS (lb)	STRAIN GAGE READING (10^{-6} IN/IN)		DIFFERENCE (10^{-6} IN/IN)	E (PSI) 10^6	STRESS (PSI)
					P_1	P_3			
A	Distortion	Upper gage	7	23.8	7	5	2	0.485	0.97
				43.8	17	12	5		2.43
				63.8	25	18	7		3.40
				83.8	34	24	10		4.85
				103.8	41	30	11		5.34
				123.8	47	36	11		5.34
		Lower gage	2	23.8	- 20	- 17	3		1.46
				43.8	- 42	- 35	7		3.40
				63.8	- 63	- 55	8		3.88
				83.8	- 84	- 76	8		3.88
				103.8	-105	- 96	9		4.37
				123.8	-124	-115	9		4.37
B	Distortion	Upper gage	8	23.8	23	- 19	4		1.94
				43.8	49	- 40	9		4.37
				63.8	75	- 62	13		6.30
				83.8	102	- 85	17		8.25
				103.8	129	-108	21		10.20
				123.8	157	-126	31		15.04
		Lower gage	9	23.8	- 14	- 9	5		2.43
				43.8	- 29	- 18	11		5.34
				63.8	- 43	- 31	12		5.82
				83.8	- 58	- 43	15		7.28
				103.8	- 73	- 55	18		8.73
				123.8	- 88	- 68	20		9.70